Sex determination of Romano-British neonatal remains via advanced biomolecular and anthropological techniques

UNIVERSITY OF
LINCOLN

Robert Jackson

07113369

A report submitted in part fulfilment of the examination requirements for the award of an MScRes Forensic Science awarded by the University of Lincoln, September 2014, supervised by Dr. R. Dixon and Mrs G. Fowler, M.Sc.

This is to certify that I am responsible for the work submitted in this thesis, that the original work is my own, except as specified in the acknowledgements, and in references, and that neither the thesis nor the original work contained therein has been previously submitted to any institution for a degree.

Signature: Robert Jackson
Name: Robert Jackson
Date: 07 October 2015

Abstract

The aim of this study was to amplify the ancient DNA from a collection of 63 Romano-British neonatal skeletons, in order to determine their sex. The DNA testing strategy has been designed to overcome the issues associated with ancient DNA investigations, including degraded template DNA, inhibition of PCR, and modern contaminants.

Ancient DNA has been extracted using a silica based method using the GENECLEAN Kit for Ancient DNA. Three different PCR-Cleanup kits were investigated to determine their effectiveness in the removal of PCR inhibitors. The PowerClean kit (MoBio Laboratories) proved the most effective, and was used throughout.

Two different sets of primers were used to provide amplicons from the Amelogenin gene. The Amel-A and Amel-C primers used by Arnay-de-la-Rosa (2007) proved to be ineffective, with multiple problems with non-specific binding and lack of amplification of the target region. However, the amelogenin primers from the AmpFISTR Identifiler kit proved more effective and were chosen for use in testing the ancient material.

Modern DNA is used through the study to compare to the ancient material, in order to allow for pre-testing of the techniques and optimisation of the PCR without the loss of precious material. Modern DNA was also artificially degraded in order to determine whether the PCR technique can amplify fractured DNA. In this experimentation, the Identifiler primer PCR successfully amplified modern DNA that had been degraded for 15 minutes in an ultrasonic bath, to a length of approximately 100-500bp in size.

Measurements of the skeletons have also been taken in order to determine the exact age of the neonates at time of death, to identify potential patterns in the deaths of the individuals, and to identify a potential link between the age of the individual at time of death and the probability of survival of the DNA within their remains. Of the remains, 72% of the individuals were of an age of at least 38 prenatal weeks, indicating a full term child considered as an infant death. 8% of individuals provided an age range above 24 weeks, and were potentially stillbirths rather than infant deaths, while 20% of the remains showed sufficient damage to prevent complete age ranges that utilise both the length and width of the skeletal material from being calculated and therefore may have been miscarriages of younger foetuses or the fragmented remains of older infant remains.

Following the DNA analysis of the remains, three of the individuals provided amplicons of the target region and therefore their sex could be determined. All three of these individuals provided an XY male genotype. All other remains tested gave negative results. Many of the results showed severe problems with PCR inhibition even after the use of the PowerClean PCR Cleanup kit. Therefore, the conclusions that can be drawn are limited. The potential for contamination to be the cause of these three results is discussed, but the low sample size of positive results makes it difficult to determine the source of the amplified DNA. Further work is suggested, including more rigorous inhibitor removal methods and qPCR to provide a larger sample size of positive neonatal DNA results, allowing for the validity of the results to be assessed more thoroughly.

Inhibition and DNA degradation have proved to be the largest challenges faced in this research, which is consistent with other research that utilises ancient DNA. Further analysis of soil samples from the excavation and of the remains themselves is suggested, to determine the type and quantity of inhibitory substances present. Biochemical assessment to determine the level of preservation of the microstructure of the bone, and the use of cloning and sequencing to identify DNA damage and rule out contaminants is suggested.

Acknowledgements

The author wishes to thank Dr Ron Dixon and Ms Gillian Fowler, and Prof. Jonathan Cooper for all of their help and support throughout this thesis, providing inspiration for many ideas and adjustments. Secondly, I would like to thank Alice Green for consistent inspiration and motivation throughout my practical and written work, even when I am terribly frustrating. Thirdly, I would like to thank Tom Faire, for his support and providing me a place to stay, without which, I would not have been able to complete this thesis.

I would also like to thank my friends and family, who have been very supportive throughout this project.

Contents

1. Chapter One: Introduction

The determination of sex is an important part of forensic anthropology. This is typically done using morphological techniques, in the examination of the pelvis (Phenice, 1969) and skull (White & Folkens, 2005). During puberty, a high degree of sexual dimorphism develops in these bones and this dimorphism is used to identify male and female characteristics, therefore allowing for the determination of sex.

However, morphological examination is not always possible in anthropological specimens. In many cases, damage to the skeleton has obliterated the dimorphic characteristics present on the bone, or the bones themselves have been lost. In juvenile remains, morphological assessment of sex has remained a persistent problem for forensic anthropologists as the dimorphism induced during puberty is not yet evident.

With modern improvements to ancient DNA analysis, it has become more common to sex even small pieces of skeletal remains using molecular biology. DNA has been used for identification in forensic cases in the UK for over 25 years, but is typically carried out with fresh, modern samples of blood, saliva or semen. Both nuclear DNA and mitochondrial DNA (mtDNA) analyses are used in forensic cases, as both can provide useful information for a police investigation.

Mitochondrial DNA is very resilient and has a high copy number per cell, so is often preferential for analysis over nuclear DNA. However, mtDNA is not unique to a particular individual. Mitochondrial DNA is inherited maternally and will be shared in siblings, as well as any older generations following the maternal line. Even so, mitochondrial DNA is still useful in forensic cases, as it can be used to exclude individuals from the investigation or identify a possible victim or perpetrator through a maternally linked relative on the National DNA Database.

Nuclear DNA by comparison is not as resilient to damage and only has one copy per cell. Therefore, nuclear DNA is more likely to degrade over time and will generally be present in a lesser concentration than mitochondrial DNA. However, the key characteristic of nuclear DNA is that it is unique to each individual and therefore has much more power to identify a specific perpetrator or victim.

Nuclear DNA is present in almost every single cell in the human body, with some exceptions such as red blood cells. Most forensic DNA analysis is done with body fluids due to their accessibility and the rate at which they are found in crime scenes. However, both nuclear DNA and mtDNA are present in bone cells and can be recovered and analysed from skeletal remains.

Ancient DNA (aDNA) analysis has rapidly improved in recent years and has become a much more viable technique available to the forensic anthropologist in order to investigate

skeletal remains. Ancient DNA is simply any DNA which is recovered from an ancient specimen, such as skeletal remains, fossils, mummified remains and remains frozen in permafrost.

While the principles behind aDNA analysis are the same as modern DNA analysis, there are a number of issues that are unique, or much more problematic, to ancient DNA. Modern DNA analysis relies upon the use of Polymerase Chain Reaction (PCR) technology, which amplifies low copy numbers of DNA into large quantities that can then be manipulated and analysed much more effectively. PCR reactions are very successful in amplifying DNA, but are also very finely balanced. A PCR reaction must be optimised effectively in order to deliver a high efficiency of DNA amplification, must exclude contamination from other unwanted DNA sources and must contain no inhibitors.

These problems are much more of an issue in aDNA analysis, as the template DNA has typically undergone some level of degradation. Therefore, the optimisation of the PCR technique must be very precise in order to deliver an efficient amplicon yield from a very low copy number of DNA. In addition, contamination must be very tightly controlled as the low copy number of ancient template DNA means that even the slightest contamination by modern DNA can be overwhelming. Inhibitors must also be effectively removed from the PCR reaction as even very small levels of inhibition can prevent aDNA from being able to amplify to a detectable level.

The aims of this project are to develop a strategy to recover ancient DNA from a collection of Romano-British neonatal skeletons and to use this ancient DNA to determine sex for each individual. The experimental protocol will be designed to overcome contamination issues, remove inhibitors and overcome PCR issues with degraded template DNA in order to provide an optimised technique to recover aDNA from neonatal skeletal remains.

2. Chapter Two: Literature Review

2.0. Introduction

The analysis of human remains is an important part of a forensic investigation. Forensic anthropologists have extensive knowledge of the morphology of the human skeleton and how it varies dependant on sex, age, ancestry and stature. All of these factors can be used to identify a victim when a decomposed body or skeletal remains are found.

Typically, human remains are identified using their morphological characteristics. The human skeleton varies visibly over its lifetime, allowing for a visual examination of these characteristics that will allow the anthropologist to determine age. Also, during puberty the hormonal changes within the body cause skeletal changes which typically cause a more masculine or feminine morphology to form. The ancestry of the individual will lead to a large degree of morphological changes in the face, or splanchnocranium. Finally, the stature of the individual will be reflected by the variance in morphology and size of the long bones of the skeleton (White and Folkens, 2005).

2.1. Morphological Assessment of Sex

Sexual dimorphism is shown in many species and is characterised by a difference in morphology between male and female individuals of one species. A classic example of sexual dimorphism is the brightly coloured male against the brown colouring of the female peacock. In humans, sexual dimorphism is evident across a very wide range of bones, from head (Walker, in Buikstra and Ubelaker, 1994) to toe (Fessler et al, 2005). White and Folkens (2005) describe the overall disparity between male and female skeletal size, stating that masculine skeletons are typically larger and more robust, while female skeletons are typically smaller and more gracile in construction. However, White and Folkens identify the issue that while some skeletal dimensions may show 20% larger proportions in male skeletons, in other dimensions there may be little or no sexual dimorphism. However, the widest degree of sexual dimorphism is found in the pelvis and skull and these are typically used to determine sex in a forensic investigation when present.

2.1.1. Pelvis

The pelvis is regarded as the most sexually dimorphic set of bones in the human body. In 1969, Phenice proposed a method for sexing a skeleton via the os pubis, by determining whether a marked ventral arc, subpubic concavity and sharp medial aspect of the ischiopubic ramus were present. Phenice achieved an accuracy of 96% correct sex determinations in his experimentation and this technique has been continuously and extensively tested and proven to be successful. A range between 59% accuracy (MacLaughlin and Bruce, 1990) and 96% accuracy (Sutherland and Suchey, 1991) has been found during these tests, dependant on the population type that the skeletons originated

from. However, typically the accuracy of the Phenice method of sex determination is found to be between 80% and 90%, with reports of 83% accuracy in experimentation by Lovell in 1989, 83% accuracy in English remains from MacLaughlin and Bruce's 1990 experimentation and Ubelaker and Volk reporting 88.4% accuracy in 2002.

2.1.2. Skull

The skull has also been widely studied in order to determine whether morphological differences can be used to provide sex determinations. The overall observation that male skeletons are typically more robust than their smaller female counterparts continues to be true in the skull. Five key points have been identified by Walker (in Buikstra and Ubelaker, 1994) that show useful sexual dimorphism; the nuchal crest, mastoid process, supraorbital margin, supraorbital ridge and mental eminence. The mental eminence is found on the mandible rather than the cranium, where dimorphism is also readily apparent in the muscle attachments and overall shape of the mandible. Gülekon and Turgut (2003) found that masculine mandibles typically show a squarer chin with stronger gonial eversion and deeper mandibular rami. Walrath et al (2004) investigated the accuracy of the 5 key points described by Walker in addition to 5 other sexually dimorphic traits and found that there was no significant interobserver error in the overall determination of sex. The scores given to individual traits did show significant difference between two observers, occurring to a greater degree in traits with subjective definitions and no diagrams. However, the traits described by Walker have structured definitions and diagrams to accompany them and therefore should have little interobserver error.

2.1.3. Post-Cranial Skeleton

Sex determination via the morphology of the post-cranial skeleton has also been examined, with dimorphism found across many of the long bones of the arms and legs. For example, sexual dimorphism is found in the humerus, across six measurements determined by Iscan in 1998. Iscan determined that the maximum length of the humerus, vertical diameter of the humeral head, circumference of the midshaft, maximum and minimum midshaft diameters and the epicondylar breadth were all variable regions that could determine between masculine and feminine skeletons. This could be done using each individual measurement for up to 93% accuracy (using the epicondylar breadth to examine Thai specimens) or by stepwise discriminant function analysis to utilise all of the available measurements, achieving 97.1% accuracy in Thai remains.

However, there is a large degree of variation between individual populations. In 2005, Frutos examined a Guatemalan sample using the measurements described in Iscan's research. Guatemalan populations have a similar skeletal structure to Asian populations, sharing a lot of traits that are used to identify ancestry. Frutos achieved an accuracy of 98.2% using the discriminant function analyses described in Iscan, indicating how well a

Guatemalan population can be analysed using a methodology developed on Asian specimens. However, when Frutos used the discriminant functions developed by Mall et al (2003), using a collection of German remains, 0% of male remains were correctly classified via the maximum length and humeral head diameter, due to the larger body size and body mass of Germanic populations compared to Asian populations.

2.1.4. Juvenile Sex Assessment

There are many problems with the identification of juvenile skeletons in a forensic and archaeological context. The largest of these is sex determination, because sex is very difficult to identify using skeletal morphology in juvenile remains. This is largely due to the fact that the sexual dimorphism seen in the adult skeleton develops during puberty. In juveniles who have yet to reach sexual maturity this dimorphism is not yet evident (Cardoso, 2008). Komar and Buikstra stated in their 2008 book that convincing evidence of sexual dimorphism in juvenile skeletons has not been found.

However, extensive work has been done to try to develop morphological techniques to determine sex in juvenile remains. Typically this work has been focused on the skull and pelvis, as these are the most dimorphic bones in the adult skeleton. As a modern example, in 2012 Gonzalez examined cephalometric radiographs from living juveniles aged 5-16, identifying 8 craniometric points and developing 20 measurements that utilised these points. Gonzalez found that the neurocranium is the most sexually dimorphic region of the juvenile craniofacial skeleton, until puberty begins. Males typically have larger heads than females in all stages of growth between 5 and 16 years of age. However, Gonzalez identifies the fact that the sexual dimorphism which develops in the juvenile skull is created by the interactions of every craniofacial structure and its growth patterns.

Therefore, the accuracy of sex determination is dependent on the age of the individual. The juvenile remains must be accurately aged before they can be sexed, since the major source of sexual variation is simply a size difference. This is reflected in Gonzalez' data, with the older 15-16 year old skulls allowing for sex determination with an 85% accuracy after cross-validation, while younger age groups such as the 5-6 year olds and 11-12 year olds having a lower cross validated accuracy of 74% and 72% respectively. This would imply that in even younger juvenile remains, such as infants, the sexual dimorphism is so slight that an accurate determination becomes very difficult.

Research has also been undertaken to determine whether there is sexual dimorphism present in juvenile teeth. Garn et al (1962, 1964) found sexual dimorphism in certain parts of certain permanent teeth, which also exists in a lesser extent in deciduous dentition (Black, 1978). The durability of the dentition compared to actual bone is much higher and their ability to survive even in bad burial conditions makes teeth an invaluable resource for the forensic investigator.

During the development of the permanent teeth, the crown forms very early and remains unchanged during growth and development. Cardoso (2008) therefore states that any sexual dimorphism present in the permanent teeth of adults should also be present in the developing permanent teeth in juvenile remains. However, as the shape and dimensions of the teeth are linked to the ancestry of the population, using a method that has been developed on a different population to the population that is being studied has been shown to cause poor results, such as those gained in Teschler-Nicola and Prosinger's 1998 study. Therefore, it is recommended in Cardoso (2008) that adult individuals with well-defined sex characteristics on the pelvis and skull are used as a basis for the dimensions of permanent dentition in a population before juveniles from the same population can be analysed alongside it.

Viciano et al (2011) used a unique "living" population in this way to determine whether juveniles could be accurately sexed via the emerging adult dentition. This population was a group of 117 volcano victims that were preserved by the pyroclastic flow of the Vesuvius eruption in 79AD. Of these, 87 individuals were adults between 20 and 60 years old and had previous sex determinations described using the pelvis and skull, indicating 52 males and 32 females. The remaining 30 individuals were subadults between the ages of 4 and 20 years, whose sex had been examined using the mandible and ilium in a method described by Schutkowski in 1993. Viciano took 6 different measurements of each tooth; the maximum mesiodistal crown diameter, maximum buccolingual crown diameter, mesiodistal cervical diameter, buccolingual cervical diameter, mesiolingual-distobuccal crown diameter and mesiobuccal-distolingual crown diameter.

Using discriminant formulae developed based on these measurements; Viciano was able to correctly assign adult sex determinations between 76.5 and 100% of the time, using the crown and cervical measurements of the canine teeth. These formulae were then applied to the 30 juvenile individuals, which allowed for 22 of them to be assigned a sex determination. These 22 individual sex estimates were then compared to the sex estimates given using Schutkowski's method utilising the ilium and mandible, which corroborated the sex determination in 76.19% of cases.

Therefore, there is definitely the possibility to form quite accurate sex determinations with juvenile remains. However, the population that Viciano used was quite small, so care must be taken to assume that this technique would work across other populations. While the recent developments in juvenile sex determination have definitely advanced the possibilities and options available to the forensic anthropologist, there are still a number of difficulties that prevent juvenile morphological sex estimation techniques from being as widely accepted as morphological sex estimation for adult remains.

2.2. Bone Structure

White and Folkens (2005) states that all bones in the human skeleton are made of two typical structures: the compact (cortical) bone and spongy (trabecular) bone. Cortical bone is the strong dense bone that forms the outer surface of the bone, while trabecular bone is a porous and lightweight bone which is found within the bone itself. This trabecular bone forms a honeycomb-like structure and is the location of the red marrow, where blood cells are produced. The outer surface of the bone is then covered with a thin layer of tissue known as the periosteum. While this is not present in the dry bone found in ancient remains, in life it covers all bone that lacks cartilage coverage. The periosteum is a strong membrane which provides nutrients to the bone and intertwines with tendons, entering the surface of the bone to coat it fully.

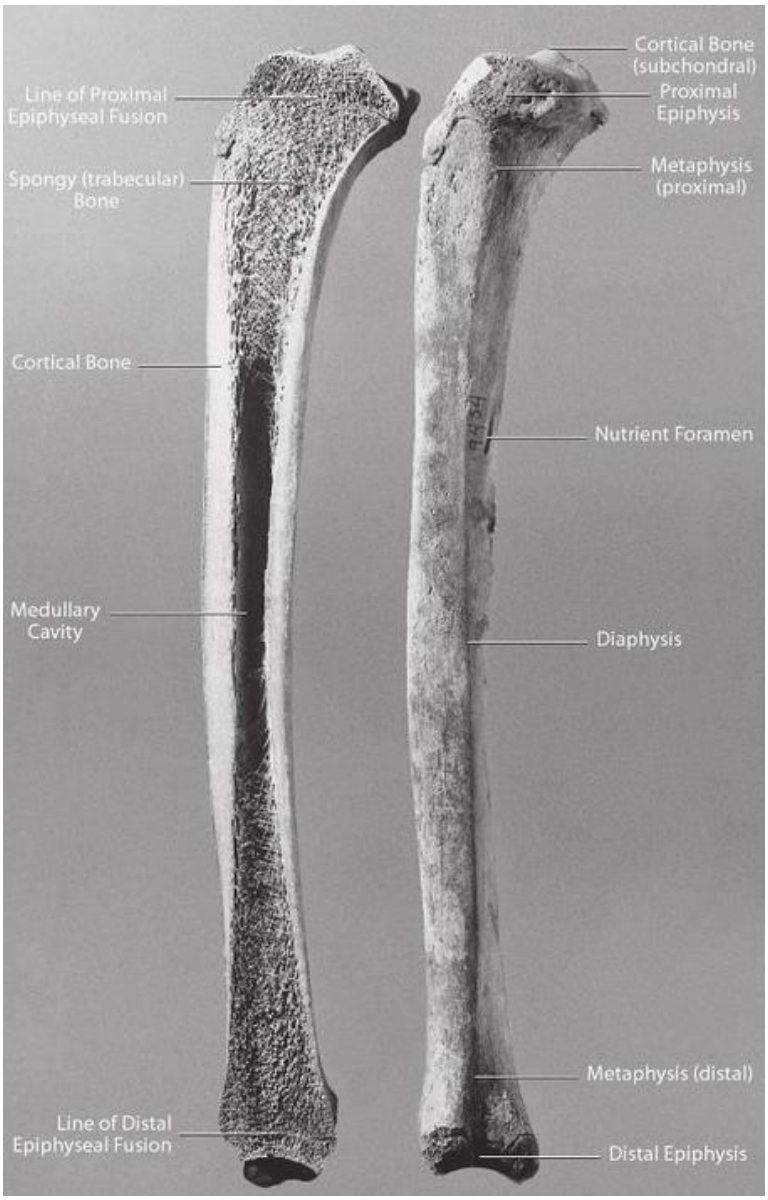

Fig 1**:** Left tibia showing the key elements of bone anatomy, including the cortical and trabecular bone. Reproduced from White and Folkens, 2005.

On a molecular level, bone is a composite material formed of collagen and hydroxyapatite. Collagen forms around 90% of the organic component of bone and is a flexible elastic fibre that forms a matrix within the bone tissue. This matrix forms banded fibrils, with 40nm wide "gap zones" where there are a high density of gaps between collagen molecules and 27nm "overlap zones" where collagen molecules align and become closely packed (Nudelman et al 2010). Hydroxyapatite is a calcium phosphate mineral that forms crystals within the collagen matrix, beginning in the gap zones and extending along the surface and interior of the fibrils to provide strength and hardness (Campos et al 2012). In combination, these provide bone with its strong-but-flexible properties that make it so valuable in the human body.

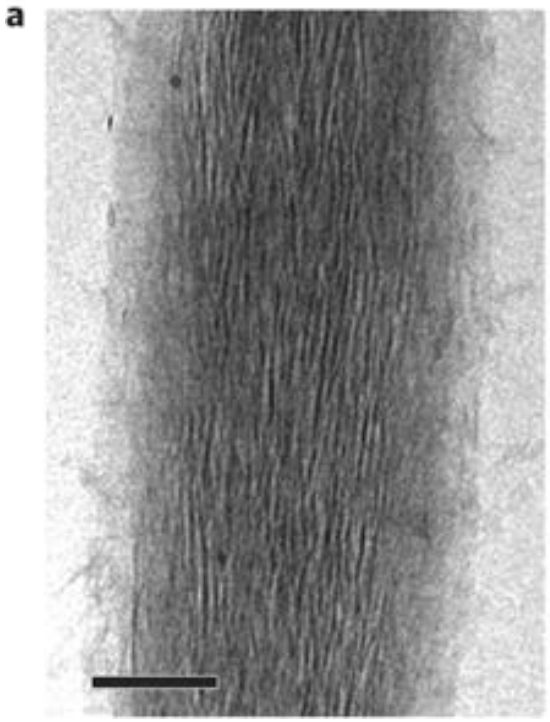

Fig 2: Two dimensional cryo-electron tomography image showing striations in collagen fibrils in bone. Reproduced from Nudelman et al (2010)

2.2.1. DNA Location within Bone

In 2012, Campos et al attempted to determine where the DNA was located within the collagen-hydroxyapatite matrix of bone tissue. While it had been previously established that DNA can bind to hydroxyapatite by Lindahl's 1993 experimentation and Okazaki et al's later 2001 research, there was little information about the relationship between collagen and DNA. Campos suggested that DNA does bind to collagen, but long strands of DNA would not bind to mineralised collagen as this would change the structure of the fibrils. This structure change has not been observed in previous research, so is unlikely to take place. However,

short strands of nuclear or mitochondrial DNA may bind to fibrils during the mineralisation process, potentially being trapped in the gap zones as hydroxyapatite crystallises the fibrils, surrounding and protecting the DNA.

Campos used two parallel data sets in order to investigate this; a set of four modern cow bones that were degraded in a range of environments for 4 years and a dataset of genuine ancient musk-ox bone that had been preserved in permafrost for over 14,000 years. An 82bp fragment of the control region in cow mtDNA was then amplified with qPCR in order to determine the level of usable DNA over time and the percentage levels of DNA bound to hydroxyapatite and collagen parts of the bone.

Campos discovered that after the first year of burial, a very sharp loss in overall recoverable DNA occurs, falling to less than 10% of the total mtDNA recoverable from a frozen control bone. This is due to the loss of the soft bone tissues such as osteoblasts, blood cells and periosteum cells. The percentage mass of collagen in the bone also falls, but Campos states that this is likely a contributory factor to the loss of total DNA rather than the sole reason. After this initial decrease, collagen and mtDNA loss both stabilise and slow.

In a frozen control bone, 75% of DNA retrieved is recovered from collagen, while 25% is recovered from hydroxyapatite. After the initial sharp decrease in DNA yield after the first year of burial, this ratio reverses, with 75% of retrievable DNA being contained in the hydroxyapatite and 25% in collagen. Therefore, it is suggested that the hydroxyapatite fraction of bone is at least as important as collagen in long-term preservation of DNA.

In the ancient musk-ox bone, good collagen survival was shown to be present and a ratio between 1:1 and 1:4 of mtDNA recovered from collagen and hydroxyapatite was shown, which would indicate that both fractions are important and allow for the potential of significantly large amounts of DNA loss if either fraction is discarded. This could suggest that extractions utilising EDTA, or EDTA in combination with Proteinase K, will have good rates of success in recovering amplifiable DNA.

2.3. DNA Structure

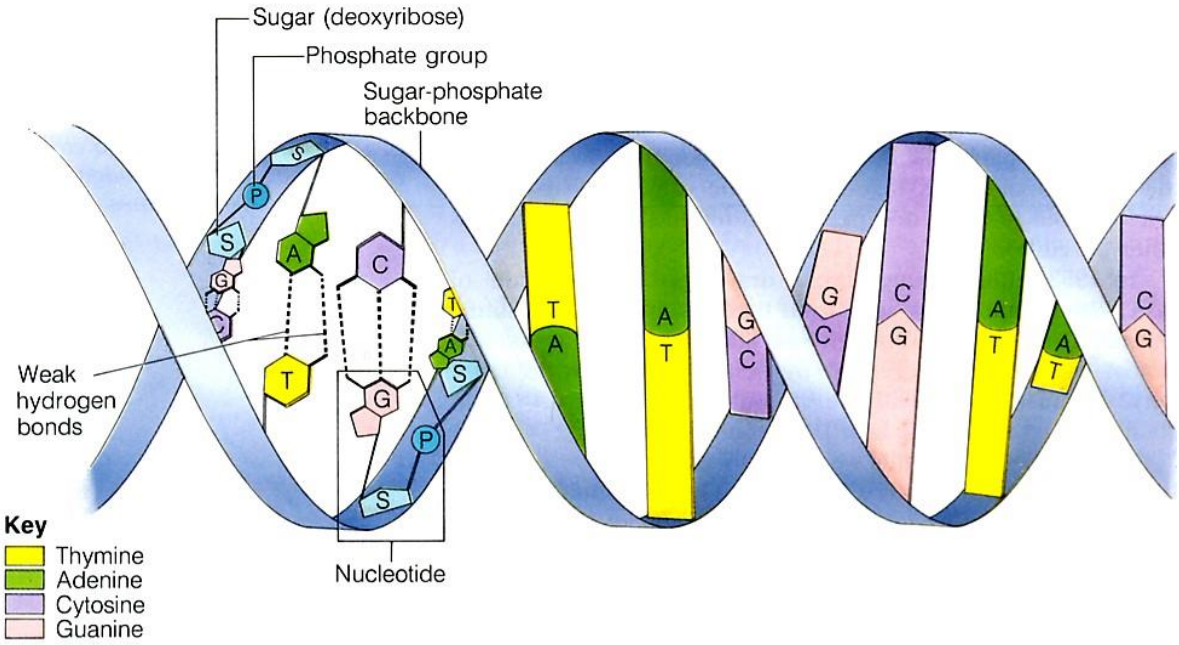

Fig 3: The structure of DNA in its typical double helix shape. Reproduced from - http://ehrig-privat.de/ueg/dna_-_structure.htm

DNA naturally occurs as a double helix structure, with two strands of DNA tightly wrapped around each other. The structure of DNA is similar to a helical ladder, with the backbone of the molecule formed of a sugar phosphate chain and the 'rungs' of the ladder formed of nitrogenous bases. There are four distinct types of nitrogenous base: guanine, cytosine, adenine and thymine. Each nitrogenous base is attached to a sugar-phosphate group to form a 'nucleotide'. The sequence of these bases determines our genetic characteristics and the two strands have complementary sequences due to the fact that the two strands of DNA are arranged in opposite directions (5' to 3'). The bonding of each nucleotide is specific to a corresponding base to form a pair, with guanine bonding to cytosine through three hydrogen bonds and adenine bonding to thymine with 2 hydrogen bonds (Turner et al., 2005).

2.3.1. Non Coding DNA

DNA is typically divided into two categories; non coding DNA forms regions known as 'Introns' and 'Intergenic Regions', while coding DNA forms regions known as 'exons'. Both introns and exons are found within a gene, but the introns are spliced out during the production of mRNA and do not contribute to the coding of a protein (Alberts et al, 2007). By comparison, intergenic regions are the sequences of DNA located between genes (Tropp, 2012). It is estimated by Kinra (2006) that more than 90% of human DNA is non-coding, with repetitive sequences of nucleotides seen in 20-30% of introns.

2.3.2. The Polymerase Chain Reaction

The Polymerase Chain Reaction (PCR) was first developed in 1983 by Kary Mullis and follows the principle that two short oligonucleotide primers that were complementary to the targeted DNA strand could amplify the region between them. This could be repeated multiple times to add the product of one repeat of the PCR process to the target pool of the next, thereby exponentially increasing the amount of product DNA that is formed (Bartlett and Stirling, 2003).

The PCR process begins with a single strand of unamplified DNA that contains the target region desired by the researcher. This DNA is then denatured using a high temperature, typically 95°C, which separates it into two individual strands. Complementary primers then bind to sequences of DNA that surround the targeted region at a temperature specific to the primers, typically 40-60°C. Taq Polymerase, a thermostable DNA polymerase from the bacterium *Thermus aquaticus* (Saiki et al, 1988) then extends these primers by adding free nucleotides to the growing chain at a temperature of 70-74°C. Once completed, the cycle begins anew by returning to 95°C for denaturation (Promega, 2011).

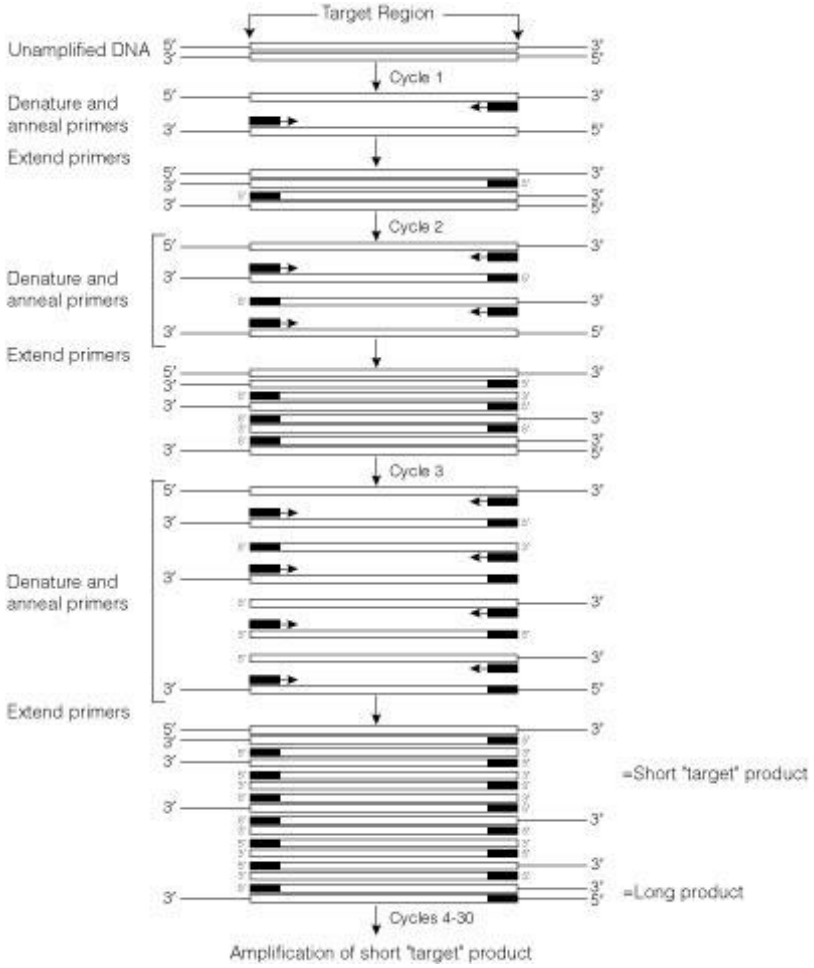

Fig 4 (previous page): The process of PCR, showing the exponential increase in target products formed through multiple cycles. Reproduced from Promega, at http://www.promega.co.uk/resources/product-guides-and-selectors/protocols-and-applications-guide/pcr-amplification/

2.3.3. Nuclear DNA Analysis in Forensics

DNA Analysis has been utilised in forensic investigations since 1986. It was originally used to exonerate a suspect in the murder of two 15 year old girls; Dawn Ashworth and Lynda Mann. It was then further used in the same case to screen a large sample of 5000 local men and was presented as evidence to convict Colin Pitchfork of murder in 1988 (BBC News, 2006).

The process of nuclear DNA analysis in forensics is known as "DNA Fingerprinting. In the UK this revolves around the use of the SGM Plus system developed by Applied Biosystems, which uses a multiplex PCR to amplify ten genetic markers (loci) in addition to a locus on the Amelogenin gene. These loci are all short tandem repeat markers (STRs), which are repeated sequences of 2-6 bases of DNA typically located in non-coding regions of DNA (Turnpenny & Ellard, 2011). Each genetic marker will have a pair of numbers indicating how many repeats of that STR are present in the locus, known as an allele. These numbers are in pairs as one allele is inherited from each parent and if the alleles inherited are the same number of repeats in length, then only a single number is given.

When all of the 10 loci are examined in one individual, a genetic profile is formed. Applied Biosystems estimate that with a full profile, the probability of two random individuals having matching genetic profiles is approximately 1 in 1.3×10^{13} in African American populations and 1 in 3.3×10^{12} in Caucasian populations (Applied Biosystems, 2012). However, the Crown Prosecution Service typically uses a conservative figure of 1 in 1×10^{9} for a chance match (Crown Prosecution Service, 2011).

2.3.3.1. The Amelogenin Gene

The amelogenin gene is a single copy gene that codes for proteins used in the development of tooth enamel (National Library of Medicine, 2011), and is located on the X and Y chromosomes at Xp22.1-Xp22.3 and Yp 11.2 (Nakahori et al, 1991). These two forms are known as AMELX and AMELY respectively. Sullivan et al (1993) states that a 6bp deletion exists in the DNA sequence within intron 1 of the AMELX homologue. This allows for a PCR reaction to amplify this region in a sample to give PCR products of 106bp and 112bp in the X and Y chromosomes respectively. When separated via gel electrophoresis, this allows the forensic scientist to distinguish between male (XY) samples that show two bands at 106bp and 112bp lengths and female samples that show a single band at 106bp indicative of a female (XX) genotype.

However, the amelogenin sex determinations provided using this method are not 100% accurate. In rare cases, there can be deletions in the AMELY gene that can cause a dropout of the Y allele. In 2006, Kashyap et al investigated the failure rate amongst the Indian population, as this population has been previously reported as showing a high rate of failure of up to 1.85% in the amelogenin sex test (Thangaraj et al, 2002). Kashyap utilised a large sample of 4257 known Indian males and reported a failure rate of 0.23%, indicating that caution should be taken when analysing amelogenin within Indian and other asian populations.

2.3.4. Mitochondrial DNA Analysis

The mitochondria are organelles present within almost all eukaryotic cells and produce ATP through the process of respiration. Mitochondria also contain DNA (known as mtDNA) that is a separate entity to the nuclear DNA present in the cell. The mtDNA present in humans is a circular genome of 16569 base pairs that is inherited through the maternal line (Baker et al, 2001). mtDNA is valuable in forensic investigations as there are much higher copy numbers present in the cell. Miller et al identified in 2003 that the copy number of mtDNA per nuclear genome in skeletal muscle was 3650 ± 620 and this high copy number means that it is much more likely that an intact sequence will survive in a crime scene sample to allow for later analysis by the forensic investigators, compared to the single copy of nuclear DNA.

2.3.5. Nuclear DNA vs. Mitochondrial DNA

The disadvantage of using mitochondrial DNA in forensic investigation is that mtDNA is not unique to an individual, instead appearing within family groups due to its inheritance down the maternal line. This is due to the fact that the mitochondria present in the sperm cells are lost during fertilisation (Sutovsky et al, 1999), so only the maternal mitochondria are passed on to the child. While this maternal lineage does have use in forensics in the identification of a suspect or missing person from familial samples, it has to be used alongside other evidence to truly identify an individual, such as in the Romanov case. In the direct relation to this experimentation, while mtDNA may be easier to recover from the neonatal samples, there are no genetic markers for human sex identification present in the mitochondria, so nuclear DNA must be used.

2.4. Degradation of DNA

DNA is a fairly unstable molecule and accumulates damage over time in any decaying specimen, even those which appear well preserved. Pääbo (1989) examined dry soft tissue remains from animal specimens aged 4-13,000 years old. The DNA recovered was fragmented into low molecular weight sections and had substantial chemical damage, including inter-strand cross links, deamination products and modified pyrimidines. The

damage that DNA receives can be explained through a number of different sources which all combine to cause substantial damage over time.

2.4.1. Temperature

The temperature in which the remains exist is arguably the most important factor to the amount of damage that DNA will receive. Lindahl and Nyberg calculated in 1972 that the activation enthalpy for the loss of purine bases was 31.2kcal/mol, which equates to approximately 0.5 purine bases every 40 minutes at 37°C. A linear correlation between base loss and temperature was established over a wide range of temperatures, which Lindahl used to demonstrate that it is implausible for a "threshold temperature" to exist as a cut off point, below which depurination of DNA would not occur. Lindahl further estimated in his 1993 work that up to 5000 depurinations would occur every day in a typical human cell. While these would usually be repaired via the base excision repair pathway that repairs damaged DNA in a living cell (Liu et al, 2007), this repair does not occur after death and the damage slowly builds up. Mitchell et al (2005) calculated a 1000-fold decrease between depurination rates at 37°C and 0°C, with a further 350,000-fold decrease as temperature drops from 0°C to -50°C, indicating the huge impact that temperature has on purine base damage. When these purine bases are lost, the new aldehyde form of the deoxyribose sugar can then be cleaved by β-elimination leaving degraded sugar residues and DNA fragments with 3' and 5' ends. The average lifespan of an unrepaired site that has lost a purine or pyrimidine base before this cleaving occurs is 10 hours at 37°C (Shapiro, in Seeberg & Kleppe, 1981).

DNA bases are also susceptible to hydrolytic deamination which also has an increase in activity under increased temperatures. Mitchell et al (2005) states that the double stranded structure of DNA does provide substantial protection against hydrolytic deamination, cytosine bases are deaminated at 0.5-0.7% the rate of depurination. At 0°C, this rate of deamination is estimated to be 0.1-0.2 events per million bases each year. These deaminations cause cytosine to be replaced with uracil, which is then read as thymine during PCR and results in a C→T change in the final sequence (Molak et al, 2011). While this does not cause a change in the length of PCR products obtained, a C→T change in a primer binding site may cause primers to bind incorrectly and causes allelic drop out. Briggs et al (2007) also found a high frequency of C→T misincorporations at the 5' ends of aDNA strands, with a complementary high frequency of G→A misincorporations at 3' ends. This may indicate that cytosine may be more susceptible to deamination at the ends of DNA molecules. In combination with the DNA cleavage caused by β-elimination of depurinated bases, this may lead to increased rates of deamination in ancient DNA.

2.4.2. Time

While it can be seen that DNA degradation is very slow at <0°C temperatures, over time the damage will accumulate to form significant DNA degradation. Abyzov et al (2004) has done substantial research into the microbiological fauna present in ancient Antarctic ice, examining strains of *Pseudomonas* and Actinomycete bacteria. Abyzov determined the number of viable microbial cells in various ice core depths. As the core depth increases, the age of the sample increases due to the slow accumulation of glacial ice. Abyzov also discovered a decrease in the number of viable bacteria as the depth and age of the core sample increased. Mitchell et al (2005) theorised that this inverse correlation reflects the accumulation of endogenous DNA damage that the glacial bacteria have developed over time.

The age of the specimen is largely important in connection with the environmental temperature of burial. Smith et al (2001) developed the concept of "thermal age", which determines the 'age' of a sample when standardised to a temperature of 10°C. Thermal Age is therefore defined as the time after which, if it had been deposited at 10°C, the sample would show equivalent levels of DNA degradation. Smith theorised that the amount of DNA damage present in an ancient sample is more likely to be correlated with thermal age than with actual chronological age. However, thermal age only considers damage done by depurination and does not include other forms of damage such as cross-links and deamination driven miscoding, so the actual damage levels may be higher. The equations used to determine thermal age can be found in Appendix 9.1.

2.4.3. Chemical

There are a number of environmental toxins that can cause damage to DNA. For example, methylene chloride (dichloromethane) is used as a solvent in industrial processes and insecticide. When released into the environment, methylene chloride undergoes slow biodegradation in soils, while being highly mobile in leaching groundwater (World Health Organisation, 2003). The WHO states that dichloromethane has been found at concentrations up to 743µg/L in surface water, with higher concentrations of up to 3600µg/L in groundwater. Graves et al (1995) examined the potential damage from dichloromethane and determined that it will cause single stranded breaks in DNA as well as potentially being broken down into formaldehyde which can cause DNA-protein cross links (World Health Organisation, 2000).

Environmental free radicals are also a threat to the survival of DNA in an exposed sample over a long period of time. Carbon tetrachloride is used as an industrial solvent and has been used in the past as a refrigerant. When released into the environment it is extremely stable in the atmosphere with a lifespan of 25-100 years, while in soil, carbon tetrachloride will rapidly be broken down by biotic degradation pathways in both aerobic and anaerobic

conditions (World Health Organisation, 1999). As carbon tetrachloride is broken down, it forms the $\cdot CCl_3$ (trichloromethyl) radical which can then covalently bond to DNA (Thomas & Aust, 1986). Thomas & Aust also states that trichloromethyl and other environmental free radicals which are oxidized by O_2 molecules produce superoxide ($O_2\cdot$) which can then be converted to other oxygen radicals such as the hydroxyl radical ($\cdot OH$), which is capable of cleaving DNA.

2.4.4. Burial Environment

The burial environment in which a skeletal sample is deposited can have a substantial impact on the survival of both the morphological features of the bone and the DNA contained within. Acidic soils such as peat bogs, fens and other wetlands (Gorham, 1957) are characterised by an abundance of H^+ and Al^{3+} ions in the soil which can be caused by a number of environmental factors, such as high rainfall leaching base cations from the soil, or ammonium fertilizers undergoing nitrification and releasing H+ ions (Sparks, 2003). These acidic soil conditions can increase the rate of DNA depurination due to the acid catalysis of the hydrolytic reaction of depurination (Gates, 2009).

Soils can also result in damage to the physical structure of the bone. Chhem & Brothwell (2007) state that burial in chalk can lead to a deeply etched bone surface, while Quigley (2001) describes post chalk-burial bones as “eroded and friable”. Manifold (2013) examined burials in various soil conditions and found a significantly higher percentage of remains showing 75-100% cortical surface erosion in chalk burials than in neutral, alkaline or waterlogged soils. While this can occur, alkaline soils may still contain well preserved remains; Nicholson (1996) found that acidic moorland (pH 3.5-4.5) was the most destructive soil type for bone, while chalk soils (pH 7.5-8.9) were much more favourable for preservation. However, some remains showing excellent preservation have been recovered from peat bogs, such as the “Tollund Man” which still retain soft tissues due to the minimal microbial activity found in the acidic and anaerobic bog environment. Unfortunately, while the physical remains are very well preserved, the bog conditions destroy any DNA present in the remains, preventing genetic analysis (McGrath, 2013)

2.4.5. Microbial Activity

Microbial activity in skeletal remains has strong links to burial environment and other taphonomical factors. Jans et al (2004) state that microbial damage is an important factor in bone deterioration and that both bacterial and fungal attack can occur. Bacterial damage is typically found in complete burials and is therefore likely to be linked to the early stages of putrefaction. Turner-Walker (in Pinhasi & Mays, 2007) states that the autolysis process that breaks down a recently dead organism creates an anaerobic environment that benefits both the bacteria released during gut decomposition and those naturally occurring in the soil, which may explain this link. Jans further states that fungal damage and fungal enzyme

release can occur in well preserved bone at any time during burial, excavation and storage, providing that environmental conditions are correct for the growth of saprophytic fungi.

Wisshak & Tapanila (2008) identifies the different types of damage caused by microorganisms as six different types of tunnelling in bone. Wedl Type 1, Wedl Type 2 and Hackett tunnelling form empty tunnels of 10-15µm, 5µm and 50-250µm respectively and are caused by fungi and cyanobacteria. Linear Longitudinal, Budded and Lamellate tunnelling is characterised by spongiform bone-filled tunnels of 5-10µm, 30-60µm and 10µm respectively. In all cases, this destruction of bone tissue will damage morphological features as well as reducing the levels of bone tissue that can be used for DNA recovery.

2.5. Inhibition

Inhibitors are substances which are co-extracted from a sample in the DNA extraction process, which then interact in the PCR process to prevent PCR amplification. Eckhart et al (2000) suggests that this can be due to the inhibitor binding to DNA polymerase, while Opel et al (2009) suggest that the inhibitor may also bind directly to the DNA or interact with the polymerase during primer extension. The inhibitors typically found in samples extracted from buried remains come from two areas; those present in the soil and those present in the body itself.

2.5.1. Inhibitors in the Soil

Humic compounds (humic and fulvic acids) make up a major component of soil (Robe, 2003) and inhibit PCR. Robe further states that humic acids bond to amides in biological molecules to denature them, or oxidise to form quinines which then bond covalently to DNA molecules. Opel et al (2009) states that skeletal remains commonly contain humic acid inhibitors and that the most common method of inhibition via humic acid is due to them binding specifically to DNA to limit the amount of template available for PCR, a problem that is compounded in ancient DNA studies where the amount of template DNA is already low. Matheson et al (2010) examined both humic and fulvic acids and determined that humic acids are much more of a problem in PCR inhibition than fulvic acids. However, Matheson raises the issue that the inhibitory effects of humic compounds in PCRs vary to a wide degree. Yankson & Steck (2009) also discuss the difficulties of soil bound inhibitors in DNA extractions, describing humic acids as “recalcitrant” in nature and identifying humic substance-containing clay as the most difficult soil environment to recover DNA samples from.

Tannic Acid is another inhibitor which may be found in soil samples, due to its presence in certain types of plant material such as leaves. Samples exposed to leaf litter or soils formed

by decomposition of leaf litter may show inhibition due to the Tannic acid inhibiting Taq polymerase and reducing the availability of the template DNA (Opel et al, 2009).

2.5.2. Inhibitors in the Body

The human body releases a number of PCR inhibitors during the process of putrefaction. Firstly, in skeletal remains, the calcium that makes up a majority of the inorganic part of bone can act as an inhibitor. Opel et al (2009) established that calcium acts as a Taq inhibitor, competing with magnesium to reduce the reaction efficiency of the PCR and therefore reduce the total product amount. Collagen, the organic component of bone and connective tissue may also act as a PCR inhibitor. Opel states that while collagen does bind to DNA in a similar way to humic acid, additional Taq polymerase and magnesium will not improve the amplification of the sample, which would indicate that the binding of collagen to DNA affects the ability of the Taq polymerase to catalyze consecutive nucleotide additions and form a full replicated sequence during the PCR process.

The soft tissues of the body can also contain inhibitors released during decomposition. Melanin is a pigment found in hair and skin tissues, which inhibits PCR through two main routes. Opel et al (2009) states that melanin acts like humic acid and binds to specific sequences in DNA to limit the amount of template available for replication. Eckhart et al (2000) states that melanin preferentially forms a complex with Taq Polymerase which inhibits its efficiency. Haematin is another potential inhibitor found in the soft tissues and is present in red blood cells. Opel suggests that haematin acts as a Taq inhibitor to reduce PCR efficiency and noted a reduction in the amount of final product in all amplicons that they tested.

2.6. Contamination

The possibility of contamination in human DNA investigation has always been of concern, especially in forensic cases. DNA is present in almost every cell in the human body and as such is shed with our skin cells to objects that we touch in our everyday lives. Primary transfer of DNA from an individual to an object is used in forensic cases to indicate that a person must have been present at a crime scene. For example, Geddes (2012) utilises the UK murder case of Steven Lawrence in 1993 to demonstrate that trace blood and hair evidence found on a suspects clothes were analysed and used to imply that the suspect was present during the crime. Primary DNA transfer between an analyst and the experimental samples must be minimised in order to prevent the analyst's DNA from amplifying and presenting themselves in PCR products taken from the experimental samples.

However, secondary transfer can also be an issue. Goray et al (2012) used the proposed events from a murder case to demonstrate the possibility of an object contaminated with an individual's DNA then coming into contact with a second object and transferring the DNA. This would allow for DNA from an individual to be found on an object that they had never

been in contact with and possibly lead to a false conclusion that they were present at a crime scene. It was shown that an individual that handled an object such as a child's toy or article of clothing could be identified from DNA transferred when that toy or article of clothing came in contact with another object, with no direct contact between the individual and the final object. In research involving the chain of custody with human DNA samples under study, care must be taken that the tools, workspace and reagents used are not contaminated with DNA that can then be secondarily transferred to the sample. In forensic cases, a recent example of this is in the Amanda Knox trial (Hogenboom, 2014), in which a knife was recovered that had traces of the victim's DNA on the blade. However, no blood or other bodily fluids were found on the knife and the defence argued that the minute traces of DNA may therefore have been post-PCR laboratory contamination.

2.6.1. Control of Contamination

Due to the issues which arise when contamination occurs, it is vital to control contamination as much as possible. Ideally, contamination could be completely eliminated. However, even under the strictest containment situations, contamination is still a major and relatively uncontrollable hazard (Deguilloux et al, 2011). While it is impossible to guarantee complete removal of any contaminating DNA traces, there are many possible methods that can be used to drastically reduce the chance and level of contamination in an ancient DNA amplicon.

2.6.1.1. Sample Contamination

One of the avenues for contamination is that DNA from the archaeologists excavating the skeletal remains can be transferred to the surface of the remains themselves, through direct contact or sample washing (Gilbert et al, 2005). Gilbert suggests that it is crucial to have knowledge of the history of the sample handling prior to the analysis by the investigator, as the excavation of the remains may not have been under controlled DNA-free conditions and the samples may have been handled by other archaeologists, anthropologists or research personnel before the study in question has taken place. To reduce the level of contamination coming from the sample itself, Bouwman et al (2006) suggests that the outer 1-2mm of surface bone should be removed from the sample with a sterile scalpel. Chilvers et al (2008) further decontaminate the sample using UV irradiation at 254nm for 5 minutes on each bone surface to destroy any remaining DNA on the bone surface. While this technique does destroy any aDNA remaining in the surface layer of bone along with the modern contaminant DNA, the aim is to drastically reduce the ratio of modern contaminant:ancient DNA, retaining the aDNA remaining in the inner cortical bone and trabecular bone. However, Sampietro et al (2006) suggests that contaminant DNA on the surface of the bone can permeate deeply into the bone if it is washed before analysis. Due

to the bone becoming more porous as the organic portion degrades, water-borne DNA such as skin cells in sweat or the washing water can penetrate deeply into the body of the bone.

Daskalaki et al (2011) treated their sample bone with 0.05% hypochlorite bleach in addition to UV irradiating and removing the outer surfaces with a drill. Malmström et al (2007) states that this process, with the inclusion of the bleach decontamination, removes >99% of contaminant DNA from the sample, yet also reduces the amount of authentic DNA by 77%, which is identified as a potential cause of allelic dropout with low concentrations of aDNA. However, the difference in fragment sizes between the small aDNA and larger contaminating modern DNA is retained and this can be used to identify remaining contamination.

2.6.1.2. Laboratory Contamination

Laboratory contamination can come from three potential sources. Firstly, there is the possibility of contamination from the laboratory itself, with contaminant DNA on the instruments and work surfaces. Secondly, contamination may come from the reagents used in the process of DNA extraction and PCR amplification. Finally, contamination may come from previous amplifications of the same species analysed in the same laboratory.

To reduce the contamination coming from the laboratory equipment and previous amplifications, many dedicated ancient DNA laboratories such as those at the University of Bordeaux, France (Deguilloux et al, 2011) and the Australian Centre for Ancient DNA (Adler et al, 2011) have physically isolated laboratories for pre-PCR aDNA work, separate from the post-PCR laboratories in order to prevent high copy number aDNA from contaminating fresh aDNA samples. Both of these laboratories have high pressure systems with filtered incoming air, overnight 30-50nm UV irradiation of the entire rooms and tools, laminar flow hoods, bleach, decon and isopropanol cleaning of all surfaces and bleaching and UV irradiation of tools and instruments (both before they first enter the lab and then routinely before, during and after their use). Laboratory personnel are protected through the use of freshly laundered clothing, full body suits, shoe covers, boots, face masks, face shields and triple-gloving with latex or nitrile gloves to reduce the potential for contamination from their DNA and are not allowed to move from the post-PCR laboratory to the aDNA laboratory within a single day.

Reagent contamination is minimised almost entirely through the use of high quality DNA-Free reagents. Care is taken not to use pipette tips more than once, or expose potential contaminant sources to stock solutions of reagents. However, Deguilloux et al (2011) identifies that even when DNA free reagents are used and all precautions taken to minimise DNA contamination, contaminants can still arise during genetic analysis. Using DNA-Free reagents in a highly controlled dedicated aDNA lab, contaminated samples were still detected throughout analyses performed. These contaminant sequences formed at least

44.3% of PCR products, with a further 11% of PCR products being ambiguous potential contaminant sequences. Negative controls contained PCR products in 31.2% of analyses and contained 16 different contaminant sequences, none of which matched DNA sequences from the researchers involved in the experimentation. Deguilloux hypothesises that these may have been due to contamination in the primers or PCR reagents, with almost 20% of the contaminant sequences analysed associated with one specific primer lot. Reagents can therefore not necessarily be trusted to be "DNA-Free", especially Primers, as primers cannot be treated with DNAase like other reagents and all reagents are handled during manufacture. Deguilloux states that an absolutely contaminant free environment and analysis is unobtainable in reality, even when the strictest controls are in place during all stages of the analysis, from excavation to sequencing.

2.6.1.3. Authentication Criteria

The famous and well used criteria of authenticity were developed by Poinar in 2003 and comprise of 10 key things which should be utilised to prove an authentic ancient DNA result. Firstly, the ancient DNA work must be carried out in a physically isolated laboratory which is dedicated to ancient DNA or low copy number DNA samples. Post-PCR analysis should be carried out in a separate location. Secondly, PCR control amplifications should be carried out regularly containing the pre-PCR reagents used but no template DNA in order to detect random low-copy number contamination. Positive PCR controls should generally be avoided to reduce risk of contamination.

The behaviour of the amplicons should also be examined. Amplicons larger than 1000bp in size should not appear, due to the hydrolytic cleavage that takes place during degradation over time, as in aDNA. As a general rule, amplification strength of the PCR product should be inversely related to the size of the product, providing that the primers used are equal in sensitivity.

The copy number of DNA should be analysed using quantitative real time PCR (qPCR) or through the use of competitive PCR assay. It may be impossible to exclude sporadic contamination in low copy number analyses, and it is noted that contamination levels in ancient human DNA vary drastically both in samples and reagents.

The results obtained should be reproducible from different DNA extracts of the same specimen, but also the same DNA extract used in the original analysis. PCR products should also be verified via cloning of the amplicons and sequencing of a minimum of 10 clones in order to determine the ratio of endogenous:contaminant sequences and any errors caused by DNA damage.

Further reproduction of results should be undertaken in an independent laboratory. Full DNA extraction, amplification and sequencing should be carried out by different scientists in

an independent lab, from the same specimens. This is especially vital in human aDNA analyses.

Biochemical preservation should also be examined, as it can be useful as corroborating evidence for the survival chances of ancient DNA in a specimen. The total amount of organic solids, composition and condition of the specimens can all be useful as markers to indicate survival of DNA.

Any associated remains such as animal remains should be analysed for aDNA, especially alongside human studies. The survival of DNA in faunal material is a good indicator for survival in the human remains and can be used as negative controls for human PCR amplifications in order to provide evidence for contamination.

Finally, any sequences determined from the amplicons should be able to be placed into a phylogenetic tree with other haplotypes in order to ensure that they are authentic.

While these 10 criteria do provide an excellent foundation to ensure that work carried out with ancient DNA is completed to a very high standard, there are some arguments against the use of these criteria. Gilbert et al (2005) instead suggests that researchers take a self-critical approach to authentication, rather than strictly following guidelines which may not make sense in their specific case. Gilbert states that the age and preservation conditions of the specimens under study, the time elapsed since excavation and recovery, and the thermal history of the site are the most important factors that allow a researcher to evaluate whether it is possible for DNA to survive to be recovered.

Gilbert suggests that the 10 criteria put forward in Poinar (2003) were never intended to be a checklist that must be followed to the letter in order to guarantee authenticity of aDNA results, and yet in practice they are used as such. Gilbert observes that several aDNA studies only follow a few of the guidelines in their research, which would imply that those not followed must prove the data unreliable and are therefore omitted by choice by the researchers. However, it is also possible that researchers view the usage of all of the criteria as a waste of time, as the problems raised in different studies are all dependent on the types of samples used and the DNA that is trying to be recovered. For example, contamination is going to be much more of an issue when dealing with the amelogenin gene of ancient human remains than it is when dealing with the DNA of well-studied extinct species.

Deguilloux et al (2011) individually invalidates the criteria put forth in Poinar's research, highlighting the issues that researchers face when trying to determine authenticity. With samples that are contaminated during excavation or storage, replication of results may not detect the contaminants since they will all yield the exogenous DNA. If this contamination has taken place during excavation, then carrying out this replication of results in an independent laboratory will still not highlight this. Negative controls, while useful, cannot

rule out contamination as the contaminants may not be present in negative controls, but are detectable in the aDNA extracts themselves. Furthermore, Deguilloux highlights that the detection of low-level contaminants in PCR controls is dependent on the number of PCR cycles used and therefore can be difficult in certain situations.

The suggested use of cloning in Poinar to determine authentic sequences can cause sequences to show errors if a contaminant sequence is more prominent than an endogenous sequence in a sample.

2.7. Experimental Techniques

2.7.1. Cell Lysis

The first stage in any DNA extraction is to lyse the cells in order to access the DNA within the nucleus. This can be done in a number of ways, including chemical, mechanical and thermal lysis. Chemical lysis in forensic applications typically involves the use of a detergent such as SDS and Proteinase K in a buffer solution such as EDTA or PBS that mimics the internal chemistry of the cell in order to prevent damage to the DNA upon release. This will then be heated to 65°C to provide the optimum temperature for Proteinase K and incubated for a minimum of 4 hours (Robertson et al, 2002).

Robertson further suggests that in the case of DNA extraction from bone, the bone must be mechanically broken down due to its strong physical nature. It is suggested that the bone is broken down into small pieces before being homogenized in a blender or grinder with liquid nitrogen to make the bone more brittle and reduce heat build-up from friction.

Mechanical lysis involves breaking down the cell wall or cell membrane via physical damage. An example of this is used in Okungbowa et al (2007), via the use of an ultrasonic bath at 003 RMS for 5 minutes, in the course of ten 30-second intervals. This technique allowed for the recovery of proteins and functioning enzymes from the cells in a fast and efficient way.

Thermal lysis involves the heating of a sample in order to disrupt the proteins that form the cell membranes and cause lysis. This can be achieved via incubation of the sample at 90°C for 20 minutes. However, this technique is considered a ‘quick and dirty’ method that leaves a lot of cell debris in the sample, including salts that may inhibit enzymes used in PCR (QIAGEN, 2002) and therefore can have high failure rates and fast sample degradation post-extraction.

2.7.2. DNA Extraction Techniques

2.7.2.1. Chelex Extraction

Chelex-100 is a resin produced by Bio-Rad that acts as a chelating agent in DNA extractions. The sample is added to 5-10% Chelex-100 and then either boiled for a short period of time, such as 20 minutes (Sepp et al, 1994) or incubated at a lower temperature for a longer period of time (Hoff-Olsen, 1999) to lyse the cells. Chelex binds to metal ions and cell debris that are released during the cell lysis, but does not bind to the DNA. When centrifuged, the DNA will remain in solution while cell debris and Chelex beads will pellet at the bottom and can be removed.

Walsh et al (1991) examined the effectiveness of the Chelex extraction in comparison to phenol-chloroform extractions and found that with forensic-style bloodstain analysis, Chelex performed on par or better with phenol chloroform, removing PCR inhibitors effectively. Chelex binds to the metal ions released during lysis, including MG^{2+} ions which act as cofactors for DNAase enzymes, thus making the DNAases inactive and preventing the degradation of the DNA. However, the heating used in a Chelex extraction denatures the double-helix structure of DNA and results in less stable single-stranded DNA, which while usable for PCR, is less stable when stored and therefore should be used quickly.

2.7.2.2. Silica-based Extraction

A silica based extraction utilises silica beads or resin to chelate the DNA. The sample must first be incubated and agitated at 60°C for at least 4 hours in an extraction buffer of Guanidine Thiocyanate, typically overnight. The sample is then centrifuged and the supernatant is added to the silica suspension. The solution is then incubated at room temperature to allow for the DNA to bind to the silica, before being centrifuged into a pellet, washed in buffers and ethanol to remove cell debris and eluted into a solution for use in PCR (Höss & Pääbo, 1993)

Hoff-Olsen (1999) examined the effectiveness of silica based extractions in the recovery of DNA from degraded human tissues. Hoff-Olsen found that Silica was a reasonably expensive technique, but when utilised correctly would provide the best chance of extracting typeable DNA from decomposed human remains, only failing to recover typeable DNA in 4 of 70 STR analyses (5.7%), compared to the 22.8% fail rate found in Phenol-Chloroform extractions and the high 80% failure rate of chelex extractions.

2.7.2.3. Phenol/Chloroform/Isoamyl Alcohol Extraction

Phenol-Chloroform (PCI) extractions are a type of liquid-liquid extraction that separates the organic protein and fat molecules in a sample from the aqueous DNA. The phenol present in the mixture denatures proteins that are present in the sample, while DNA remains in a

double-stranded state within the aqueous phase. The Isoamyl alcohol is a detergent that assists in the breaking down of the cell wall or cell membrane to release the cell debris and DNA and reduces foaming when the organic and aqueous phases are mixed. The aqueous phase is often then extracted and submitted to repeated PCI extractions to further remove any contaminants. However, the process of repeated extractions involves multiple instances of centrifugation and mixing and this will damage the DNA and can cause some sample loss. An alternative method to this repeated PCI extraction technique is to use Proteinase K before submitting the sample to the extraction in order to break proteins down into smaller polypeptides that can more easily be removed by the phenol. (Brown, 2010)

Hoff-Olsen (1999) determined in their analysis of extraction techniques that phenol-chloroform provided a high yield in 90% of cases, with the remaining 10% of cases extracting a detectable yield and no instances of DNA not being detectable after extraction. PCI extractions were found to be the most expensive method of DNA extraction, but were effective in providing DNA that could be typed via gel electrophoresis, with a success rate of 77.1%.

2.7.2.4. Extraction Kits

Many companies now provide kits for DNA extraction which work utilising one of the methods listed above. An example of this is the GENECLEAN Kit for Ancient DNA from MP Biomedical, which utilises a silica extraction method to recover DNA. There are a number of potential advantages of using purchased extraction kits over preparing extractions in the experimental lab. Namely, the extraction kits are created to a very high commercially exacting standard and therefore there should be very little error in concentrations of solutions between kits, while there can be larger errors in repeatedly making up reagents in the laboratory. Also, the risk of contamination of reagents is much lower when using purchased extraction kits due to the strict DNA-Free safeguards put in place and the fact that the extraction kits are produced away from any post-PCR DNA sources, using equipment that is designated for the production of reagents and has never been used in DNA analysis.

2.7.3. Polymerase Chain Reaction

The Polymerase Chain Reaction (PCR) is a method of copying small sections of targeted DNA in many orders of magnitude, to amplify the concentration of the target DNA in a solution and allow for further analysis of the DNA even when dealing with very small amounts (low copy number DNA). By repeating the process of denaturing the DNA, annealing primers and finally extending the primers with deoxyribonucleotides (dNTPs) to form double-stranded DNA again, a single piece of DNA can be amplified up to billions of copies within the space of a few hours.

The PCR technique was first developed by Kary Mullis in 1983 and has since been widely improved and adapted to a range of applications in molecular biology, to the extent that PCR has now become the foundation of modern molecular biology techniques (Bartlett & Stirling, 2003).

2.7.3.1. Standard PCR Process

The process of PCR is a repeated thermal cycle of three steps, which can be repeated a variable number of times in order to amplify template DNA of varying copy number. As a general rule, with low copy number DNA such as that used in aDNA studies, a higher number of cycles are required in order to amplify the small sample to a useable concentration of DNA.

The first stage of PCR is the "Denaturation" stage, in which the sample is heated to 95°C to break the hydrogen bonds that hold the two strands of DNA together as its standard double-stranded helical formation.

Once the DNA has separated into two single strands, the sample is cooled to a temperature that is dependent on the choice of primer, usually between 50 and 65°C. This is the "Annealing" stage. The primers bind specifically to the DNA that they target, only in locations where the sequence of the primer very closely matches the complementary sequence of the template.

The third step is the "Extension" stage, in which free dNTPs are added to the primer in a 5' to 3' direction by a DNA polymerase. The choice of polymerase dictates the temperature used in the extension stage, with Taq polymerase typically requiring a temperature of 72°C.

This process is then repeated, with each cycle doubling the number of DNA strands in the solution. However, a typical PCR begins with a preliminary initialisation step in which the reaction is heated to 95°C for up to 10 minutes in order to activate thermally triggered DNA polymerases and begin DNA denaturation. A PCR is concluded with an extended version of the "Extension" stage, for 5-15 minutes, to ensure that any single stranded DNA remaining in solution is fully extended into double-stranded DNA.

Due to the exponential amplification of DNA, the post-PCR solution of is of a very high concentration and can then be used in further work (See Fig 5). The solution is stable and can be stored at -20°C for several weeks.

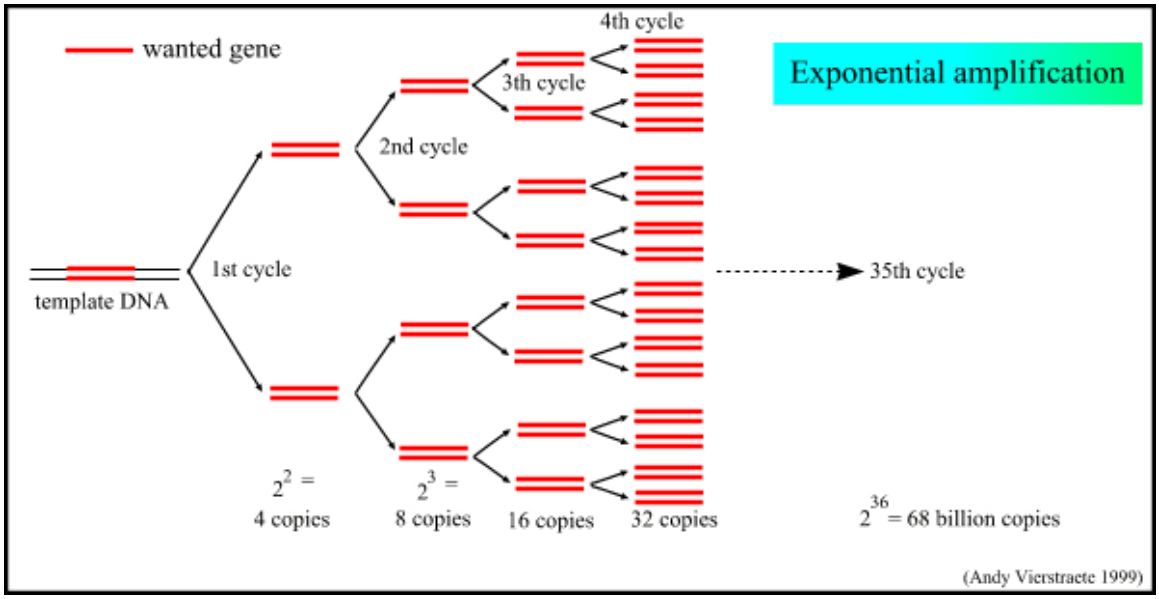

Fig 5: The exponential amplification of a target sequence of DNA via PCR.

2.7.3.2. Real-Time PCR

Real-Time PCR (RT-PCR) is defined by Shipley, in Dorak (2007) as "the continuous collection of fluorescent signals from one or more polymerase chain reactions over a range of cycles". The RT-PCR machine is both a fluoroscope and thermal cycler and the addition of fluorescent reporter probes allows the RT-PCR machine to detect the concentration of the targeted DNA sequence in solution at the end of each cycle. This provides a graph of the increasing DNA concentration over time, allowing the researcher to determine the concentration of DNA in the original sample through the use of regression. Popping et al (2010) states that current detection platforms using RT-PCR can detect less than 10pg of DNA in a sample.

Typically, fluorescent reporter probes will be oligonucleotides with two fluorescent reporters, which are specific for the target DNA sequence. One fluorescent reporter will be a fluorescent dye, on the 3' end of the oligonucleotide, while the other is a fluorescence quencher on the 5' end. During the annealing stage of PCR, the reporter probe will hybridise with the target DNA and will be extended much like a normal primer. The Taq polymerase will release the fluorescent dye during the extension phase and the strength of the fluorescence will increase, as the quencher no longer functions. The change in fluorescence is proportional to the increase in the concentration of the PCR product in real time (Popping et al, 2010).

Real Time PCR has become a widely used technique in ancient DNA analysis and is considered a very important technique for determining the authenticity of results since its inclusion in Poinar's criteria of authenticity (2003).

2.7.3.3. "Touchdown" PCR

One of the issues that are faced when creating a PCR protocol is the choice of annealing temperature. Primer hybridisation with DNA is correlated to temperature in that at higher temperatures than the optimum, the specificity of the binding is increased, yet yield of the specific product is decreased. At lower temperatures than the optimum, yield improves but the specificity is reduced and can lead to non-specific binding and amplification of unwanted DNA (Hecker & Roux, 1996).

Touchdown PCR (TD-PCR) takes a different approach to standard PCR in that the annealing temperature varies through the cycles of the PCR. The initial annealing temperature in the first two cycles is higher than the melting temperature of the primers and will therefore prevent amplification from occurring. However, in each following pair of cycles, the annealing temperature is run at 1°C less than the previous cycles. When the melting temperature of the primers is reached, annealing begins with a very high degree of specificity, but low yield. As the PCR continues, the yield increases but specificity drops as the annealing temperature decreases further. By the point where non-specific binding would usually occur, there will theoretically be such a high concentration of the target product that it will outcompete non-specific binding to yield a single, targeted, amplicon. In practice, Hecker & Roux found that TD-PCR improves both specificity and maximum yield, compared to standard PCR in which one must usually be sacrificed.

2.7.3.4. Primers

Primers are oligonucleotides - short strands of nucleic acid that are typically between 18-22 bases long. They will bind to complimentary sequences present in single stranded DNA and are used in pairs of forward and reverse primers to bracket a section of DNA which is then amplified by DNA polymerase.

In the development of PCR protocols, primer choice is very important. The target sequence must be framed by the two primers, which limits the actual sequence of the primers, so the size, structure and location of the primers are the variables that must be considered for good primer design.

In ancient DNA work, careful choice of primers can have a large effect on the production of detectable PCR products. Due to the random degradation of DNA over time, the recovery of large amplicons is difficult. An inverse relationship between amplicon length and efficiency of amplification is standard of aDNA results (Alonso et al, 2004) and is even required for authentication of ancient DNA following the criteria set by Poinar (2003). Ancient DNA is known to be highly fragmented, typically only occurring in sizes less than 500bp in length (Willerslev & Cooper, 2005). As such, primers that amplify smaller fragments are favoured in aDNA analysis.

An example of this is found in Arnay-de-la-Rosa et al (2007), in which primers amplifying very small fragments of intron 1 in the amelogenin gene, 66bp and 72bp in length, were used to genetically determine sex from prehispanic remains from burials approximately 1213-1410 years BP.

2.8. Aims of the Current Investigation

The aim of this research is to recover viable aDNA from neonatal skeletal remains and determine the sex of the individuals. Multiple techniques to remove inhibitors from the samples are to be tested in order to identify the inhibitors present and determine how best to combat them. The level of DNA degradation will be tested via comparison to artificially degraded modern DNA. The possibility that DNA recovery probability is linked to the biological age and size of the individuals at time of death will be assessed. In determining the sex of the neonatal individuals, an attempt can be made to assess the possibility of infanticide. Infanticide was common throughout the ancient world, including the Roman Empire, and may be expected in this collection of remains due to the density of neonatal burials of a similar age.

3. Chapter Three: Materials & Methods

3.0. Sampling

The remains are a collection of Romano-British neonatal skeletons from the 1st-4th Century AD, recovered from a 8436m^2 area of farmland in Rudstone Dale, Newbald in 2005. The geology of the burial site consisted of a base layer of grey chalk brash, overlain with up to 0.5m of alluvial layers deposited by a flooded palaeochannel that ran through the site. Up to 0.8m of silty colluvium then lay upon this layer, washed down from a north-eastern slope. Finally, the top soil consisted of dark brown silty clay up to 0.4m deep. The skeletal remains were buried within the floor plan of houses, or within the garden or yard area associated with a house. These burials were separate, rather than a singular mass grave. (Network Archaeology Ltd., 2005)

The remains were recovered in a standard archaeological excavation, with no additional precautions to prevent DNA contamination. Due to the excavation occurring several years before this project, this excavation practice could not be controlled with the future DNA work in mind. The remains were stored individually in sealed plastic bags, within cardboard boxes and were in darkened conditions at room temperature since excavation. The skeletal material had previously been cleaned and catalogued before analysis began.

All of the neonates are between the age of 20 prenatal weeks and 40 prenatal weeks. Therefore, the remains are likely to have been from miscarriages, stillbirths, or infant mortality. However, the possibility of foul play in the deaths of the remains is not excluded.

The remains were sampled in a physically separate room to any DNA or Post-PCR analyses. The researcher wore a full “Howie” style lab coat, with two pairs of nitrile gloves. Firstly, the mass of the total skeletal material for each individual was recorded. Following this, the petrous portion of the temporal bone was identified from the mixed skeletal remains of each individual, before being measured. These measurements allow for the metric age determination of the remains. The petrous portion was then placed within a sealed plastic bag and stored at room temperature.

3.1. Sample Preparation & Decontamination

The skeletal remains were prepared in the same physically separate room in which sampling took place. Benches and equipment were UV irradiated overnight, then repeatedly between uses for 10 mins. All work surfaces and instruments were also cleaned thoroughly with 20% Sodium Hypochlorite and 100% ethanol. Microcentrifuge tubes and pipette tips autoclaved at 121°C for 20 minutes, then UV treated overnight.

The samples were decontaminated following a modified procedure from Adler et al (2011). The bone samples were exposed to UV radiation for 20 mins, before being wiped with 5%

w/v sodium hypochlorite. The outer 2mm surface layer of bone was removed via scraping with a sterile scalpel, decontaminated with work instruments as above.

The decontaminated bone was pulverised in liquid nitrogen using a SPEX SamplePrep 67770 Freezer Mill, using a modified version of the manufacturer's methodology, in that a 5 minute cooling step was used rather than a 10 minute cooling step, due to sufficient pulverisation with the faster time.

3.1.1. Method Development

Initial sampling was achieved using a sterilised dremel with a circular saw bit. However, it was noted that even on the lowest speed setting, the bone would be charred on the cut edges and would glow orange-hot during cutting due to the friction generated. Adler et al (2011) found that high temperatures caused by high speed drilling or cutting significantly reduced the levels of recoverable DNA, with pulverised samples yielding 5-30 times more mtDNA than samples drilled at 1000rpm. Due to concerns about the loss of recoverable DNA caused by these temperature spikes, the decision was made to physically break the neonatal bones using the hands rather than high speed cutting.

The thin and fragile bone of the neonatal petrous portion was placed within a UV sterilised plastic bag and was easily crushed into smaller pieces using the hands. This allowed for the crushed bone to fit within the liquid nitrogen freezer mill without causing temperature spikes.

3.2. Silica Extraction

Initial experimentation began with decalcification of the skeletal remains following the method proposed by Deguilloux et al (2011). The powdered skeletal material was heated to 55°C overnight with agitation, in a solution of 0.5M EDTA at pH8.5, 1-2mg/ml Proteinase K and 0.5% sodium lauroyl sarcosinate.

Following this, the silica extraction technique from Hoff-Olsen's (1999) experimentation was implemented. A silica suspension was formed by dissolving 60g of silica in 500ml PCR-grade water. This was left for 24 hours at room temperature; 430ml of supernatant was removed and replaced with 430ml clean PCR-grade water. This second solution was incubated at room temperature for a further 5 hours. 440ml supernatant was removed and 600µl of concentrated hydrochloric acid was added.

The skeletal material was incubated overnight at 60°C with gentle mixing, in a 2ml solution of extraction buffer. The extraction buffer was constituted of 10M Guanidine Thiocyanate, 0.1M Tris-HCl at pH6.4, 0.2M EDTA at pH8.0 and 1.3% Triton-X. This is made up in small volumes by dissolving 0.26g of Triton X in a mixture of 60ml 0.1M Tris-HCl at pH6.4 and

22ml 0.2M EDTA at pH8.0, then adding 72g of Guanidine Thiocyanate followed by continuous stirring overnight in the dark to dissolve.

Following incubation, this extraction buffer was centrifuged at 6000rpm for 5 minutes. 600µl of supernatant was removed and added to a further 400µl of fresh extraction buffer (as above) and 40µl silica suspension (as described above). The solution was incubated at room temperature for 30 minutes for DNA to bind to the silica and then centrifuged at maximum speed for 3 minutes.

The supernatant was removed and stored in 10M sodium hydroxide to avoid the formation of hazardous by-products. The remaining silica pellet was washed twice in 750µl of pH 6.4 washing buffer, containing 10M guanidine thiocyanate and 0.1M Tris-HCl. Following this, it was washed a further two times in 750µl of 70% ethanol and once in 750µl acetone. The pellet was dried at 56°C before the DNA was finally submerged twice in a 65µl TE elution solution, each time for 10 minutes at 56°C.

3.2.1. Method Development

The original silica based extraction was changed to utilise a purchased extraction kit, in an effort to reduce potential avenues of contamination and speed the process of DNA extraction by using a simpler technique. The GENECLEAN™ Kit for Ancient DNA from MP Biomedicals was chosen (Raff., 2008, Bennett & Kaestle., 2010, Xie et al., 2007), as it is a silica based extraction that takes considerably less time to complete and therefore requires less hands-on time with the reagents, reducing the risk of contamination by the researcher.

The GENECLEAN™ Kit was used following manufacturer's instructions, with minor changes. The length of the initial incubation was extended from the required 2-12 hours to 18 hours (overnight).

3.3. Chelex Extraction

Modern DNA samples were extracted using Chelex 100, due to the much faster processing time and satisfactory quality of DNA extraction when working with modern DNA. The Chelex extraction used was adapted from the method described by Bloom, in Goldman (1994), 15ml of mouthwash was vigorously swirled in the mouth, using the teeth to graze the sides of the mouth for several minutes. The mouthwash was expelled back into a plastic universal and centrifuged at 3398g for 10 minutes. The supernatant was poured off and the tube stood upside down on paper towel to dry.

The stock solution of 10% Chelex 100 beads were resuspended via trituration and 500µl of Chelex 100 was added to the cheek cell pellet. The pellet was resuspended in the Chelex 100

solution via trituration and 500µl of the resuspended cells were transferred to a 1.5ml microcentrifuge tube.

The microcentrifuge tube was incubated in a boiling water bath for 10 minutes, then allowed to cool. The solution was then centrifuged at 17,000g for 30 seconds to pellet the chelex beads and 100µl of the resulting supernatant was transferred to a fresh microcentrifuge tube. The Chelex pellet is discarded and the DNA solution is stored at -20°C until ready to use.

3.3.1. Quantification of DNA Concentration

Following extraction of DNA, the concentration of the resulting DNA solution was quantified in order to allow for consistent concentrations and masses of DNA to be used in further stages of the investigation. DNA was quantified using a NanoDrop 1000 spectrophotometer to determine concentration of DNA via the level of absorbance of light passed through the sample. Between the testing of each sample, the NanoDrop was zeroed using ultrapure DNA-free water. The extracted DNA was then labelled with its concentration and stored at maximum concentration. DNA was diluted immediately before later use to avoid storage of low-concentration extracted DNA solutions.

3.4. Artificial Degradation of DNA

DNA was artificially degraded using an ultrasonic bath. The ultrasound generated degrades purified DNA in solution through two methods. Firstly, cavitation is seen to cause single-strand ruptures at ultrasound strength of above 2 W/cm^2, by creating free radicals. Secondly, a thermal and mechanical effect can shear DNA strands (Elsner & Lindblad, 1989). Elsner also states that after sonication, DNA fragments have a size limit of approximately 100-500bp in size. Elsner further states that the DNA is broken in a non-specific fashion, predominantly between oxygen and carbon atoms, to form a DNA fragment with a 3’ end finishing with a free alcohol and a 5’ end that is phosphorylated.

The degradation of DNA was carried out using a modified technique from Grokhovsky (2006). 20µl of purified DNA was added to 20µl of Tris-HCl at pH 7.0, in 1.5ml thin-walled microcentrifuge tubes. Samples were then subjected to sonication at 44kHz, for 15 minutes. The microcentrifuge tubes were placed in racks, before being placed into an ultrasonic water bath, containing ice water to such a level that the ends of the microcentrifuge tubes containing the sample were fully submerged.

3.5. Removal of Inhibitors

Three methods of inhibitor removal were tested for their quality and compatibility with this investigation. These were the PowerClean kit from MoBio Laboratories, the PowerSoil kit from MoBio Laboratories and the OneStep PCR Inhibitor Removal kit from Zymo Research.

The Powerclean kit was used following manufacturer's instructions. A series of acids and bases are used to precipitate unwanted ions from the solution, which are removed. Following this, the DNA is bound to a spin filter and washed with several differing solvents in order to remove further impurities. The optional wash of 100% ethanol suggested by the manufacturer was used in this experimentation. The DNA was then eluted as a 100µl volume to concentrate the sample.

The PowerSoil kit was used following manufacturer's instructions with slight modifications. A dry sample of soil is required for the first stage of extraction, however as the DNA had previously been extracted using the GENECLEAN kit, the entire volume of extracted DNA solution that is the output of the GENECLEAN Kit for Ancient DNA was used as an alternative input for the PowerSoil kit.

While the PowerSoil kit is designed for use with DNA extractions from soil, it was considered an interesting prospect to test due to the extreme amounts of humic acid that must be removed from soil samples before DNA can be extracted. As humic acid was considered the likely culprit for the lack of DNA amplification in early extractions, a kit designed to cope with large concentrations of humic acids may work well on bone material.

The OneStep kit was used following manufacturer's instructions with no modifications. The sample is centrifuged through a spin filtration column to remove unwanted inhibitors, specifically humic acids.

Following the comparison of the PCR Clean-Up Kits (As seen in Section 4.3.3), the PowerClean kit was chosen as the most effective clean-up kit and was used in all extractions from the neonatal remains.

3.6. Sample Amplification

Once the DNA had been extracted and inhibitors removed, it was amplified through PCR to allow for visualisation.

3.6.1. Arnay-de-la-Rosa Method

The initial experimentation was completed using the Amel-A primer from Sullivan (1993) and the Amel-C primer from Maca-Meyer et al (2005). The sequence of these primers can be found in Section 9.2 in the Appendices. These primers amplify a region in intron 1 of the Amelogenin gene found within the X and Y chromosomes. The amplified region includes a

locus for a 6bp deletion in the X chromosome, resulting in a product length of 66bp amplified from the X chromosome and a 72bp long fragment amplified from the Y chromosome. Upon electrophoresis, these fragments will resolve to show one band for XX female genotypes and two bands for the XY male genotype.

The method followed to amplify the target with these primers was a modified version of the method in Arnay-de-la-Rosa (2007). The amplification was changed to take place in a 25µl reaction instead of a 10µl reaction and Taq 2x Mastermix was used in place of a mixture of individually added Tris-HCl, dNTPs, $MgCl_2$, Taq polymerase and bovine serum albumin (BSA). Also, the volume of DNA extract was modified to a consistent 10ng of DNA, regardless of the volume of DNA extract required for this mass. These modifications were made for several reasons. Firstly, the reaction volume was increased to reduce pipetting error with smaller volumes and to reduce the inhibiting effect on efficiency caused by the small level of evaporation that occurs in any PCR reaction without a mineral oil overlay.

Secondly, the decision to use Taq Mastermix instead of individual components was made to reduce the amount of error associated with pipetting multiple small volumes and also to provide a consistent concentration level of all of the PCR reagents. The reduction in time spent in physical contact with the PCR reaction that is achieved by pipetting in one volume of mastermix instead of repeatedly pipetting in multiple small volumes also reduces the chances of contamination from the researcher.

Thirdly, the use of 10ng of DNA was decided through testing of varying concentrations of sample DNA in amplification efficiency. The results of these tests can be found in Section 9.4 in the Appendices. This modification was made due to the fact that a "3µl volume of DNA Extract" as required in the original methodology can have huge variations in actual DNA content, due to the varying concentrations of extracted DNA in solution. Therefore, to make the results comparable and the method consistent, volume of DNA extract was deemed less important than concentration. In practice, the required volume of DNA extract varied between 1 and 3µl to ensure that there was 10ng of DNA in the reaction volume, with samples containing a DNA concentration above 10ng/µl being diluted before addition to the PCR reaction, and samples containing a DNA concentration of less than 10ng/µl having 2 or 3µl of DNA extract used in the reaction volume. Therefore, the volume of PCR grade water used in the reaction volume was variable and was changed in order to make up the total reaction volume of 25µl.

Therefore, the 25µl reaction volume used in this method consisted of 10ng of DNA, 12.5µl of Taq 2x Mastermix, 1µl of Amel-A primer solution and 1µl of Amel-C primer solution, made up to 25µl with PCR grade water.

A PCR Blank was also made simultaneously, containing the above but with no DNA extract added and additional PCR grade water to make up the 25µl volume.

The PCR reactions were then subjected to 40 cycles of the following temperatures: 1 minute at 95°C, 1 minute at 53°C, 1 minute at 72°C. Following this, a final 10 minute stage held at 72°C was included to ensure that all primer extension had been completed. The post-PCR amplicons were then stored at 4°C until use.

3.6.2. Method Development

Initial testing of the above method resulted in successful amplification of modern DNA. However, further amplifications using the same technique resulted in no amplification. Modern DNA was subjected to the PCR conditions described above, with variable annealing temperatures used in order to identify the optimal annealing temperature. The results of these can be seen in Section 9.4 in the appendices and had very faint bands with non-specific binding and primer dimerisation.

In an attempt to improve specificity of the PCR and in doing so remove the non-specific bands and improve efficiency, Touchdown PCR was used. The method of this Touchdown PCR can be seen below in Section 3.6.2.1. Touchdown PCR results can be seen in Section 9.4, and show no amplification.

This led to the understanding that there may have been an issue with the primers themselves. Small MetaPhor Agarose electrophoresis gels prepared on microscope slides ("Slide gels") were used in order to test the primers. Firstly, the Amel-A and Amel-C primers were tested alongside each other, the results of which can be seen in Section 9.4. Following this, a second slide gel was run against a known working primer. It was deemed that no issues could be seen with the Amel-A and Amel-C primers that would cause lack of amplification.

New reagents were purchased and tested, both alongside the previously used reagents and also in PCRs using entirely new stock. Even with all new reagents, the primers seemed not to amplify.

3.6.2.1. Touchdown PCR

Following the unsuccessful trials with the Amel-A and Amel-C primers, touchdown PCR was attempted in order to remove issues with non-specific binding and increase the yield of PCR products in later cycles in order to produce visible DNA banding. A PCR was carried out in a 25µl volume, containing 10ng of DNA extract, 12.5µl Taq 2x Mastermix, 1µl of Amel-A primer solution, 1µl of Amel-C primer solution, and a variable volume of PCR grade water to make up to final volume. Simultaneously, a PCR blank was made which contains the above but with no DNA extract and additional PCR grade water to maintain a consistent total volume.

However, no amplicons at all were recovered from multiple touchdown PCR tests, so it was decided to change the primers used in the analysis. The negative results of this testing can be seen in 9.4 in the Appendices.

3.6.2.2. Identifiler Method

Following the repeated failure of the Amel-A and Amel-C primers used in Arney-de-la-Rosa (2007), a decision was made to test the skeletal material with new primers to ensure that inhibition was not the cause of the failed amplifications.

The Identifiler Amelogenin Forward & Reverse primers were chosen based on their regular and successful usage in forensic science, especially in the analysis of DNA for storage in the CODIS database in the US (Butler (2009), Sapse and Kobilinsky (2011)). These primers amplify a slightly larger part of the same region as the Amel-A and Amel-C primers, producing amplicons of 106bp from the X chromosome and 112bp from the Y chromosome. Therefore, these amplicons should still be recoverable based on the hypothesis that small fragments <100-500bp in length are of the theoretical maximum size for heavily degraded ancient DNA (Elsner & Lindblad, 1989).

The Identifiler PCR was carried out in a 25µl volume containing 10ng of DNA extract, 12.5µl Taq 2x MasterMix, 1µl Forward primer solution, 1µl Reverse primer solution, and a variable volume of PCR grade water to make up the total volume.

These PCRs were carried out using the following steps: Pre-denaturation for 11 minutes at 95°C, denaturation for 1 minute at 95°C, annealing for 1 minute at 61°C, extension for 1 minute at 72°C, and finally post extension for 5 minutes at 72°C. The denaturation, annealing and extension steps were cycled 35 times.

Following preliminary successes with the Identifiler primers, they were fully adopted for all further analyses. A range of DNA concentrations and annealing temperatures were tested in order to determine the optimum PCR and it was determined that 10ng of DNA in the solution, with an annealing temperature of 61°C, provides optimum amplification.

Some primer dimerisation was observed when using the Identifiler primers, at 50bp in length. In an attempt to remove this, varying quantities of Mg^{2+} were added to the PCR reactions, but seemed to have very little effect to reduce the presence of dimers.

3.7. Sample Electrophoresis & Visualisation

Samples were resolved in a 50ml 3% MetaPhor Agarose gel. Electrophoresis conditions were 80V, 500mA, for 1hr 45 minutes. Samples were run alongside the NEB Biolabs Low Molecular Weight Ladder, the size markers of which can be seen in Appendix 9.3. Orange G loading dye was used alongside Ethidium bromide to stain the DNA and the gels were viewed and photographed under UV light.

4. **Chapter Four: Results & Discussion**

4.0. Metric Measurements of the Remains

Measurements were taken of the skeletal remains. Where possible, these measurements were carried out on the left petrosa. When unavailable, the right petrosa was measured. If both petrosae were missing or heavily damaged, then other parts of the skeleton were used. In those cases, there is some variation in the bone used due to attempts to use bone that would not result in the loss of very important physical material for anthropological investigations. Therefore, broken and fragmented bone was targeted as a replacement for petrous portions when unavailable. The measurements of the remains can be seen below.

Skeleton Number	Side	Average Petrosa Measurement		
		Length (mm)	Width (mm)	Mass (g)
SK22684	L	43.51	18.08	4.01
SK25105	L	38.85	14.59	2.60
SK25165	L	35.28	15.58	2.03
SK25208	R	31.82	19.26	3.22
SK25209	L	40.42	19.70	3.47
SK25213	R	40.08	17.59	2.85
SK25236	L	41.41	20.34	2.91
SK25244	L	30.22	16.55	2.11
SK25245/244	R	31.06	17.50	2.19
SK25251	L	35.44	19.36	2.56
SK25272	L	37.88	15.59	3.20
SK25368	L	42.81	16.01	3.35
SK25600	L	36.99	16.30	2.90
SK26320	L	33.02	17.01	2.18
SK26391	L	37.29	14.62	2.49
SK26414	L	39.71	18.09	3.43
SK26615	L	36.52	16.29	2.42
SK26836	L	40.38	18.12	3.96
SK26851	L	36.44	14.77	2.72
SK26855	L	31.12	18.10	2.77
SK26926	L	35.35	17.81	2.36
SK26934	R	41.38	20.75	3.07
SK26937	L	32.81	14.96	2.09
SK27325	R	41.98	17.43	3.12
SK27392	R	33.01	18.07	2.62
SK27447	L	36.04	20.47	2.65
SK27771	L	39.96	19.28	3.14
SK27774	L	35.12	17.18	2.48
SK27885	L	38.63	19.62	3.32
SK27925	L	36.00	17.24	2.75
SK27935	R	42.42	15.73	3.01
SK27938	L	39.95	17.84	2.64
SK27970	L	38.94	17.42	2.59
SK28224	L	38.96	18.19	3.38
SK31118	L	35.90	15.45	1.95
SK31225	L	37.49	25.80	4.01
SK33056	L	31.54	15.77	2.47
SK51508	R	37.49	17.61	2.57
SK51510	L	37.01	25.71	2.59
SK53069	L	19.01	12.12	0.84

Table 1: Measurements of the petrous portion of the temporal bone.

Skeleton Number	Side	Bone	Average Measurement		
			Length (mm)	Width (mm)	Mass (g)
SK22668	R	PROX TIBIA	50.14	11.51	1.34
SK25149	N/A	SPHENOID BODY	13.615	15.615	1.53
SK25164/165	N/A	SPHENOID BODY	11.935	12.49	0.72
SK25167/168	N/A	RIB FRAG	N/A	N/A	1.72
SK25262	L	DIST FEMUR	44.395	18.085	1.74
SK25297	L	PROX FEMUR	28.985	18.17	1.81
SK25471	R	HUMERUS	68.29	16.665	3.945
SK25544	L	PROX FEMUR	46.095	17.25	2.285
SK25570	R	PROX HUMERUS	36.85	12.74	1.5
SK25572	R	DIST FEMUR	30.36	14.39	1.64
SK25575/576	L	PROX FEMUR	34.545	18.085	1.28
SK25729	R	DIST HUMERUS	37.35	17.95	1.34
SK26201	L	PROX HUMERUS	32.47	12.87	1.25
SK26508	R	SCAPULA	31.685	27.26	1.26
SK26846	R	DIST FEMUR	32.425	21.225	1.81
SK27449	L	CUNIFORM 3	N/A	N/A	3.165
SK27628	R	PROX TIBIA	25.285	11.885	0.985
SK27657	R	PROX HUMERUS	31.205	13.305	1.135
SK27743	L	PROX FEMUR	37.295	16.9	1.82
SK27844	N/A	SPHENOID BODY	12.585	12.835	1.555
SK27972	N/A	LUMBAR BODY	16.35	22.515	2.05
SK31089	R	ILIUM FRAG	N/A	N/A	3.075
SK31061	L	PROX FEMUR	40.38	14.14	1.49
SK51506	L	ISCHIUM	37.55	23.635	2.72

Table 2: Measurements of other bones used when the petrosa was damaged. N/A indicates a measurement that could not be used.

These measurements were taken using the dimensions shown in Schaefer et al (2009). In cases of a complete long bone, the distal end was used. Proximal ends were used when the distal end was not present. Note that due to the age of the individuals, the epiphyses were unfused and in many cases not identifiable. In every case of long bone measurement, the distal end of the diaphysis was measured, rather than the unfused epiphysis itself.

4.1. Age Determination of the Remains

The age of the remains were then determined using a number of differing techniques, dependant on which bone was measured. Primarily, the Fazekas and Kósa (1978) method was used for the petrous portion, with the projected age of the remains shown in Table 8 below. The calculations for age determination via this method can be seen in Appendix 9.3.1.

Skeleton Number	Side	Average Measurements of the Petrosa			Projected Age (Prenatal wks)		
		Length (mm)	Width (mm)	Mass (g)	Age (Length)	Age (Width)	Age (Combined)
SK22684	L	43.51	18.08	4.01	40+	38-40 (I)	40+
SK25105	L	38.85	14.59	2.60	38-40	30-34	30-40
SK25165	L	35.28	15.58	2.03	38	34-38 (I)	38
SK25208	R	31.82	19.26	3.22	36	40+ (I)	40+
SK25209	L	40.42	19.70	3.47	40	40+	40+
SK25213	R	40.08	17.59	2.85	40+	38-40 (I)	40+
SK25236	L	41.41	20.34	2.91	40+	40+	40+
SK25244	L	30.22	16.55	2.11	34	34-40 (I)	34-40
SK25245/244	R	31.06	17.50	2.19	34 (I)	38-40	38-40
SK25251	L	35.44	19.36	2.56	38	40+	38+
SK25272	L	37.88	15.59	3.20	38-40	34-38 (I)	38-40
SK25368	L	42.81	16.01	3.35	40+	34-40	34+
SK25600	L	36.99	16.30	2.90	38-40	34-40 (I)	38-40
SK26320	L	33.02	17.01	2.18	36-38 (I)	38-40	38-40
SK26391	L	37.29	14.62	2.49	40	34 (I)	40
SK26414	L	39.71	18.09	3.43	40	38-40 (I)	40
SK26615	L	36.52	16.29	2.42	38	34-40 (I)	38-40
SK26836	L	40.38	18.12	3.96	40+	38-40 (I)	40+
SK26851	L	36.44	14.77	2.72	38	34 (I)	38
SK26855	L	31.12	18.10	2.77	34-36 (I)	38-40 (I)	38+ (I)
SK26926	L	35.35	17.81	2.36	38	38-40	38-40
SK26934	R	41.38	20.75	3.07	40+	40+	40+
SK26937	L	32.81	14.96	2.09	36-38	34 (I)	36-38
SK27325	R	41.98	17.43	3.12	40+	38-40 (I)	40+
SK27392	R	33.01	18.07	2.62	36-38 (I)	38-40 (I)	38+
SK27447	L	36.04	20.47	2.65	38-40	40+	38+
SK27771	L	39.96	19.28	3.14	40	40+	40+
SK27774	L	35.12	17.18	2.48	38-40	38-40	38-40
SK27885	L	38.63	19.62	3.32	40	40+	40+
SK27925	L	36.00	17.24	2.75	38	38-40 (I)	38-40
SK27935	R	42.42	15.73	3.01	40+	34-38	34-40
SK27938	L	39.95	17.84	2.64	40	38-40	38-40
SK27970	L	38.94	17.42	2.59	40	38-40 (I)	40
SK28224	L	38.96	18.19	3.38	40	38-40 (I)	40
SK31118	L	35.90	15.45	1.95	38	34	34-38
SK31225	L	37.49	25.80	4.01	38-40	40+	38+
SK33056	L	31.54	15.77	2.47	36	34-38	34-38
SK51508	R	37.49	17.61	2.57	38-40	38-40	38-40
SK51510	L	37.01	25.71	2.59	38-40	40+	38+
SK53069	L	19.01	12.12	0.84	24-26 (I)	30-32 (I)	30+ (I)

Table 3 (previous page): Projected age of the remains, calculated using the average measurements of length and width of the petrous pyramid and the Fazekas and Kósa (1978) method. Note that age determinations indicated with an "(I)" are taken from the measurement of a broken (incomplete) bone. Therefore, these age determinations have not been used in the final combined age determination when possible.

The combined age ranges given are determined using a combination of the age ranges provided by the length and width measurements. When measurements of damaged bones indicated with an (I) have been taken, these have been avoided in the combined age determination, to avoid the individual appearing younger than they actually were at the time of death.

The results shown in Fig 8 above indicate that the overwhelming majority of the skeletons were 38-40 prenatal weeks old. Following Naegele's Rule (Fehling et al, 1907), an expected time of birth is approximately 40 weeks (280 days) after conception. However Kieler et al (1995) found a 9 day standard deviation to an average of 281 days and Bergsjø et al (1990) found a 13 day standard deviation from a 281 day average. Therefore, this would indicate that these individuals are likely of full-term or slightly early-term age.

However, it is unknown whether these are stillborn individuals, under the modern definition of "any child which has issued forth from its mother after the twenty fourth week of pregnancy and which did not at any time after being completely expelled from its mother, breathe or show any other signs of life" (Births and Deaths Registration Act 1926). Alternatively, these individuals may have been cases of infant mortality, with the child surviving childbirth but dying within the first year of life.

When the petrosa was missing, differing techniques for multiple bones were used to determine age. Age determinations were calculated using the metric measurements given in Schaefer et al (2009) and the aging tables given by Fazekas and Kósa (1978). Combined, the results of these aging techniques can be seen in Table 4. The calculations for these methods can be seen in Appendix 9.3.2 through Appendix 9.3.7.

Skeleton Number	Side	Bone	Average			Projected Age (Prenatal wks)		
			Length (mm)	Width (mm)	Mass (g)	Age (Length)	Age (Width)	Age (Combined)
SK22668	R	PROX TIBIA	50.14	11.51	1.34	30+ (I)	N/A	30+ (I)
SK25149	N/A	SPHENOID BODY	13.615	15.615	1.53	40+	36	36+
SK25164/165	N/A	SPHENOID BODY	11.935	12.49	0.72	38-40	26-30	38-40
SK25167/168	N/A	RIB FRAG	N/A	N/A	1.72	N/A	N/A	N/A
SK25262	L	DIST FEMUR	44.395	18.085	1.74	24+ (I)	34-40	34-40
SK25297	L	PROX FEMUR	28.985	18.17	1.81	18+ (I)	N/A	18+ (I)
SK25471	R	HUMERUS	68.29	16.665	3.945	40	38-40	38-40
SK25544	L	PROX FEMUR	46.095	17.25	2.285	26+ (I)	N/A	26+ (I)
SK25570	R	PROX HUMERUS	36.85	12.74	1.5	22+ (I)	N/A	22+ (I)
SK25572	R	DIST FEMUR	30.36	14.39	1.64	20+ (I)	32+ (I)	32+ (I)
SK25575/576	L	PROX FEMUR	34.545	18.085	1.28	20+ (I)	N/A	20+ (I)
SK25729	R	DIST HUMERUS	37.35	17.95	1.34	24+ (I)	40	40
SK26201	L	PROX HUMERUS	32.47	12.87	1.25	20+ (I)	N/A	20+ (I)
SK26508	R	SCAPULA	31.685	27.26	1.26	38	38-40	38-40
SK26846	R	DIST FEMUR	32.425	21.225	1.81	20+ (I)	40	40
SK27449	L	CUNIFORM 3	N/A	N/A	3.165	N/A	N/A	N/A
SK27628	R	PROX TIBIA	25.285	11.885	0.985	20+ (I)	N/A	20+ (I)
SK27657	R	PROX HUMERUS	31.205	13.305	1.135	20+ (I)	N/A	20+ (I)
SK27743	L	PROX FEMUR	37.295	16.9	1.82	22+ (I)	N/A	22+ (I)
SK27844	N/A	SPHENOID BODY	12.585	12.835	1.555	40+	26-30	40+
SK27972	N/A	LUMBAR BODY	16.35	22.515	2.05	N/A	N/A	N/A
SK31089	R	ILIUM FRAG	N/A	N/A	3.075	N/A	N/A	N/A
SK31061	L	PROX FEMUR	40.38	14.14	1.49	24+ (I)	N/A	24+ (I)
SK51506	L	ISCHIUM	37.55	23.635	2.72	40+	40+	40+

Table 4: Projected age of the remains, calculated using the average metric measurements of length and width of varying bones, utilising metric techniques outlined in Schaefer et al (2009) and the aging tables given in Fazekas and Kósa (1978). Note that age determinations indicated with an "(I)" are taken from the measurement of a broken (incomplete) bone. Therefore, these age determinations have not been used in the final combined age determination when possible.

As above, the combined age given in Table 4 has been calculated using a combination of the age determinations provided by the length and width measurements taken from the remains. Due to the heavily fragmented post-cranial skeletons, there are a considerable number of measurements from incomplete bones. Where possible, these have not been used to determine age. However, in many cases a combined age has been calculated using two, or in some cases only one, incomplete measurement. These age determinations have been indicated with an (I) and provide a lower boundary for the age of the individual, although the predicted age for the individual would be older than this.

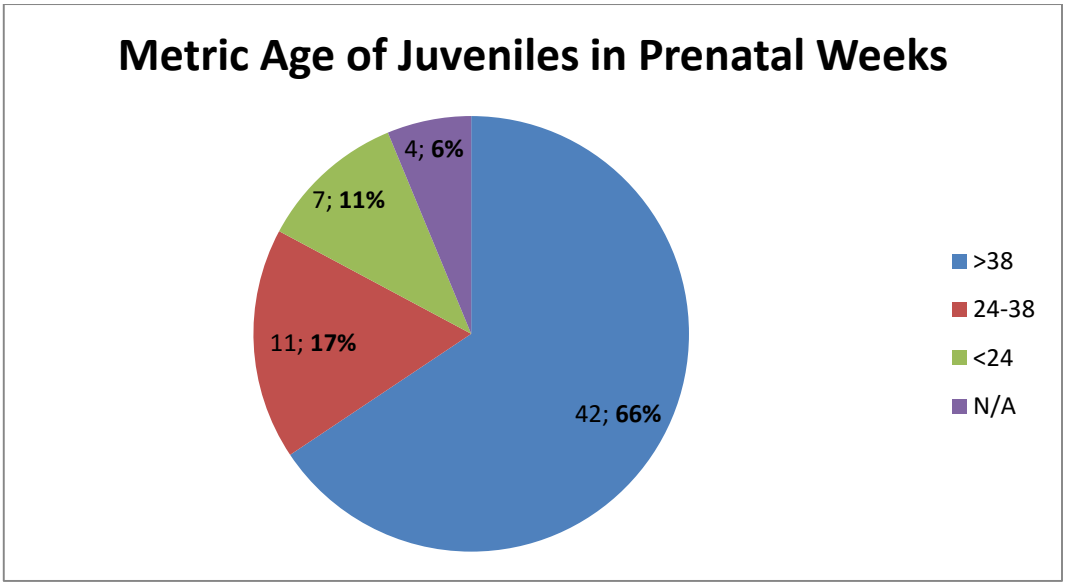

Fig 6: The age determinations of the juveniles based on the measurements and calculations shown in Tables 3 & 4, utilising petrosa and post-cranial measurements. N/A indicates that an age could not be calculated due to incomplete remains.

It can be seen from Figure 6, that while there are many individuals who have an age of 38 prenatal weeks or more and are likely early or full-term juveniles, there are many individuals who have a minimum age of 18-24 weeks. It is possible that these juveniles are also full-term individuals with fragmented skeletons, it also may be possible that these are the remains from a miscarriage or a stillborn foetus delivered before the limit of viability. The limit of viability describes the gestational age at which an individual has a 50% chance of survival outside of the uterus. In modern pregnancies this is considered to be approximately 24 prenatal weeks, but in Romano-British society the limit of viability would be much later due to the lack of modern medicine and intensive care facilities.

4.2. Arnay-de-la-Rosa Technique

The primers from Arnay-de-la-Rosa (2007) produced no viable results. However, the development of the final method rested greatly on the results of the testing with the Arnay-de-la-Rosa technique. The results of the Arnay-de-la-Rosa testing can be seen below.

Initial testing of the Arnay-de-la-Rosa primers was carried out across two MetaPhor Agarose gels, the first containing 5ng of female DNA in each sample, but using a range of annealing temperatures. The second gel contains 5ng of male DNA in each sample, across a range of annealing temperatures. This was carried out to determine the optimum annealing temperature for an efficient PCR.

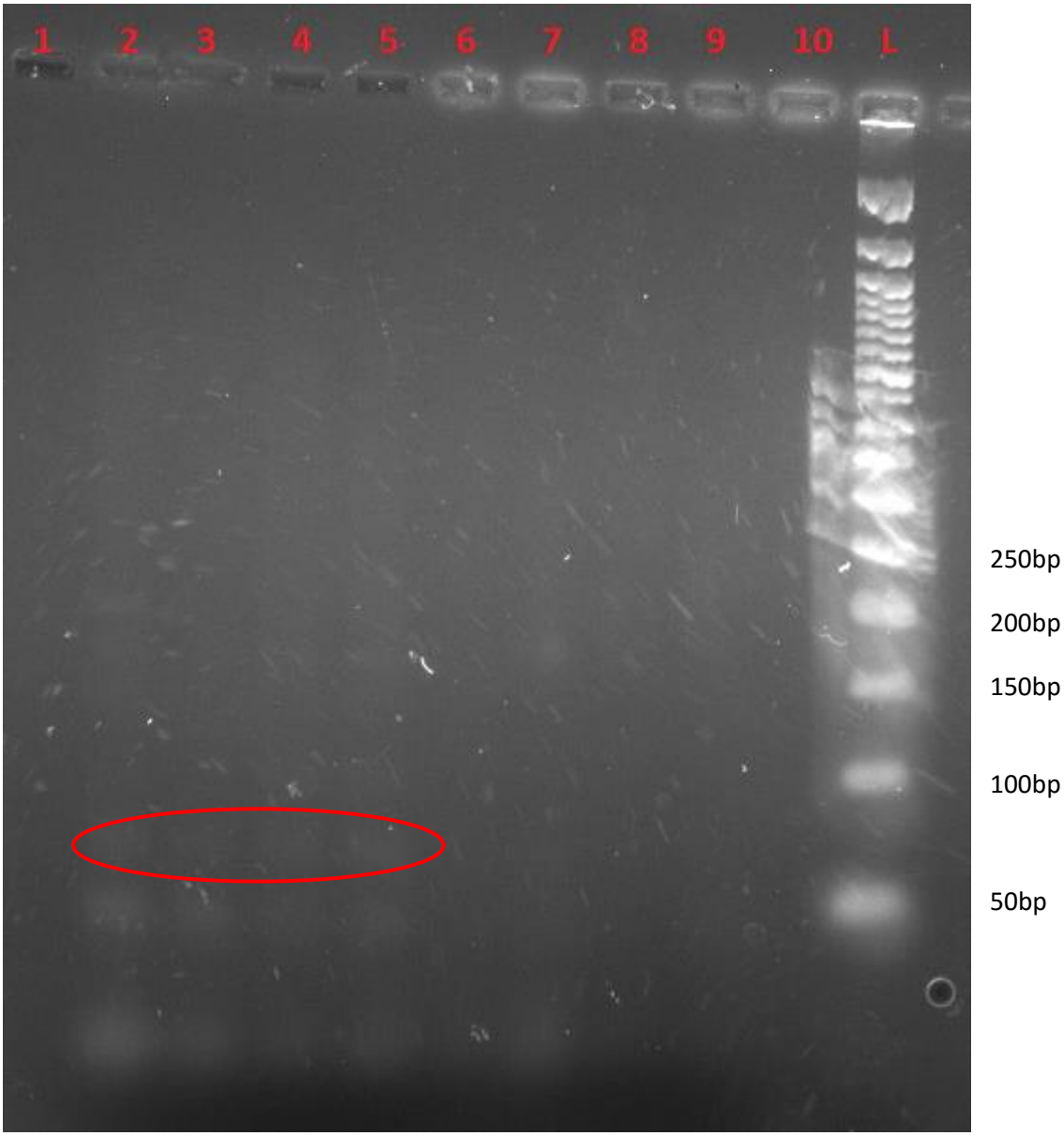

Gel Key: 1 - 50°C annealing temperature, 2 – 49.4°C annealing temperature, 3 – 48.3°C annealing temperature, 4 - 47°C annealing temperature, 5 – 45.1°C annealing temperature, 6 – 43.5°C annealing temperature, 7 – 42.5°C annealing temperature, 8 - 42°C annealing temperature. 9 – Blank, 10 – Empty, L – NEB Biolabs 50bp Ladder.

Fig 7: First testing of the Arnay-de-la-Rosa primers. All tests carried out with 5ng of modern female DNA. Bands can be seen in lane 1 at approximately 200bp and in lanes 5 and 7 at approximately 170bp. Lanes 1-4 show banding at 50bp and approximately 66bp which may be the target fragments.

From the results of Figure 7, it can be seen that there are non-specific bands appearing, in addition to the target bands at 66bp. The banding is very faint at this level and smearing is present even with the use of modern DNA.

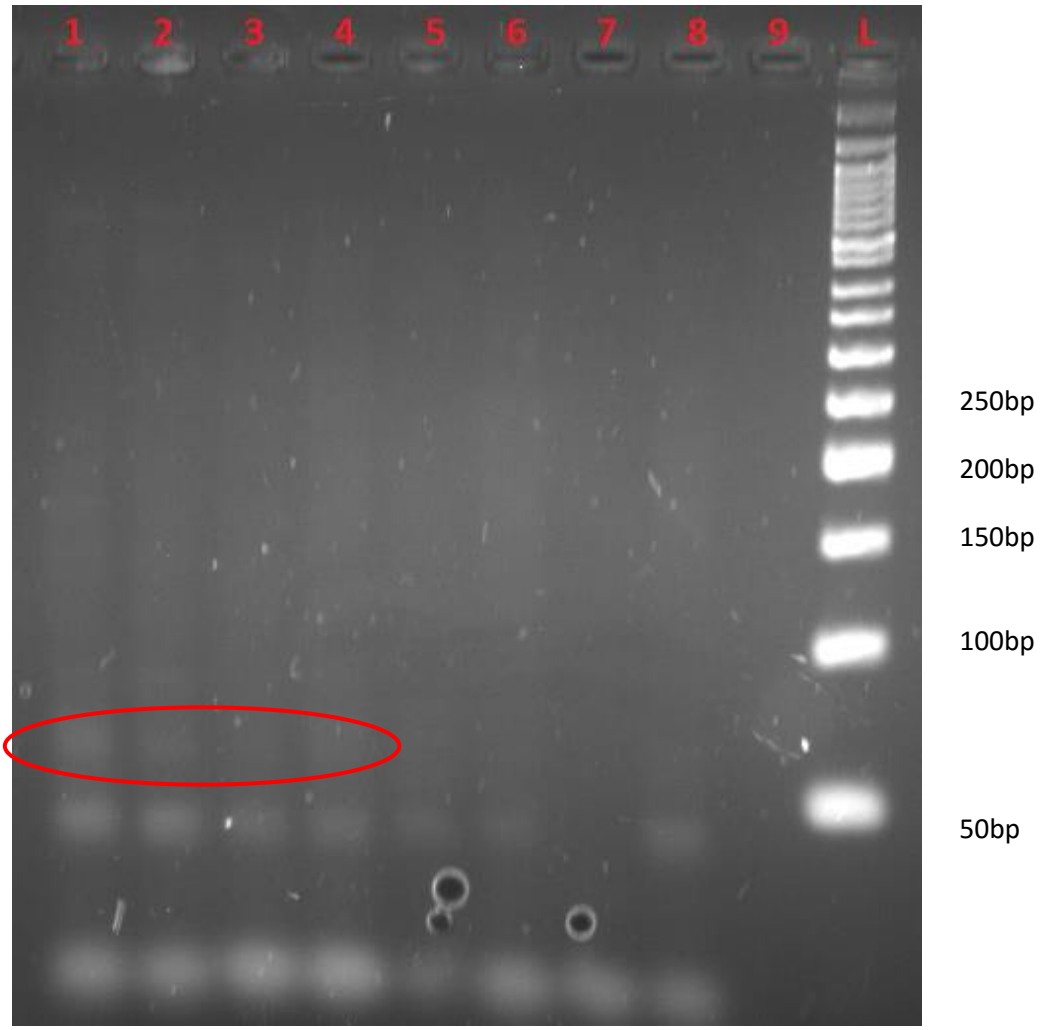

Gel Key: 1 - 50°C annealing temperature, 2 – 49.4°C annealing temperature, 3 – 48.3°C annealing temperature, 4 - 47°C annealing temperature, 5 – 45.1°C annealing temperature, 6 – 43.5°C annealing temperature, 7 – 42.5°C annealing temperature, 8 - 42°C annealing temperature. 9 – Empty, L – NEB Biolabs 50bp Ladder.

Fig 8: First testing of the Arnay-de-la-Rosa primers. All tests carried out with 5ng of modern male DNA. Banding can be seen at approximately 66bp in lanes 1-4, but also at approximately 100bp in size in lanes 1 and 2 and very large bands at approximately 600bp in length in lanes 1 and 2.

The results in figure 8 confirm that 66bp fragments can be produced at the higher annealing temperatures between 47-50°C. However, no banding can be seen for the 72bp fragment that should be produced from the Y chromosome in male DNA. Additional banding can be seen at 100bp and 600bp in the higher annealing temperature lanes 1 and 2. This indicates that there is some non specific binding occurring at these temperatures. Usually, non-specific binding occurs at lower-than-optimal annealing temperatures, so to see non specific

binding in the higher temperatures indicates that non-specific binding is likely occurring at every temperature tested on this gel, but the higher temperatures allow for better amplification and therefore the banding is more visible in lanes 1 and 2. Therefore, the decision has been made to test higher annealing temperatures and also to double the mass of DNA used in the PCR to 10ng to improve the efficiency of the PCR and to hopefully remove any non-specific binding.

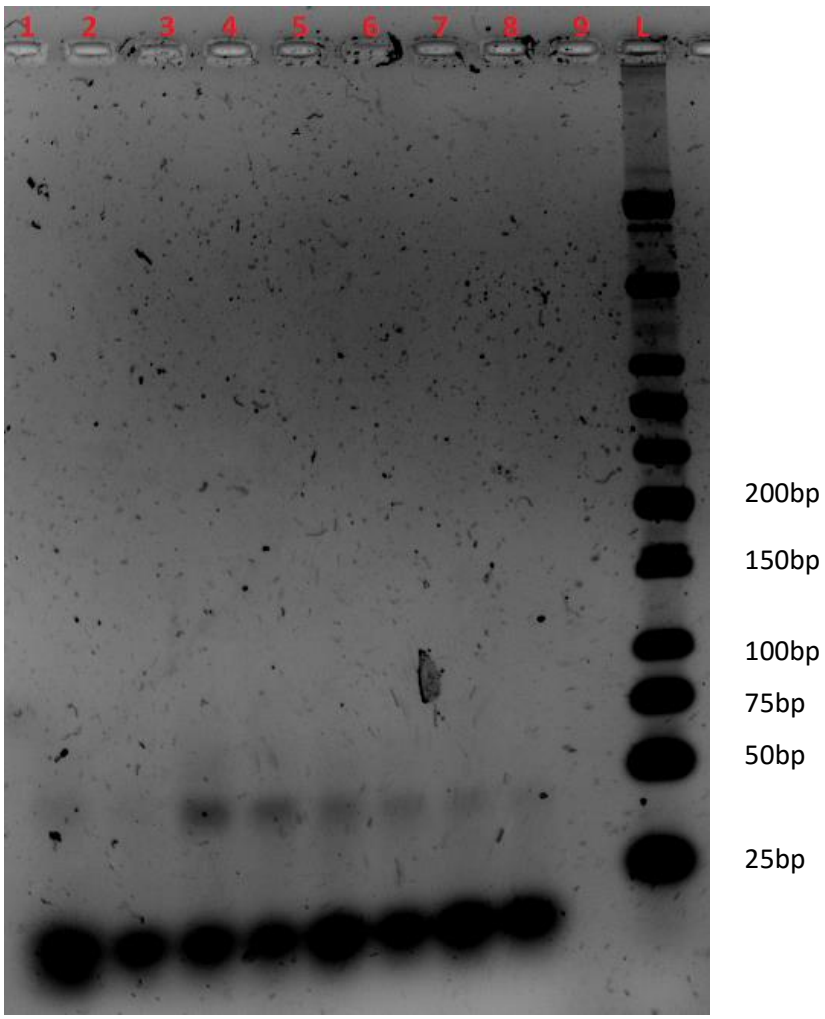

Gel Key: 1 - 55°C annealing temperature, 2 - 54.4°C annealing temperature, 3 - 53.4°C annealing temperature, 4 – 52°C annealing temperature, 5 – 50.1°C annealing temperature, 6 – 48.5°C annealing temperature, 7 – 47.5°C annealing temperature, 8 - 47°C annealing temperature, 9 – Empty, L – NEB Biolabs Low Molecular Weight Ladder

Fig 9: Second testing of Arnay-de-la-Rosa primers. All tests carried out with 10ng of female DNA. Primer dimer banding can be seen at approximately 45bp in size, with the strongest occurring with a 53.4°C annealing temperature. Very faint banding can be seen just above the 50bp marker on the ladder in lane 3, which may indicate the presence of the 66bp fragment.

At this point in the experimentation, it became seemingly impossible to amplify the target fragments of 66 and 72bp in size. There had been no changes in the techniques used and the presence of primer dimers indicates that there has been no accidental introduction of PCR inhibitors into any of the reagents. Further experimentation was carried out in order to confirm that the target fragments would not amplify and to try to determine a potential cause and solution of this issue.

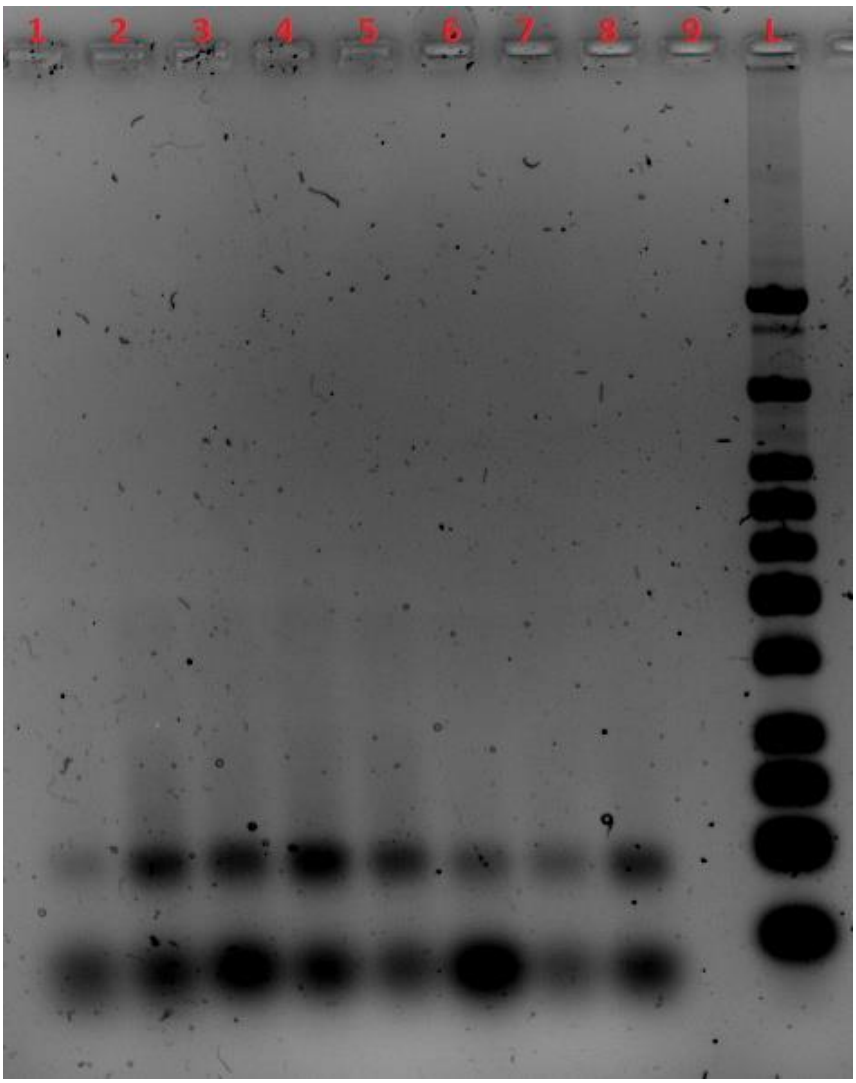

Gel Key: Gel Key: 1 - 55°C annealing temperature, 2 - 54.4°C annealing temperature, 3 - 53.4°C annealing temperature, 4 – 52°C annealing temperature, 5 – 50.1°C annealing temperature, 6 – 48.5°C annealing temperature, 7 – 47.5°C annealing temperature, 8 - 47°C annealing temperature, 9 – Empty, L – NEB Biolabs Low Molecular Weight Ladder

Fig 10: Second testing of the Arnay-de-la-Rosa primers. All testing carried out with 10ng of modern male DNA. Primer dimer bands can be seen at approximately 45bp in size and non-specific binding bands can be seen at approximately 200bp in size. Smudged, streaky bands can be seen between 50-100bp in size, with no discernible strong banding patterns within.

Figure 10 shows the continuing trend of no banding present at the 66bp and 72bp target sizes. Primer dimer bands continue to form, indicating that the PCR process itself is successfully amplifying DNA, but not the target DNA. The streaking occurring at the target size region could indicate degraded DNA but this is unlikely as the DNA was modern DNA extracted on the same day as the PCR was started. It may also indicate that too much DNA was loaded onto the gel or that the electrophoresis conditions were incorrect, however this would cause streaking throughout the gel. Strong bands have formed for the primer dimers which indicate that this is not the case. Faint non specific bands are still present in the results, demonstrating that the PCR is still not at maximum specificity.

As no strong banding was occurring and non-specific binding was still present, Mg2+ ions were added in varying concentrations in order to attempt to balance the specificity and activity of the Taq polymerase in order to remove the non-specific bands and primer dimers, but improve the strength of target bands.

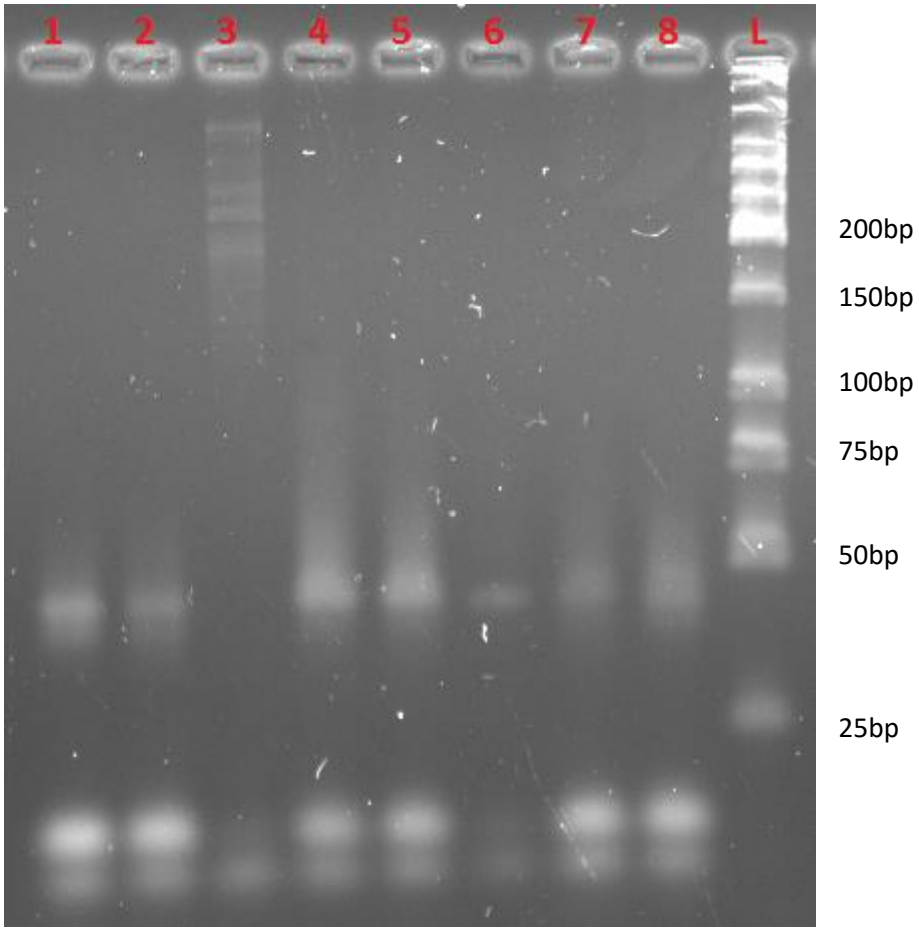

Gel Key: 1&2 – 1mM Mg^{2+} ions, 3&4 - 2mM Mg^{2+} ions, 5&6 - 3mM Mg^{2+} ions, 7&8 - 4mM Mg^{2+} ions, L – NEB Low Molecular Weight Ladder.

Fig 11: Varying levels of magnesium ions (Mg2+) in the PCR solution of the Arnay-de-la-Rosa primers. All tests carried out with 10ng of modern male DNA and an annealing temperature of 52°C.

Figure 11 again shows no target bands at 66 and 72bp in size. There are strong streaks in all lanes except lane 6. Lane 3 shows extensive banding of large fragments around 500-700bp in size, which indicate that non-specific binding is still occurring. Primer dimer bands are also still appearing in every lane except lane 3, in which the non-specific binding bands have out-competed the primer dimers.

Touchdown PCR was carried out in order to further attempt to improve specificity and reduce primer dimerisation. This will overall improve efficiency and therefore increase the chances of producing visible target banding.

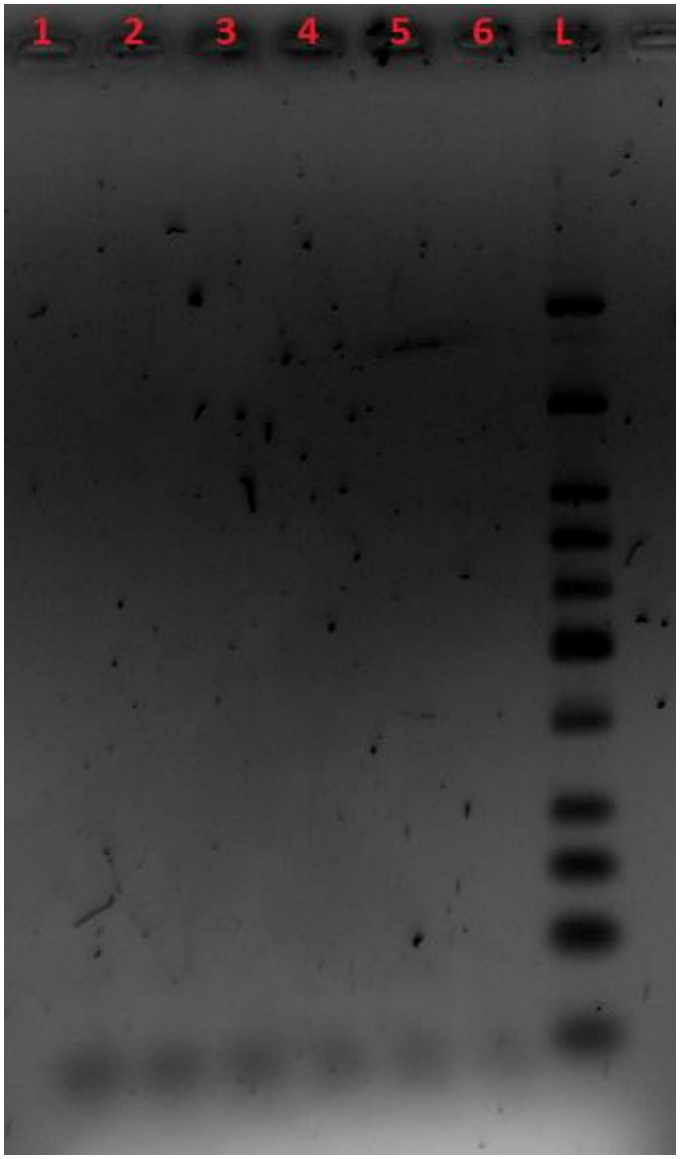

Gel Key: 1 - 61°C initial annealing temperature, reduced by 1°C per cycle, 2 – 61°C initial annealing temperature, reduced by 0.5°C per cycle, 3 - 60°C initial annealing temperature, reduced by 1°C per cycle, 4 - 60°C initial annealing temperature, reduced by 0.5°C per cycle, 5 - 59°C initial annealing temperature, reduced by 1°C per cycle, 6 - 59°C initial annealing temperature, reduced by 0.5°C per cycle.

Fig 12: Touchdown PCR of 10ng male DNA, with varying initial annealing temperatures and rate of cooling between cycles, reducing to a standard 52°C annealing temperature upon completion of the touchdown cooling cycle.

No banding can be seen in Figure 12, including primer dimers, indicating that the initial starting temperatures may be too high for the primers and are causing the primers to degrade. Therefore, a second touchdown PCR was carried out with lower initial temperatures in order to resolve this problem.

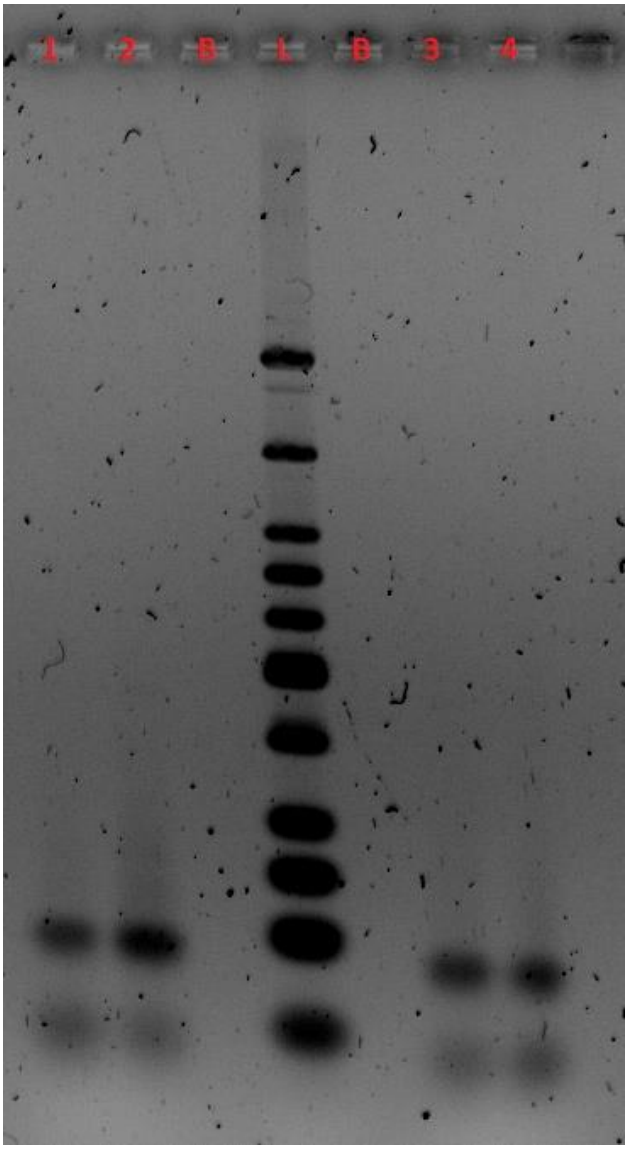

Gel Key: 1 - 58°C initial annealing temperature, reduced by 1°C per cycle, 2 – 57°C initial annealing temperature, reduced by 1°C per cycle, L – NEB Biolabs Low Molecular Weight Ladder, 3 - 56°C initial annealing temperature, reduced by 1°C per cycle, 4 - 55°C initial annealing temperature, reduced by 1°C per cycle. B – Indicates an empty lane.

Fig 13: Touchdown PCR of 10ng male DNA, with lower initial annealing temperatures, reducing to a standard 51°C annealing temperature upon completion of the touchdown cooling cycle.

Figure 13 again shows no banding at the expected 66bp and 72bp size region. Primer dimer bands are continuing to form, indicating that PCR inhibition is not the cause of the target DNA loss. Streaks of DNA also appear within the 66-72bp region, indicating that while the DNA is still not amplifying correctly, these temperatures are more effective in amplification of the target DNA than the temperatures shown in Figure 12.

Due to the lack of correct banding patterns forming, it was suspected that there may have been some issue with the primers themselves that was preventing the formation of the 66 and 72bp fragments. Therefore, the primers were run on microscope slides in order to examine for faint primer bands, or multiple bands from a primer that may indicate a fragmented primer.

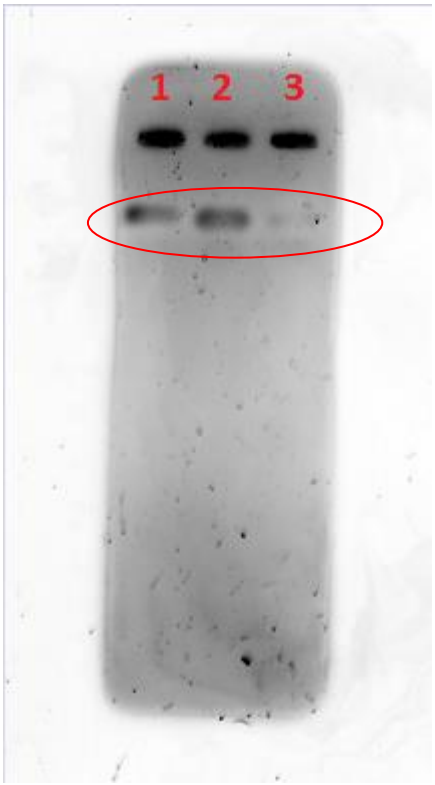

Gel Key: 1 – Identifiler Amelogenin Primer (Forward), 2 – "Amel-A" primer, 3 – "Amel-C" primer.

Fig 14: Comparison of primer bands of the Amel-A and Amel-C primers, against the known standard of a working primer (Identifiler Amelogenin Primer (Forward)). All testing carried out using 5µl of primer solution.

It can be seen in Figure 14 that there are no fragmented primer bands, indicating that the primers are still whole. However, the band formed by the Amel-C primer is substantially weaker than the band formed by the Amel-A primer and the known standard. From these results, it appeared that there was an issue with the Amel-C primer that may have been causing the lack of amplification seen in previous experimentation.

The concern that the primers or reagents were not effective in PCR amplification led to the decision to order new batches of every reagent, in order to test them individually and identify the cause of the problem. The results of this testing can be seen below.

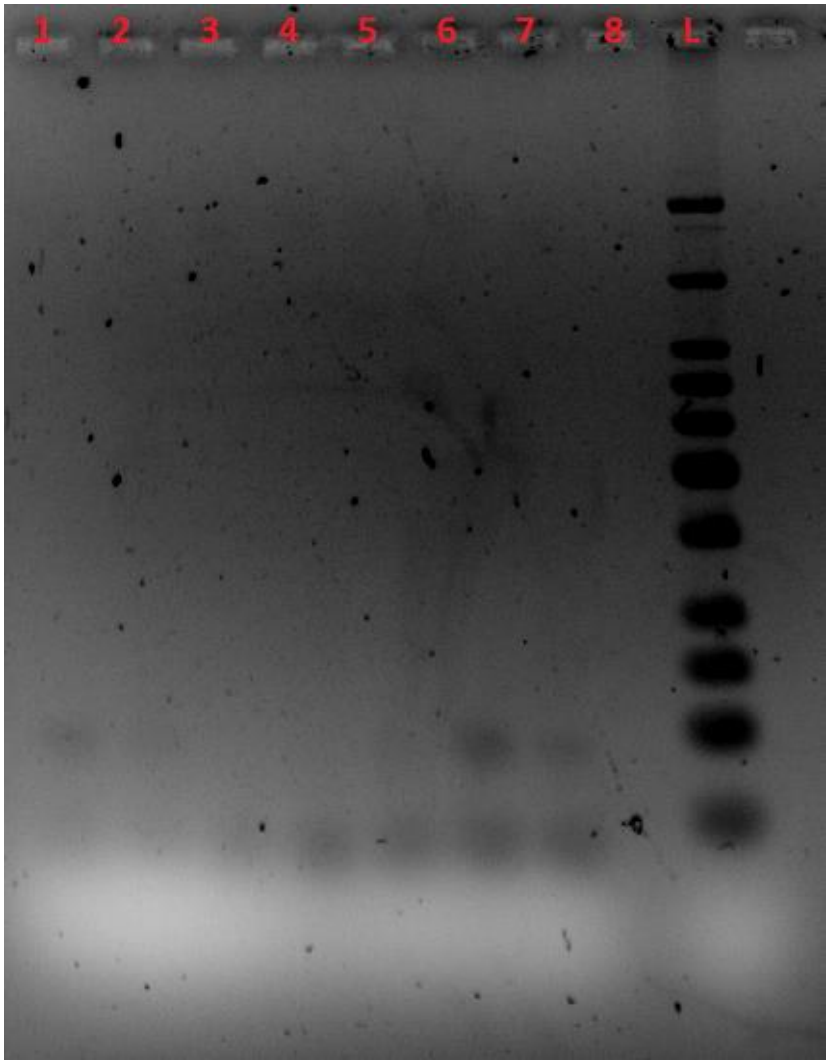

Gel Key: 1 – 5ng of DNA with new primers, 2 – 10ng of DNA with new primers, 3 – 10ng of DNA with old primers, 4 – 5ng of DNA with old primers, 5 – 5ng of DNA with new Taq Polymerase, 6 – 5ng of DNA with new Ultrapure Water, 7 – Blank control, 8 – Empty, L – NEB Biolabs Low Molecular Weight Ladder.

Fig 15: Testing of fresh reagents using the Arnay-de-la-Rosa primers. All testing carried out with an annealing temperature of 50°C, using modern male DNA.

As shown in Figure 15, the trend of no amplification of the expected 66 and 72bp fragments has continued. Primer dimer bands have failed to form in lanes 3,4 and 5, while weak primer dimer bands have formed in lanes 1 and 2. This indicates that an issue with the older primers was likely causing a failure to bind, resulting in a lack of amplification. The new primers can successfully bind and amplify, even if only with each other in this instance. Interestingly, primer dimer bands have formed from the old primers in lanes 6 and 7. This may indicate an issue with the PCR grade water that was used in previous experimentation, that had been replaced for Lane 6. Therefore, a decision was made to attempt a PCR with entirely new reagents,

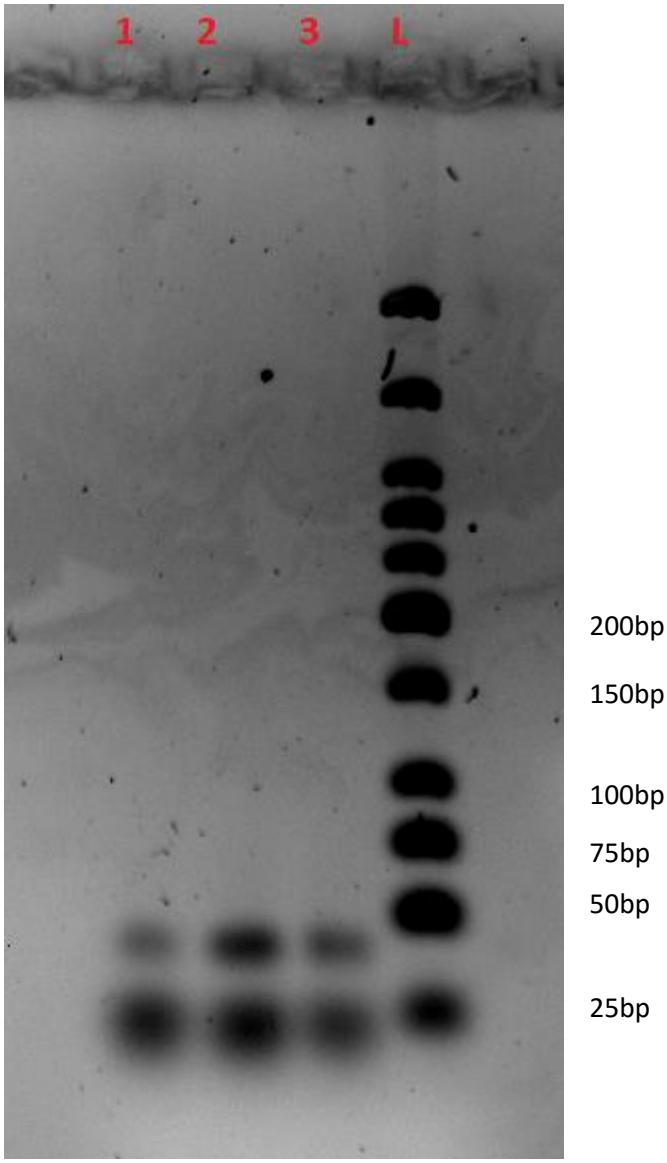

Gel Key: 1 – 5ng of DNA with entirely new reagents, 2 – 10ng of DNA with entirely new reagents, 3 – blank, L – NEB Biolabs Low Molecular Weight Ladder.

Fig 16: Testing the Arnay-de-la-Rosa technique using entirely new reagents including; new primers, new ultrapure water, and new Taq Polymerase. All testing carried out using modern male DNA.

As shown in Figure 16, there are still no banding patterns at 66 and 72bp in size, indicating that the method is still failing to provide any amplification. At this point, due to the consistent failures occurring through the use of the Amel-A and Amel-C primers suggested in Arnay-de-la-Rosa, it was decided that the best course of action would be to change the primers to the more established AmpFISTR Identifiler primers, which proved to be much more effective. The development of a PCR technique using these primers can be seen in Section 4.3.

4.3. Identifiler Technique

The final Identifiler PCR technique was the product of much testing and development. The development of the technique can be seen in the results below.

4.3.1. Testing the Identifiler Technique

Initial tests of the Identifiler primers showed promising results compared to the Arnay-de-la-Rosa primers. The first tests can be seen in Figs 17 & 18 overleaf.

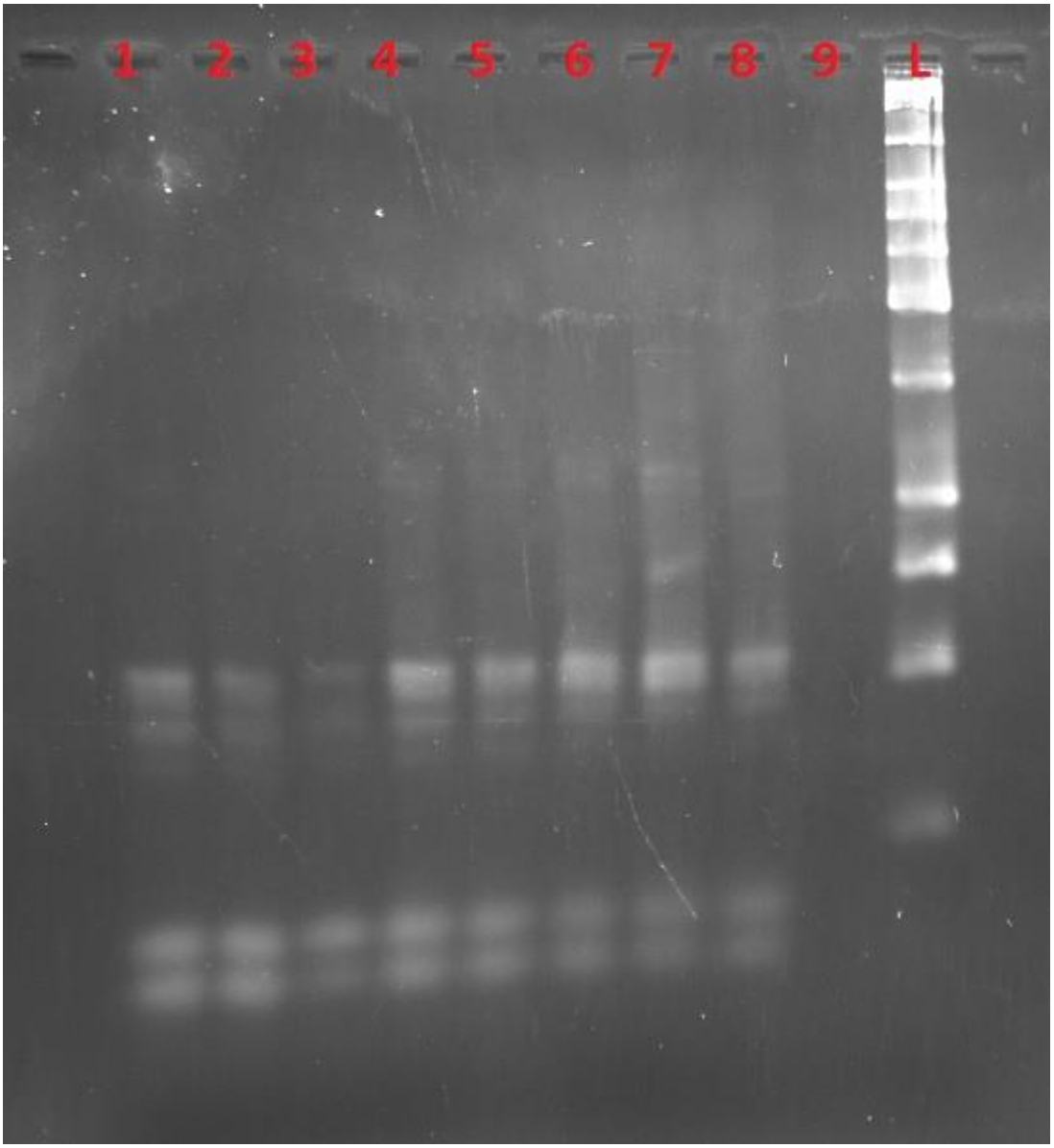

Gel Key: 1 - 63°C annealing temperature, 2 – 62.5°C annealing temperature, 3 – 61.6°C annealing temperature, 4 – 60.3°C annealing temperature, 5 – 58.7°C annealing temperature, 6 – 57.4°C annealing temperature, 7 – 56.5°C annealing temperature, 8 - 56°C annealing temperature, 9 – empty, L – New England Biolabs (NEB) Low Molecular Weight Ladder. Note: A blank was not used in this instance as the tested DNA belonged to the researcher. Personal contamination would not affect the result.

Fig 17: Initial testing of the Identifiler Primers. All testing was carried out with 5ng of modern male DNA as the template. Bands can be seen in lanes 4-8 at 106 & 112bp in length.

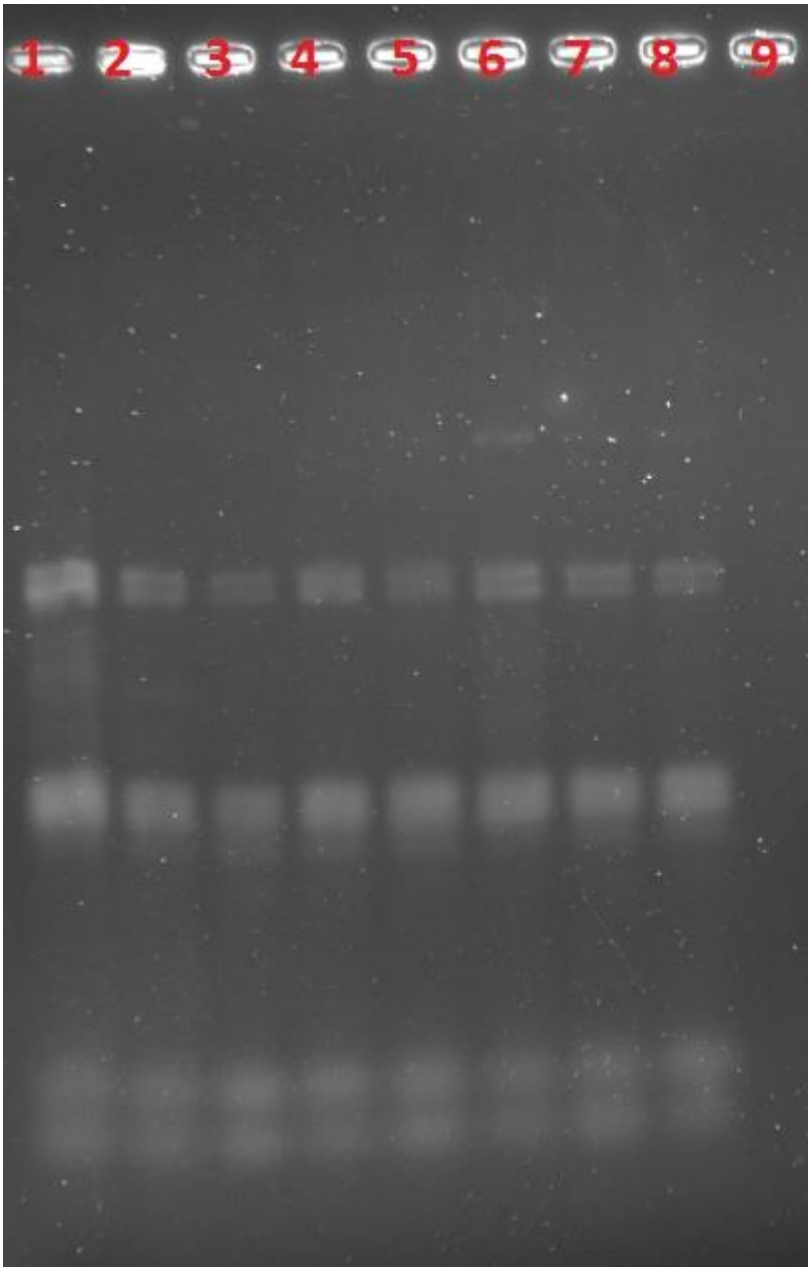

Gel Key: 1 - Gel Key: 1 - 63°C annealing temperature, 2 – 62.5°C annealing temperature, 3 – 61.6°C annealing temperature, 4 – 60.3°C annealing temperature, 5 – 58.7°C annealing temperature, 6 – 57.4°C annealing temperature, 7 – 56.5°C annealing temperature, 8 - 56°C annealing temperature, 9 – empty. Note: A blank was not used in this instance as the tested DNA belonged to the researcher. Personal contamination would not affect the result.

Fig 18: Initial testing of the Identifiler primers. All testing was carried out with 10ng of modern male DNA. Bands can be seen in lanes 1-8 at 106 & 112bp.

From the results of Figs 17 & 18, it was determined that 10ng of DNA provided a much better amplification than 5ng of DNA. This can be seen from the much clearer banding patterns provided in Fig 18. 61°C was chosen as the most effective annealing temperature

due to the presence of banding in both the 10ng and 5ng tests around 60-61°C. In Fig 18, the test at 61.6°C (Lane 3) provided the clearest bands with no non-specific binding, indicating a good specificity and strong amplification. However, in Fig 17, no amplification was recorded at 61.6°C, indicating that the yield at this temperature is quite low. Banding is shown at 60.3°C in Fig 17 (Lane 4), which indicates that the amplicon yield is only slightly too low at 61°C to provide amplification from 5ng of target DNA. The strong banding provided when using 10ng of target DNA demonstrates that this issue is not a problem with higher concentrations of DNA. It was also noted that primer dimers formed in every amplification conducted, at approximately 50bp in size. The production of primer dimers competitively inhibits the amplification of target DNA, and as such, further PCRs were carried out with varying levels of $Mg2^{+}$ ions in order to improve the efficiency of the amplification reaction.

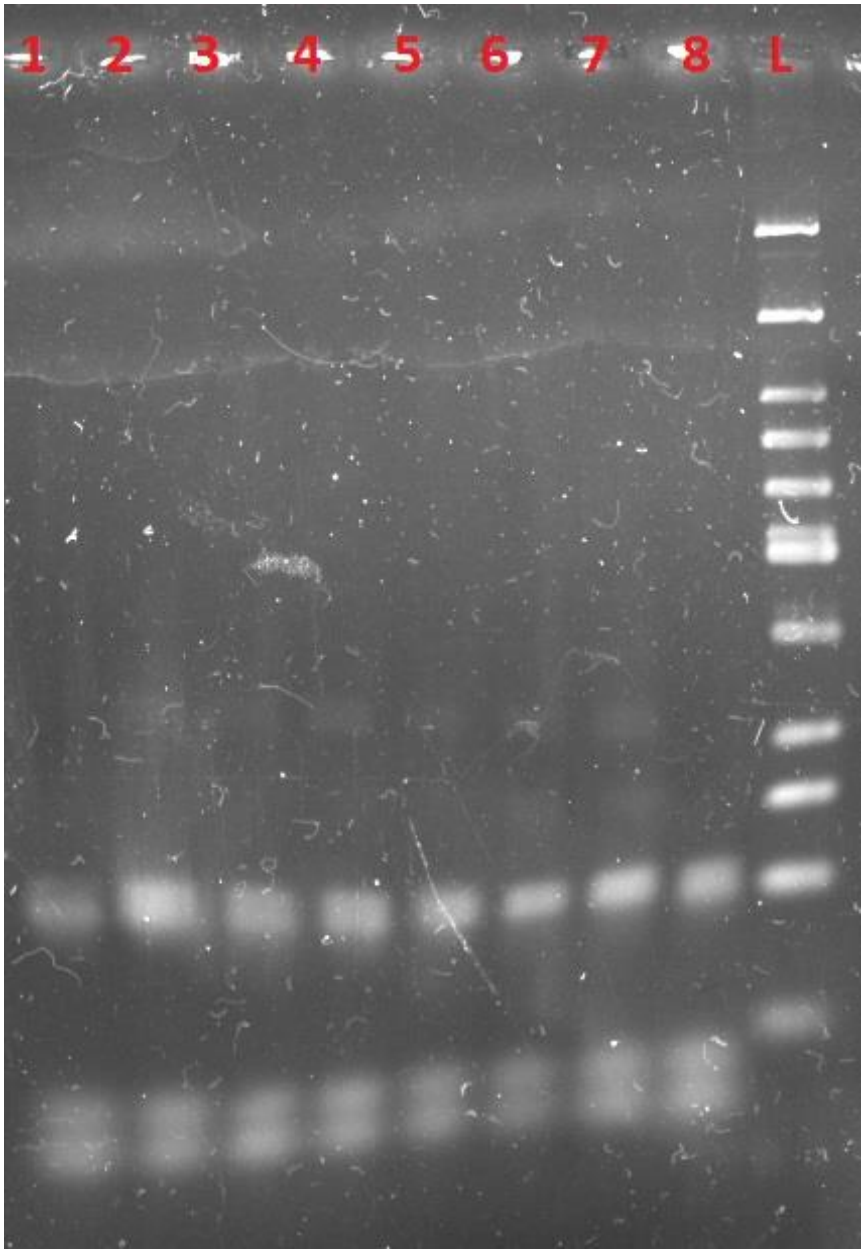

Gel Key: 1&2 – 1mM Mg^{2+} ions, 3&4 - 2mM Mg^{2+} ions, 5&6 - 3mM Mg^{2+} ions, 7&8 - 4mM Mg^{2+} ions, L – NEB Low Molecular Weight Ladder.

Fig 19: Results of varying the level of magnesium ions (Mg^{2+}) in the PCR solution. All tests carried out with 10ng modern DNA and an annealing temperature of 61°C.

As shown in Fig 19, varying the level of Mg^{2+} ions did very little to affect the production of primer dimers. Consistent amplicons intensity was seen throughout, so the decision was made to continue with the standard 1.5mM concentration of Mg^{2+} ions found in the Taq 2x Mastermix. The production of primer dimers acted in a similar fashion to an internal standard in further testing, due to the presence of strong dimer bands in every successful amplification.

4.3.2. Artificially Degraded Modern DNA

Following the optimisation of the Identifiler PCR technique, a gel was produced to compare the intensity of amplicons recovered from unaltered modern DNA, artificially degraded modern DNA, ancient bone spiked with modern DNA, and unaltered ancient bone. This was to identify the presence of PCR inhibitors in the ancient bone and identify any issues with PCR amplification of degraded DNA without any inhibition.

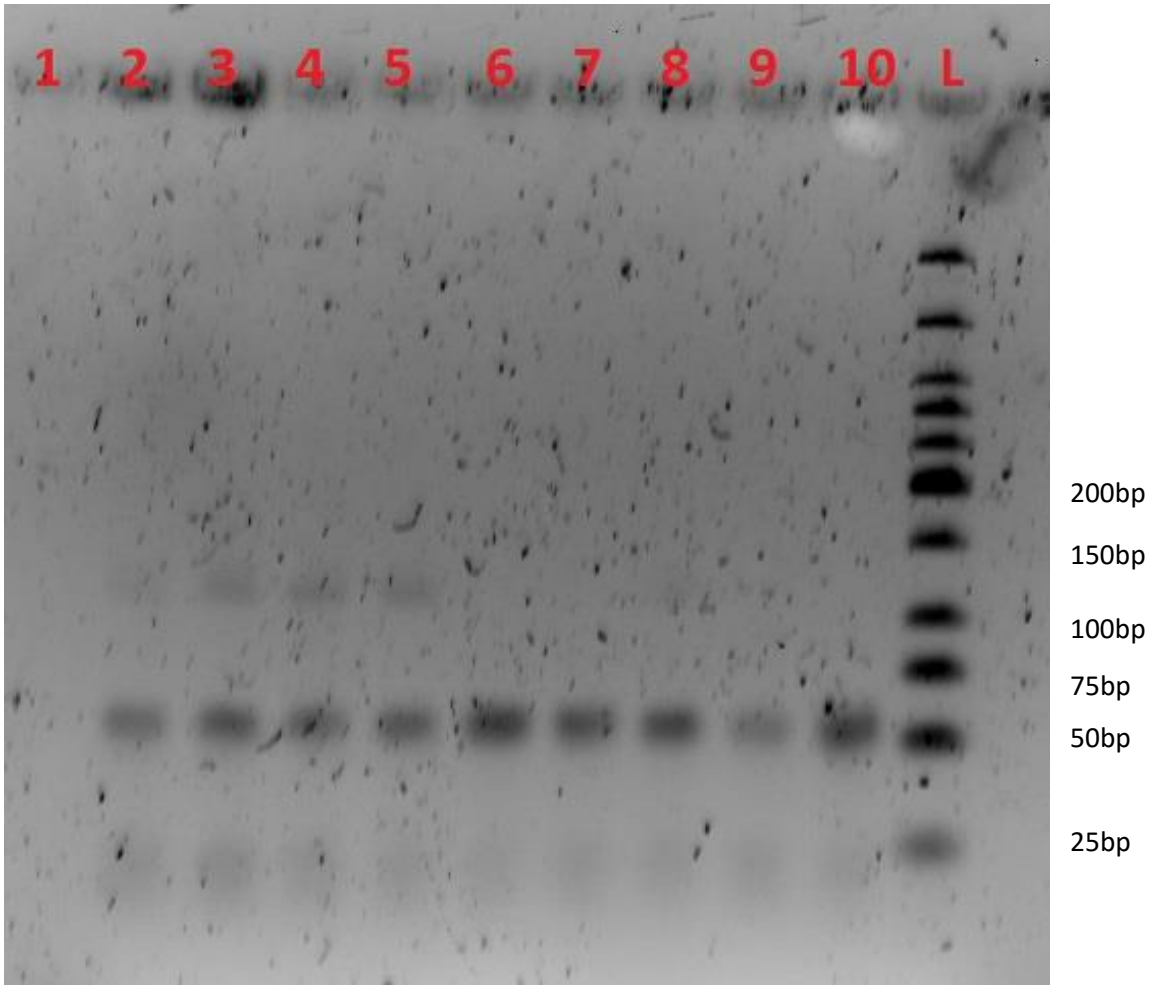

Gel Key: 1 – Empty, 2&3 – 10ng Modern male DNA, 4&5 – 10ng Modern DNA, ultrasonicated for 15 minutes at 44kHz, 6&7 – DNA extraction from ancient bone with 10ng Modern male DNA added, 8&9 – 10ng male ancient DNA extracted from bone, 10 – Blank, L – NEB low molecular weight ladder.

Fig 20: A comparison between the amplicons intensity of modern bone, artificially degraded modern DNA, ancient bone spiked with modern DNA, and original ancient DNA.

As shown in Fig 20, amplification was successful with both normal modern DNA and artificially degraded DNA. However, no amplicons were detected in DNA recovered from ancient bone material, even when spiked with modern DNA. This indicates that the

Identifiler primers are capable of amplifying heavily degraded DNA with short fragment length, broken down to approximately 100-500bp in size (Elsner & Lindblad, 1989). However, the lack of amplification in lanes 6-9 indicates there is inhibition of PCR amplification caused by the introduction of ancient bone material. The discovery of this phenomenon led to the use of inhibitor removal kits, the results of which can be seen in Section 4.3.3.

4.3.3. Inhibitor Removal

Initial tests were carried out with three different inhibitor removal kits. The results of these tests can be seen below.

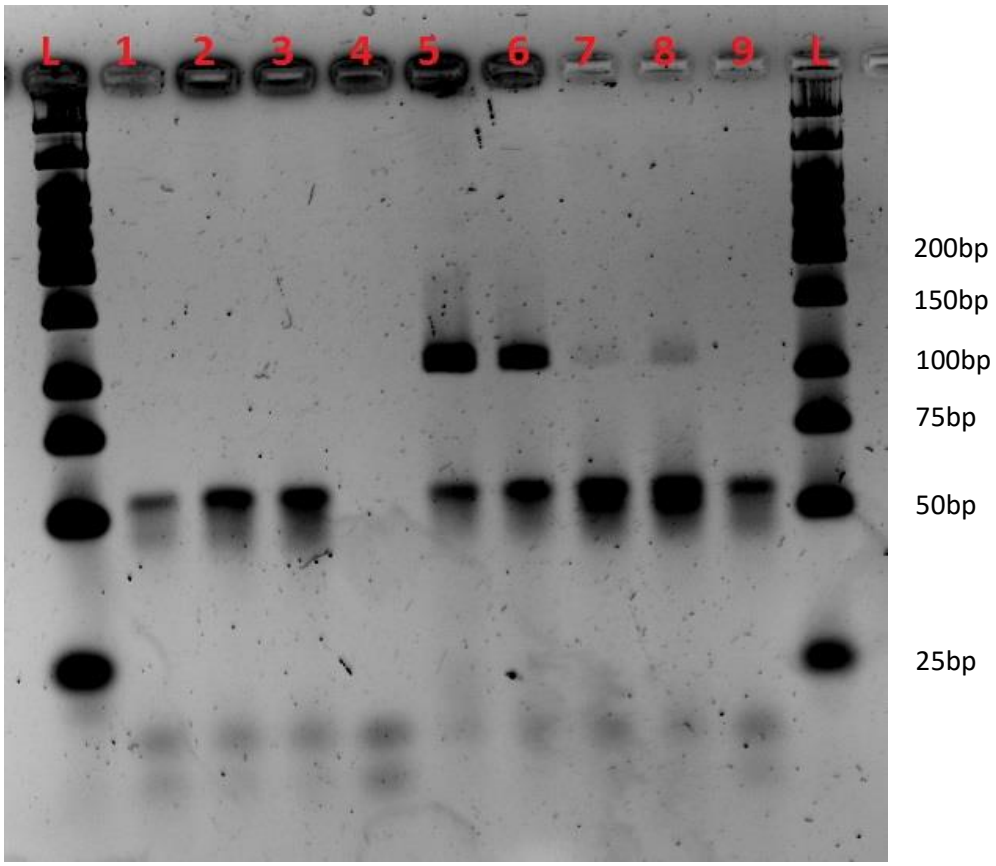

Gel Key: L – NEB Low Molecular Weight Ladder, 1&2 – No Cleanup, 3&4 – OneStep PCR Cleanup Kit, 5&6 – PowerClean for Ancient DNA, 7&8 – PowerSoil, 9 – Blank, L – NEB Low Molecular Weight Ladder. Note that all testing was carried out with 10ng of modern male DNA spiked into an extraction of ancient male DNA.

Fig 21: Comparison between the amplicons strengths generated from PCRs pre-treated with the OneStep, PowerClean and PowerSoil inhibitor removal kits.

It can be seen from the lack of bands at the target region in Fig 21 above that the OneStep inhibitor removal kit is ineffective in removing sufficient inhibitory substances to allow for

amplification. In one instance, shown in lane 4, inhibition was so severe that primer dimers could not form. The PowerClean and PowerSoil kits were both effective in removing inhibitors, but much stronger amplicon intensity was achieved with the PowerClean kit.

A further test was carried out, using 5ng of spiked modern DNA. By reducing the concentration of modern DNA, the proportion of ancient bone extract was increased in the final PCR volume. This would simultaneously increase the amount of inhibitors in the sample and reduce the mass of target DNA, making the sample more difficult for the inhibitor removal kits to clean-up. This test was used to determine whether the PCR clean-up kits would be sufficient to allow for amplification even in sub-optimal conditions.

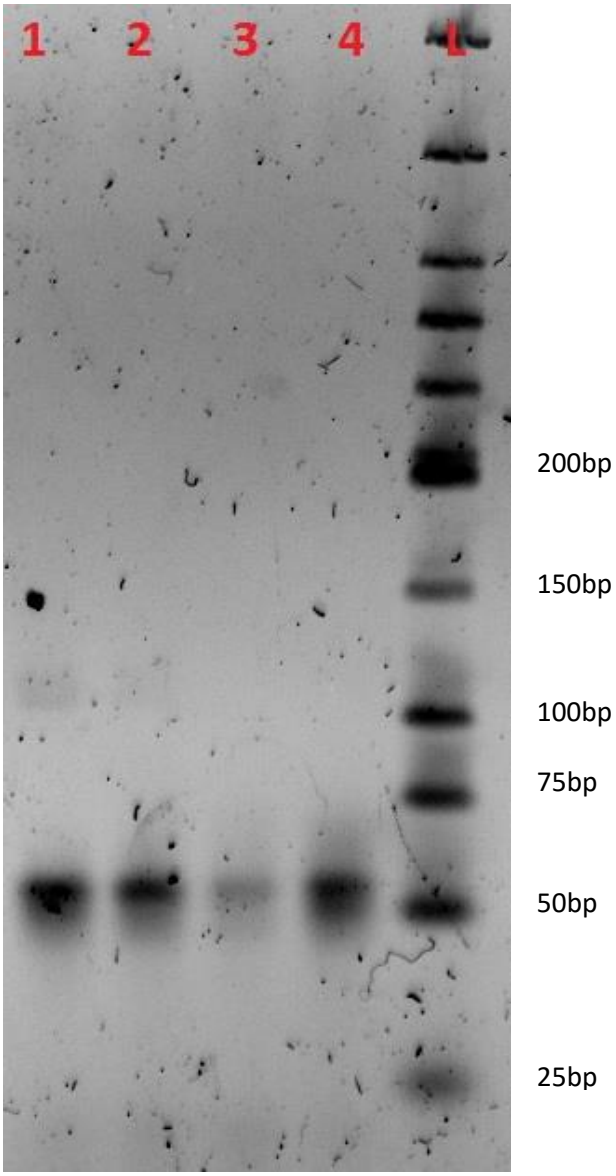

Gel Key: 1 – PowerClean Kit, 2 – PowerSoil Kit, 3 – OneStep Kit, 4 – No Cleanup, L – NEB Low Molecular Weight Ladder. All tests carried out with 5ng of modern male DNA spiked into an extraction of ancient male DNA from bone.

Fig 22: Comparison of cleanup kits with 5ng of modern DNA, demonstrating sub-optimal PCR conditions.

As shown in Fig 22, the PowerClean kit still provided two individual visible bands, indicating that the kit is beyond sufficient for the removal of inhibitors in ancient skeletal material. The PowerSoil kit provides very faint bands, indicating that some DNA has been amplified. However, the bands are so faint that it would be difficult to identify the number of bands present and their individual sizes. The OneStep kit has failed to provide any DNA amplification and again shows weaker primer dimerisation than the control sample with no

clean-up kit used. This may indicate that the process used in the OneStep cleanup kit actually reduces PCR efficiency compared to using no PCR cleanup kit at all.

4.4. Neonatal Remains

Once the technique had been tested and optimised, DNA was extracted and amplified from the Romano-British neonatal remains themselves. The results of these can be seen in the gel images overleaf.

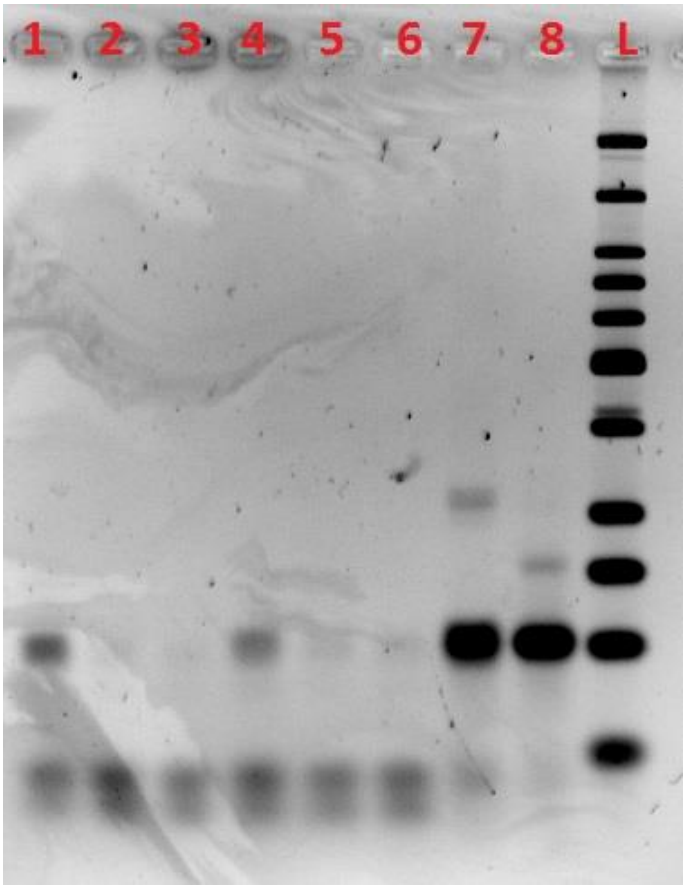

Gel Key: 1 – SK27844, 2 – SK26500, 3 – SK27449, 4 – SK25262, 5 – SK25729, 6 – SK25575/25576, 7 – Male Positive Control, 8 – Blank, L – NEB Low Molecular Weight Ladder.

Fig 23: Neonatal results 1-6. All tests carried out with 10ng of ancient DNA.

No target amplicons can be seen in these neonatal remains. There is also a lack of strong primer dimer formation in lanes 2, 3, 5, and 6 which indicates possible inhibition in these cases. However, lanes 1 & 4 show strong primer dimer formation. This indicates a variable level of inhibition in the samples, possibly due to variations in bone density affecting the uptake of humic compounds from the soil. There is also a contaminant band present in the negative control sample, at approximately 76bp in length. This contaminant is of unknown source and does not correlate with the expected alleles for the amelogenin gene being amplified. It is possible that this amplicon is due to non-specific binding to a contaminant DNA sample, yet it would be expected that if this were the case then bands would also appear at 106 and 112bp in length. If the non-specific band is competitively inhibiting the standard X/Y alleles that would be expected in a contaminant sample, then this should also occur in the positive control samples which are subjected to the same PCR conditions. Therefore, it appears that this band is from a contaminant DNA sequence which provides a 76bp long fragment from these primers.

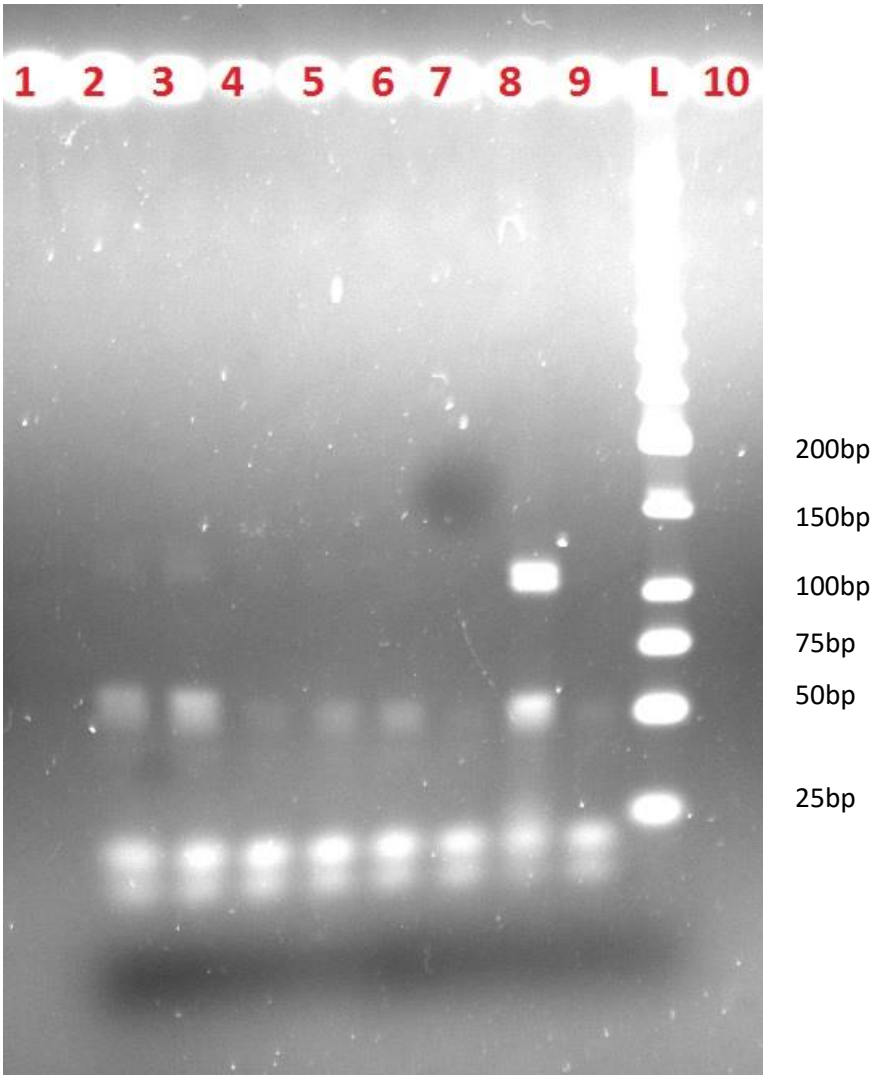

Gel Key: 1 – Empty, 2 – SK26846, 3 – SK25544, 4 – SK27325, 5 – SK25572, 6 – SK25165, 7 – Sk25213, 8 – male positive control, 9 – Blank, L – NEB Low Molecular Weight Ladder, 10 – Empty

Fig 24: Neonatal results 7-12. All tests carried out with 10ng ancient DNA.

The results in lane 2 & 3 above show faint banding at 106 and 112bp in length, indicating a male genotype for skeletons SK26846 and SK25544, respectively. The negative control in lane 9 has no amplicons, indicating a lack of contamination. As in Figure 23, there is a variation in the intensity of primer dimer formation. Therefore, this may indicate inhibition has still occurred in samples 4-7, especially in samples 4 and 7 which show very weak primer dimer formation.

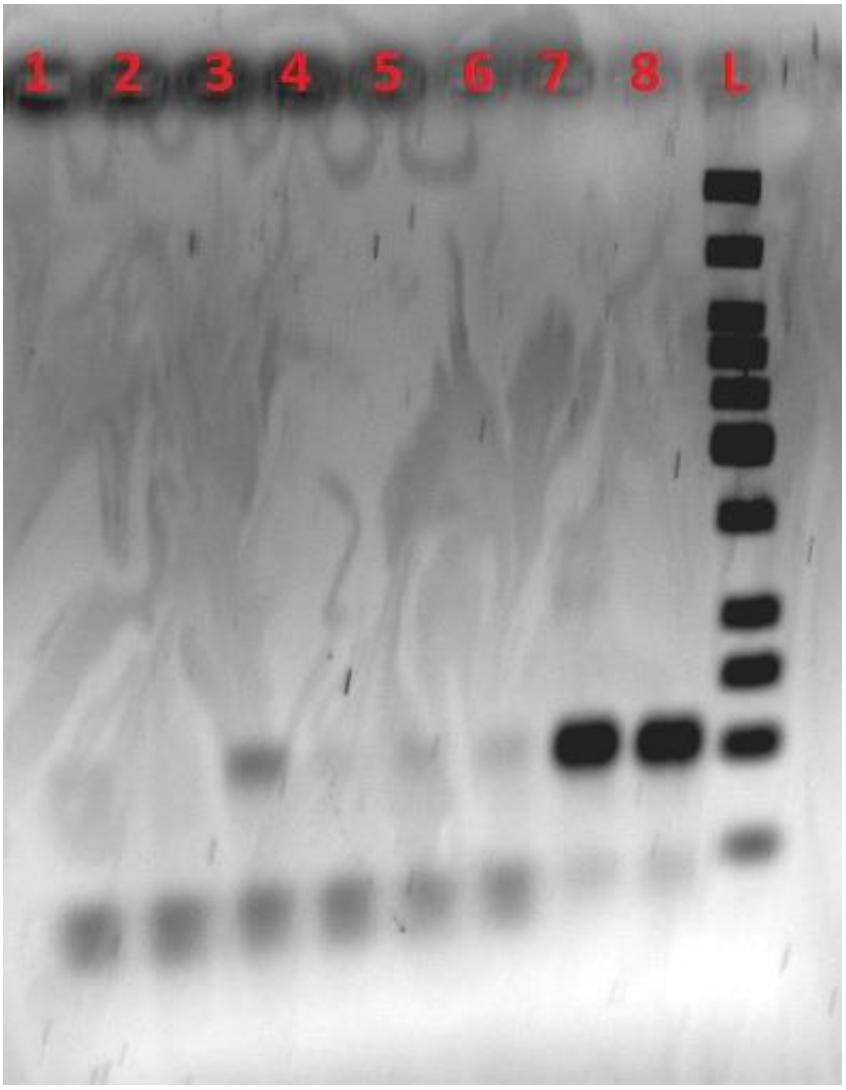

Gel Key: 1 – SK26320, 2 – SK27925, 3 – SK27447, 4 – SK27743, 5 – SK28224, 6 – SK26926, 7 – male positive control, 8 – blank, L – NEB Low Molecular Weight ladder.

Fig 25: Neonatal results 13-18. All tests carried out with 10ng of Ancient DNA.

The results shown in Figure 25 indicate that inhibition has had a strong effect on the amplification of DNA from these neonatal remains. Faint primer dimers are seen in lanes 1 & 2 and 4-6, indicating inefficient amplification. Lane 3 shows stronger primer dimer formation, but no amplicons for the 106 & 112bp target bands. No target amplicons are seen in any of the ancient DNA samples and the positive control shown in lane 7 is also faint compared to previous results. Therefore, this may indicate that the PCR used to amplify these samples has worked poorly.

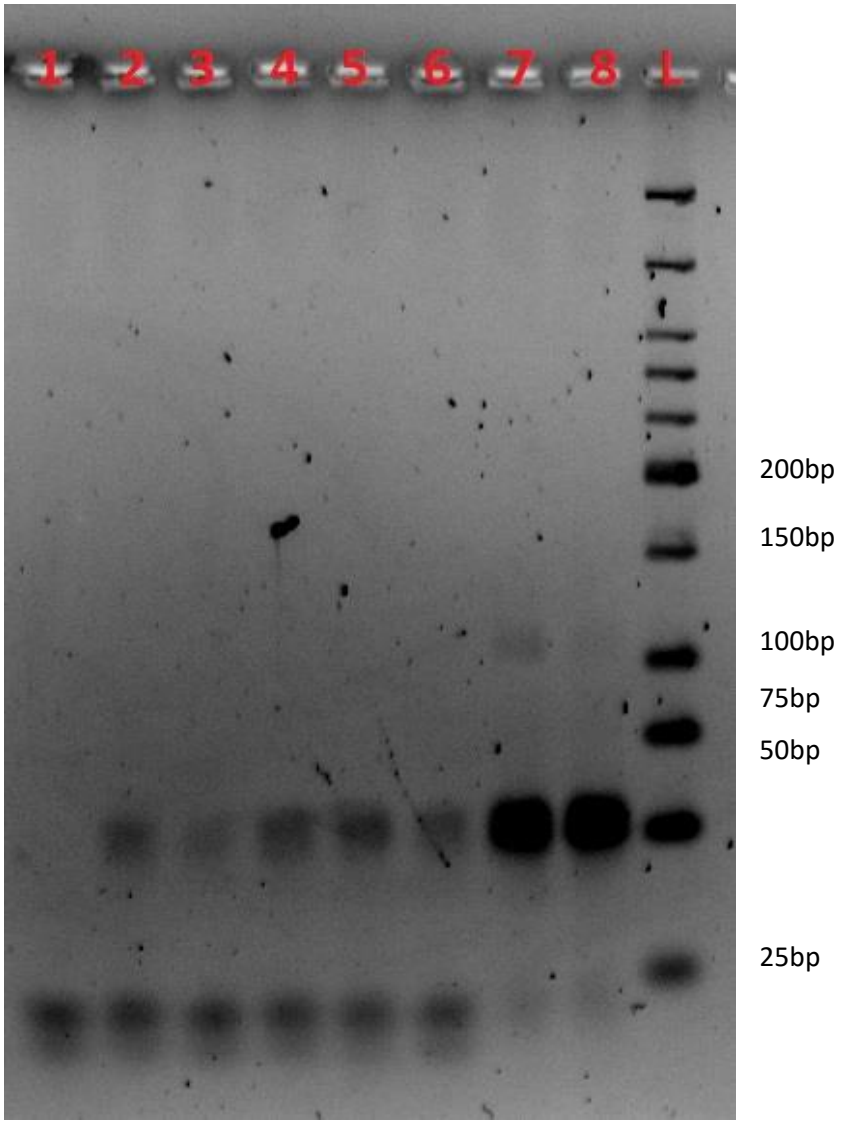

Gel Key: 1 – SK22684, 2 – SK25368, 3 – SK25167/25168, 4 – SK31225, 5 – SK25245/25244, 6 – SK27927, 7 – male positive control, 8 – blank, L – NEB Low Molecular Weight Ladder.

Fig 26: Neonatal results 19-24. All tests carried out with 10ng of Ancient DNA.

The results seen in Figure 26 show the presence of a faint contaminating DNA sequence in the blank sample, in lane 8. However, this contaminant is not seen in the ancient DNA amplifications shown in lanes 1-6. Primer dimers in lanes 2-6 are quite strong, indicating that inhibition has not had a great effect on these amplifications, yet no amplicons are seen. This may indicate that there is an insufficient level of amplifiable DNA in the neonatal remains and that the contaminant in the blank sample has not also contaminated the neonatal remains. However, it is more likely that while the levels of inhibition have not been sufficient to cause poor amplification of primer dimers, it has been sufficient to inhibit the low levels of ancient or contaminant DNA. The effect of this inhibition can be seen more

clearly in lane 1, where no amplification has succeeded and primer dimers are not present, indicating a strong level of inhibition.

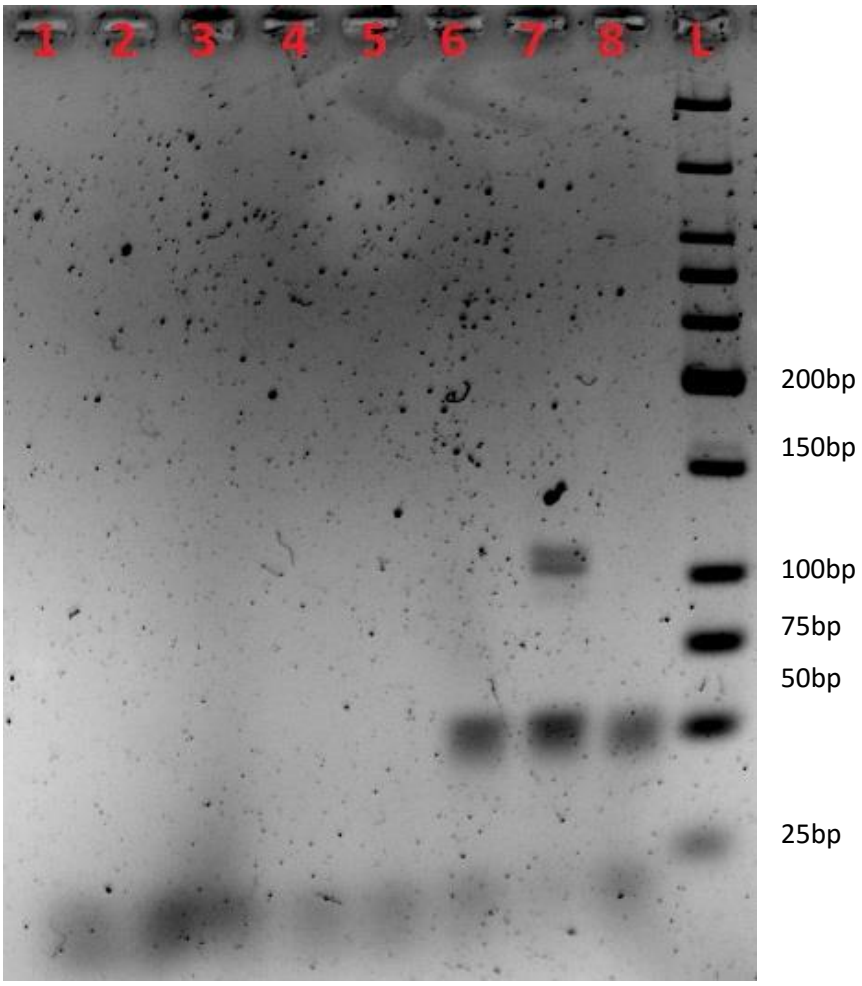

Gel Key: 1 – SK31089, 2 – SK25236, 3 – SK26201, 4 – SK27935, 5 – SK25149, 6 – SK27970, 7 – Male Positive Control, 8 – Blank, L – NEB Low Molecular Weight Ladder.

Fig 27 – Neonatal Results 25-30. All tests carried out with 10ng of Ancient DNA.

It can be seen from Figure 27 that inhibition is prevalent in these neonatal remains. Lanes 1-5 show no primer dimer formation, indicating severe inhibition. However, lane 6 shows clear primer dimer formation, with bands as strong as those found in the control samples, and as such does not appear to have been inhibited. The control samples themselves show strong and banding at 106 & 112bps in the positive control, and a clear blank. No targeted amplicons are present in the neonatal samples, but with the level of inhibition present this does not indicate that no amplifiable DNA is present in these samples.

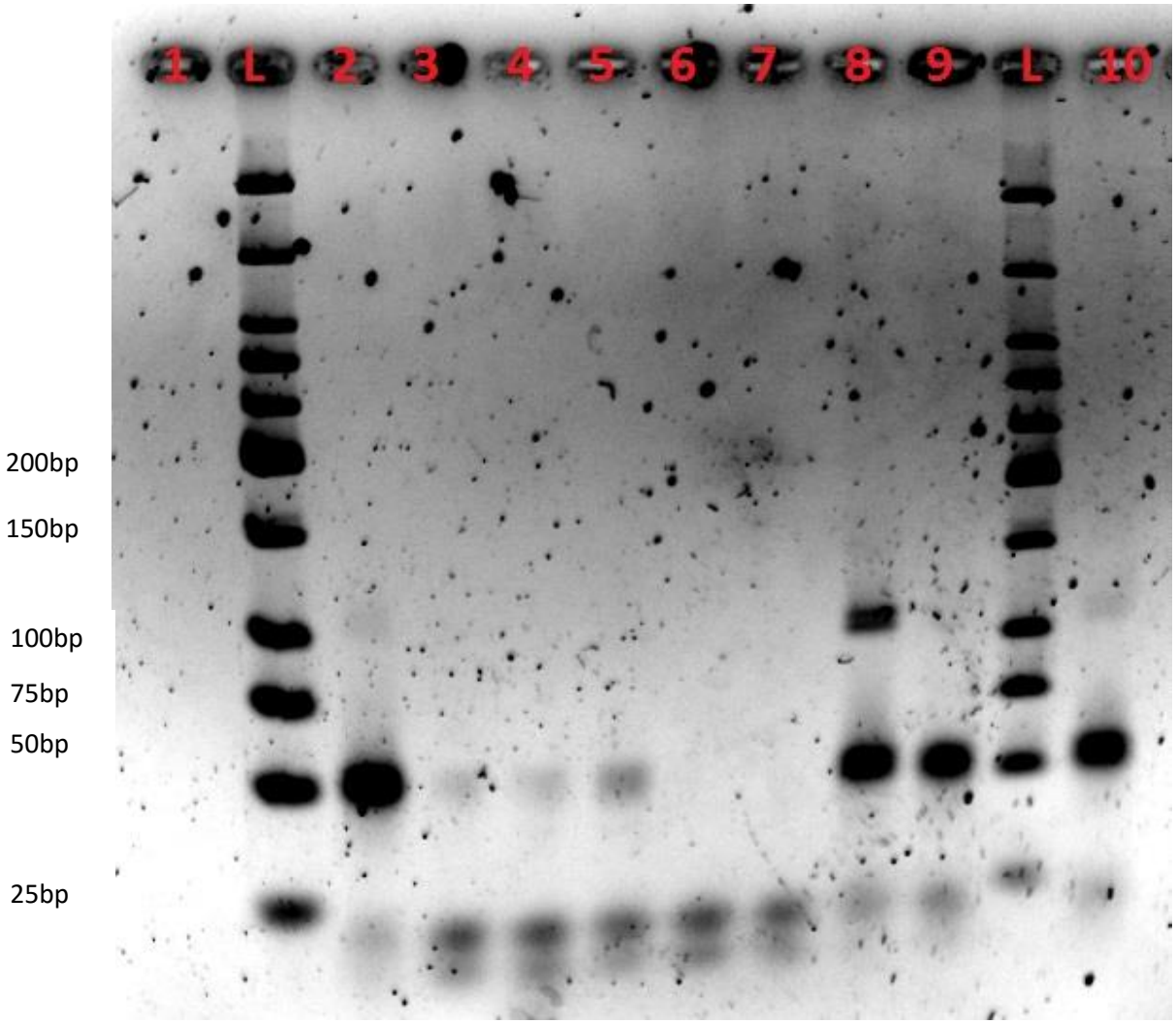

Gel Key: 1 – Empty, L – NEB Low Molecular Weight Ladder, 2 – SK25272, 3 – SK26414, 4 – SK25297, 5 – SK25105, 6 – SK25244, 7 – SK25208, 8 – Male Positive Control, 9 – Blank, L – NEB Low Molecular Weight Ladder, 10 – Repeat of SK25272 (Lane 2).

Fig 28: Neonatal results 31-36. Result 31 (SK25272) was repeated in Lanes 2 and 10, due to a feared pipetting error in lane 2. All testing carried out with 10ng of Ancient DNA.

Figure 28 shows a mixture of PCR effectiveness. Lanes 6 and 7 show no banding for primer dimer formation and therefore a strong inhibitor effect is present in these amplifications. This is further evidenced by the lack of target DNA amplification in these samples. Lanes 3-5 show faint primer dimer formation and no amplification of target DNA. This indicates that inhibition has been present to a lesser extent than in lanes 6 and 7, but has still been of sufficient intensity to prevent the amplification of any DNA.

Lanes 2 and 10 both show repeats of SK25272. This is not a repeated amplification, but a repeated electrophoresis of the same PCR product. This was carried out due to a feared pipetting error in lane 2, in which it was assumed that insufficient PCR product was added to

create visible bands. Therefore, further PCR product was pipette into lane 10 in order to ensure that the result would not be lost. SK25272 shows very strong primer dimer banding, indicating a good level of amplification. In Lane 2, the banding at the target DNA site is quite faint and is difficult to differentiate into one or two clear bands to identify whether the genotype is XX or XY, but the banding in lane 10 is clearly separated into two bands that indicate an XY genotype. The negative control shown in lane 9 does not have any amplification at the target DNA site, which indicates that the banding achieved from the amplification of ancient DNA from SK25272 is a genuine genotype for the neonatal remains.

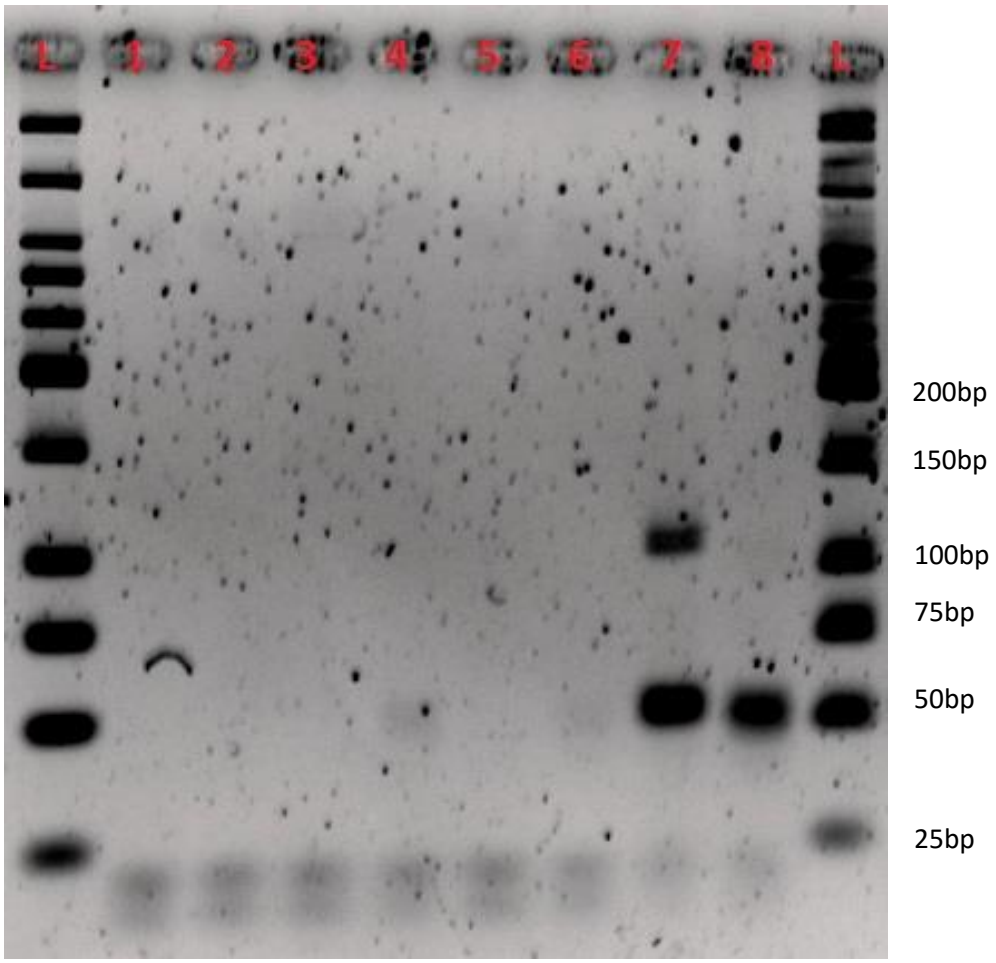

Gel Key: L – NEB Low Molecular Weight Ladder, 1 – SK26851, 2 – SK27774, 3 – SK25209, 4 – SK33056, 5 – SK27392, 6 – SK26934, 7 – Male positive control, 8 – Blank, L – NEB Low Molecular Weight Ladder

Fig 29: Neonatal results 37-42. All testing carried out with 10ng of ancient DNA.

The results of Figure 29 show a strong inhibitor presence in these remains. Primer dimers are not present in lanes 1, 2, 3 and 5, due to strong inhibition preventing amplification. Lanes 4 and 6 show some primer dimer formation but the bands are very faint, indicating

that the PCR has been very sub-optimal. All of the lanes 1-6 show strong banding for the primers themselves at the very bottom of the gel image, at <25bp in length. This indicates that sufficient levels of primer have been added to the reaction, but no amplification has occurred. No target DNA amplification has been successful from the neonatal remains. However, the positive control shows strong bands and the blank shows no contaminating DNA sequence.

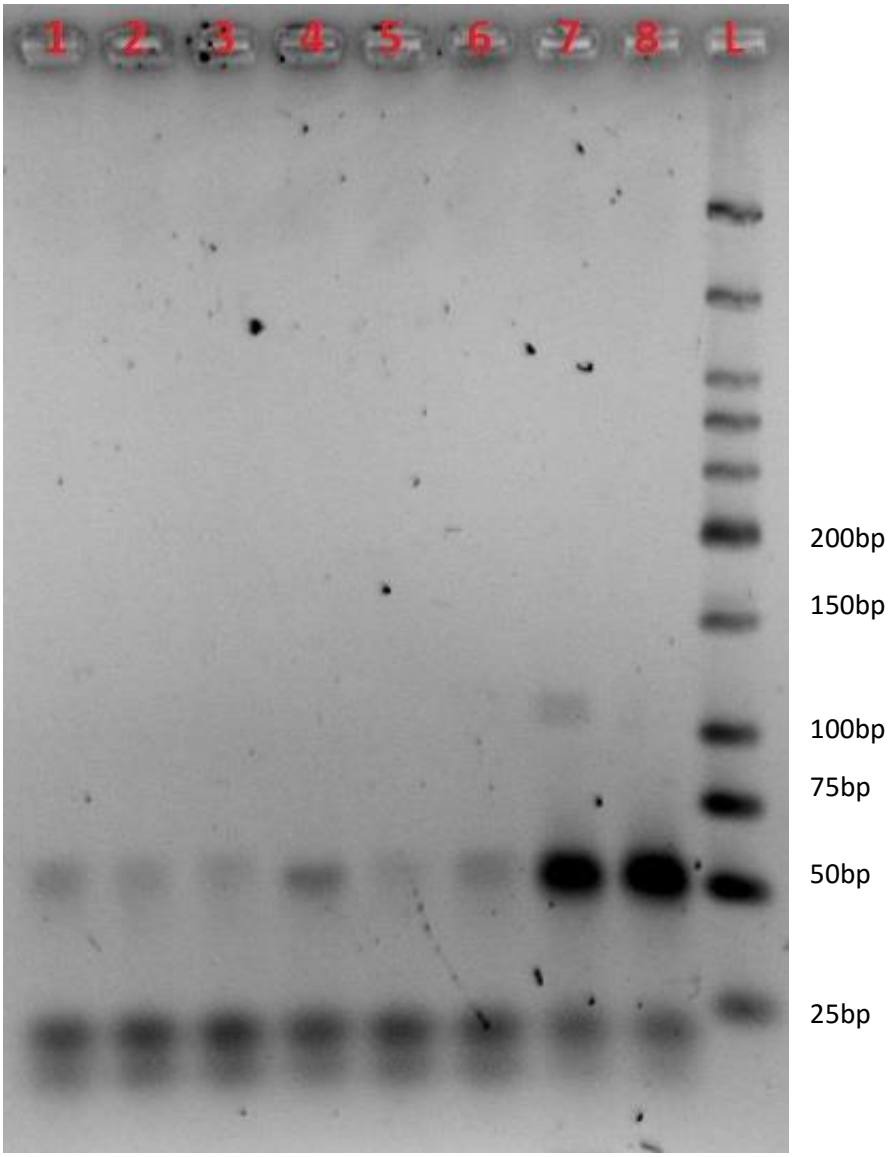

Gel Key: 1 – SK27771, 2 – SK26615, 3 – SK51508, 4 – SK31061, 5 – SK27938, 6 – SK25251, 7 – Male positive control, 8 – Blank, L – NEB Low Molecular Weight Ladder.

Fig 30: Neonatal results 43 – 48. All testing carried out with 10ng of ancient DNA.

It can be seen in Figure 30 that there are low levels of inhibition present in the neonatal amplifications. The primer dimers are present and are generally of a reasonable strength. Lane 4 shows quite a strong primer dimer band, while lane 5 shows quite a weak band. However, inhibition has not been sufficient to completely prevent primer dimer formation. The positive control shown in lane 7 is clearly defined and at the correct length and the negative control is clear with no amplification. However, there are no target DNA bands present from the neonatal amplifications. The low-level inhibition may have caused the lack of DNA amplification from these remains, or there may simply be very amplifiable target DNA in these remains that can be recovered.

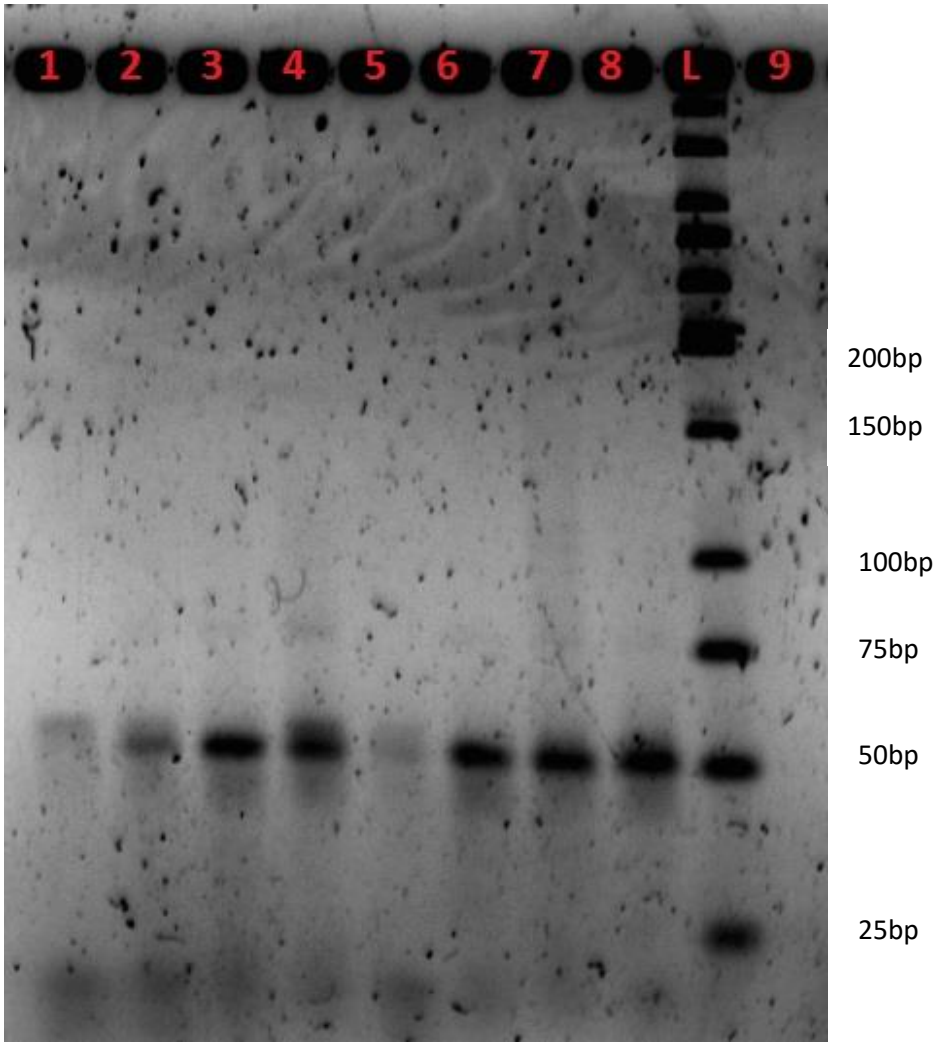

Gel Key: 1 – SK25471, 2 – SK51506, 3 – SK25570, 4 – SK51510, 5 – SK31118, 6 – SK26836, 7 – Male Positive Control, 8 – Blank, L – NEB Low Molecular Weight Ladder, 9 – Empty.

Fig 31: Neonatal results 49-54. All testing carried out with 10ng of ancient DNA.

Figure 31 shows interesting results. The male positive control bands are very faint, with some smearing present that has caused the whole of lane 7 to appear darker in colour, making it difficult to identify the faint bands against the background. This smearing may be due to DNA degradation, yet this should not occur in freshly extracted modern DNA. An alternative explanation is protein contamination due to improper DNA extraction, or a high salt content in the DNA preparation. Due to the style of the chelex extraction, this is a more likely reason for the smearing of the DNA in lane 7. However, this smearing is also seen to a lesser extent in lane 4, which has been extracted using a completely different method and should not contain proteins or a high salt concentration. Therefore, it is possible that this smearing is due to the degradation of the ancient DNA.

Strong primer bands are seen in all lanes, indicating that inhibition has contributed to the lack of target DNA amplification. DNA has been amplified in lanes 2-4 and 6-8, showing the

75bp long contaminant fragment seen previously in Figure 23, above. Again, this band is seen in the blank, but also in some of the neonatal samples and in the positive control. The presence of the 75bp fragment in the positive control is alongside the two bands at 106 and 112bp, which are correctly located compared to the ladder, so this 75bp fragment is unlikely to be an anomaly in band migration due to denaturing or improper electrophoresis conditions. Therefore, it is likely that a extraneous DNA source has contaminated these samples and provided an unexpected band at this size.

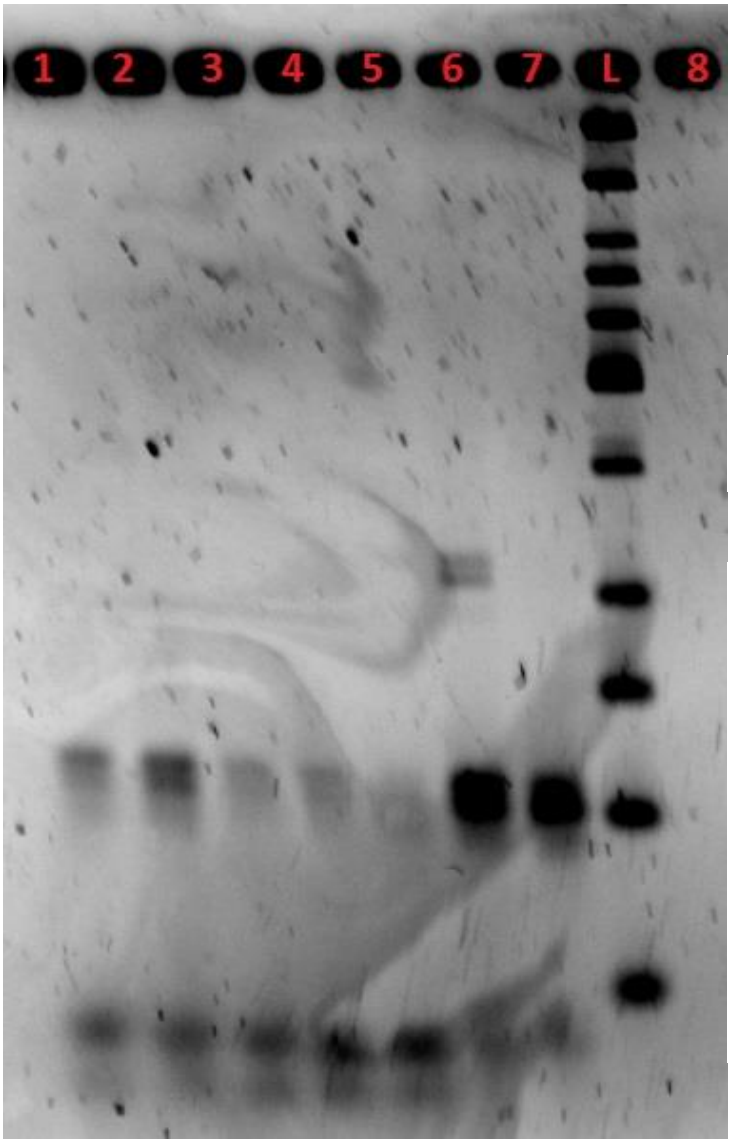

Gel Key: 1 – SK22668, 2 – SK26391, 3 – SK26937, 4 – SK25600, 5 – SK26855, 6 – Male positive control, 7 – Blank, L – NEB Low Molecular Weight Ladder, 8 – Empty.

Fig 32: Neonatal results 56-60. All testing carried out with 10ng of ancient DNA.

The results of Figure 32 show some loss of primer dimer band strength, indicating the presence of PCR inhibitors at a low level. Lane 5 has been most affected by inhibition, showing a very faint primer dimer. No target DNA has been amplified in the neonatal remains, possibly due to this inhibition. However, the positive control shows very good banding with clear resolution between the 106 and 112bp fragments, while the negative control shows no banding, indicating that these samples are clear from contaminant DNA.

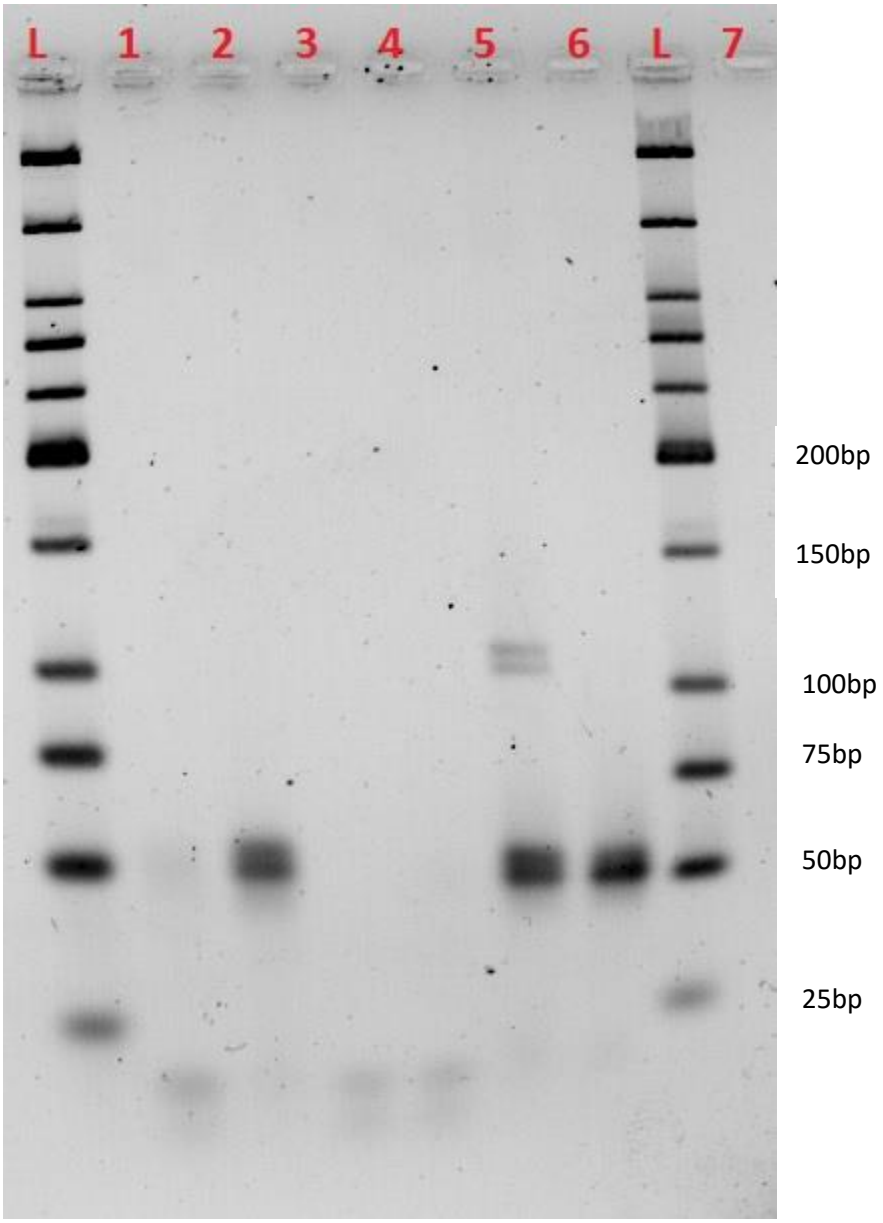

Gel Key: L – NEB Low Molecular Weight Ladder, 1 – SK27885, 2 – SK25164/25165, 3 – SK27628, 4 – SK53064, 5 – Male positive control, 6 – Blank, L – NEB Low Molecular Weight Ladder, 7 – Empty.

Fig 33: Neonatal results 61-64. All testing carried out with 10ng of ancient DNA.

The lack of primer dimer formation in lanes 3 & 4 of Figure 33 indicates a strong degree of inhibition that has likely contributed to the lack of target DNA amplification in these bands. Lane 1 has a faint primer dimer which also indicates a large amount of inhibition, again with no amplification of target DNA. Lane 2 shows strong primer dimer formation indicating a good PCR, but no amplification of the target DNA sequence. The positive control shows a good level of amplification with very clear bands showing good resolution between the 106

and 112bp fragments and the negative control shows no amplification of target DNA, indicating no contamination present in these results.

4.5. Summary of the Results

DNA recovery and amplification was successful from three of the neonatal skeletons. These skeletons are SK26846 (Fig 26, lane 2), SK25544 (Fig 26, lane 3), and SK25272 (Fig 28, lanes 2 & 10). While the removal of inhibitors has in many cases been successful, as shown by the presence of primer dimer formation, in some cases inhibition is still occurring to such a level that DNA cannot be amplified using this technique. Each of the three sets of DNA amplified have shown dual banding at 106 and 112bp in size, indicating the XY genotype of a male individual. This may indicate possible contamination, as the researcher involved in the recovery and amplification of the DNA was also male. However, the corresponding extraction blanks for these extractions and amplifications do not show contaminants.

5. Chapter Five: General Discussion

5.0. Metric Measurements & Age Determination

The initial investigation was to take accurate measurements of the neonatal remains that were to be destructively tested in order to reduce the effect of the loss of bone material on further study and to gain insight into the correlation between juvenile age and DNA recovery.

Damage to the bone was a serious problem in the measurement of the remains. The very fragile nature of infant and neonatal bone means that it is often damaged over time in a burial site, or during the excavation itself (Manifold, 2012). In this collection, 47.5% of the petrosas measured had damage that prevented a full measurement of either the length or width and 7.5% of the petrosas had damage preventing full readings of both measurements, for a total of 55% of petrous portions showing some form of damage that interfered with age determination.

This problem was amplified in the measurements of post-cranial bones that were carried out in instances where the petrosa was missing or heavily fragmented. 24 bones were measured in these circumstances, with both length and width measurements taken, for a total of 48 measurements. Of these, 15 (31%) of measurements were incomplete due to damage and 18 (38%) of measurements simply could not be carried out due to missing structures. 4 (16%) of the individuals had such severe damage to their skeleton that no age calculation could be provided, while 11 (46%) of the individuals could only have a minimum age provided, due to missing structures and incomplete measurements. Only 8 (33%) of the individuals could have an accurate age range provided from complete measurements.

This demonstrates one of the serious issues with working with juvenile, infant, or neonatal ancient remains. The small and gracile structure of the infant skeleton provides little strength when reduced to dry bone and is rapidly degraded when buried (Manifold, 2012). This causes problems with identification in both archaeological and forensic cases and highlights the need for genetic testing when working with juvenile remains.

Of the 47 individual skeletons which had intact bones allowing for a full combined age range determinations, 46 (98%) of the individuals showed an age range which fell either above, or included the age of 38 prenatal weeks. This 38 prenatal week age indicates a full term child following the definitions provided by Fehling et al (1907), modified by the research of Keiler et al (1995) and Bergsjø et al (1990). Of the remaining 13 skeletons which provided age ranges determined using incomplete measurements, a further 5 were at least 24 prenatal weeks of age. The potential youngest individual provided an age range of 18+ prenatal weeks, but as this was from one measurement of the incomplete and fragmented femur, it is likely that this individual is considerably older.

Therefore in total, 46 (72%) of the neonates examined are of a full term age, while another 8% of individuals indicating an age of above 24 weeks, the age at which a stillbirth is defined under the modern definition given in the Births and Deaths Registration Act (1926). It can therefore be said that at least 80% of the individuals shown in this sample were either stillborn or infant deaths. The remaining 20% of individuals may have been miscarriages, or may have been older than the incomplete age range has indicated and also have been stillborn or infant deaths.

5.1. Arnay-de-la-Rosa Primers

The first preliminary DNA work was carried out using the amelogenin primers described in the research of Arnay-de-la-Rosa (2007). These primers amplified two fragments of 66 and 72bp in length, with primer sequences that Arnay-de-la-Rosa had taken from earlier papers by Sullivan et al (1993) for the Amel-A primer and Maca-Meyer et al (2005) for the Amel-C primer. These primers were chosen due to the fact that the small amplicons that they produce should still be attainable from heavily degraded DNA which has broken down into <100bp fragments.

Arnay-de-la-Rosa met with success in 73.68% of cases, with 60% of cases working after the quantity of DNA in the PCR reagents had been doubled, and the remaining 13.68% of cases working after the DNA quantity had been further doubled for a total quadruple volume. However, due to the reporting of the methodology in the Arnay-de-la-Rosa paper, the actual mass of DNA used to attain successful results has not been published, only the volume of a DNA solution of unknown concentration.

My experimentation with the Amel-A and Amel-C primers used in Arnay-de-la-Rosa met with failure to amplify the target DNA. In very few instances, bands were produced at the target location with highly concentrated modern DNA, but these were both very faint in intensity and inconsistent in reproducibility. Substantial testing was carried out using the primers in multiple PCR conditions, including touchdown PCR to reduce the presence of non-specific binding which regularly occurred. However, no successful amplification could be achieved. This lack of amplification continued through the use of entirely new sets of reagents and modern DNA.

After considerable testing and modification of the protocol provided by Arnay-de-la-Rosa, it was determined that the primers were not effective in this experimentation. This may have been due to a susceptibility to inhibition, or a lack of effectiveness in amplifying degraded DNA.

5.2. Removal of Inhibitors

The Identifiler primers (Applied Biosystems) were substantially more successful in the amplification of DNA than the primers from Arnay-de-la-Rosa. However, while these primers could amplify modern DNA with an excellent success rate, the amplification of ancient DNA was substantially more difficult.

In a series of experimentation it can be seen in Figure 20 (Section 4.3.2) that inhibition was the primary issue in the amplification of DNA from skeletal material. Modern DNA amplifies very well and artificially degraded modern DNA that had been broken down to a similar fragmentation level as ancient DNA would also amplify to a similar intensity. However, no amplification was seen from DNA extracted from ancient material. Due to the fact that artificially degraded modern DNA would amplify, it is unlikely that the degradation of the DNA itself contributes much to the success rate of the Identifiler primer. Also, no amplification was seen in modern DNA that had been spiked into an ancient DNA extraction, which would indicate that some form of inhibitor that is co-extracted alongside the ancient DNA is preventing amplification of any DNA, even concentrated modern DNA.

In preliminary tests, the “PowerClean Kit for Ancient DNA” produced by MP Biomedicals provided strong amplification from samples of modern DNA that were spiked into ancient DNA extractions. This can be seen by the very intense banding produced in Figure 21. The PowerSoil Kit also produced successful amplification, but did not provide bands of such a strong intensity. This was further investigated by carrying out a PCR with 5ng of modern DNA in the PCR mixture, instead of the previously tested 10ng of DNA. In these circumstances, the PowerSoil kit did not provide a level of successful amplification that could be used to determine genotype, while the PowerClean kit continued to provide bands strong enough for visual identification of genotype.

However, in practical use, the success rate of the PowerClean kit in inhibitor removal was very low. Using the presence and strength of the primer dimers formed at 50bp in size as an internal standard, the level of inhibition can be estimated for each individual neonatal amplification. In the neonatal results, 23.8% of the results contained a strong band for primer dimer formation, 12.6% of the results contained a medium-strength band, 28.6% showed a weak band, and 34.9% showed no banding at all for primer dimer formation. Therefore, over half (63.5%) of the remains contained sufficient inhibitors to prevent amplification of the primer dimers to such an extent that either weak banding or no banding was seen. Due to the heavy degradation of the aDNA used in this experimentation only a small percentage of the final mass of DNA used in the PCR amplification would be amplifiable and in the suboptimal conditions provided by the inhibitors this amplification would be reduced to such low efficiency that target banding would not be visible.

5.2.1. Burial Site

The burial site itself is likely a large contributor to the inhibitors in the remains. The alluvium soil present at the site is left behind by flooding and is typically silty, consisting of sand and clay soil particles. The flooding will also reduce the oxygen content of the soil and cause anaerobic conditions, causing the death of organic material and providing decaying organic matter.

In combination, these conditions provide an excellent breeding ground for anaerobic bacteria and a likely source for humic substances. This increase in bacterial growth promotes the metabolism of decomposing meat into inhibitory substances. For example, the breakdown of proteins releases amino acids, ammonia, and phosphorus (Dent et al, 2003). Sachse & Frey (2003) established that amino acids do not have a negative effect on PCR amplification, but identify calcium ions as potential inhibitor, which are attracted to the insoluble complexes that form from phosphorus. Dent et al (2003) also states that the fat decomposition can produce inhibited PCR reactions. The oleic, palmitic and stearic acids which are released during the decomposition of fat form aldehydes, ketones and calcium salts. Pelt-Verkuil et al (2008) states that these aldehydes can then inhibit PCR by blocking the active site of DNA polymerase, while Maurer (2006) describes fatty acids as an alternative PCR inhibitor.

In addition to the soil of the burial site, several of the neonatal burials were alongside animal burials conducted at a similar time, possibly as part of burial rites. The animals buried included lambs, calves, and in one instance an entire articulated cow. The additional animal material decomposing at a similar time to the neonatal remains would have substantially increased the number of bacteria in the burial sites and released many more PCR inhibitors into the soil than just a small neonatal burial.

5.3. DNA of Neonatal Remains

Recovery of DNA from the neonatal remains was widely unsuccessful. In the majority of cases, this was likely due to the continued inhibition of PCR, as described above. Successful DNA banding occurred in three of the neonatal amplification gels. These individuals are SK26846 (Fig 24), SK25544 (Fig 24) and SK25272 (Fig 28). In each case, the genotype seen was XY, indicated by two bands at 106 and 112bp in length.

Due to the low number of amplified samples, there is a possibility of contamination. Therefore, the results must be considered in a self-critical approach, as suggested by Gilbert et al (2005). This self-critical evaluation has been carried out using the authentication points proposed by Poinar (2003). Firstly, the pre-PCR work was carried out in an isolated laboratory, which was only used by the researcher for this experimentation and was restricted in accessibility to reduce the number of people entering the laboratory. However, the researcher involved with this experimentation is male and therefore shares the XY

genotype, which may have caused XY contamination of the results. Post-PCR work was carried out in an independent room on a separate floor, which had lesser access restrictions.

Negative controls were used consistently, as extraction blanks. These were chosen to highlight contamination arising from any part of the extraction and amplification process. The negative controls run in Figures 24 and 28 which gave the positive neonatal results showed no contamination. Positive controls were also used, against the recommendations of Poinar, to provide a reference genotype for comparison. Although this may increase the risk of contamination, the production of a positive control for each PCR was carried out after all of the extraction and purification of the associated ancient samples was completed, in an effort to reduce the possibility of contaminating the ancient samples during their extraction process.

The amplified fragments were all below 1000bp in size, in keeping with Poinar's suggestion that any amplified fragments above 1kbp in size are likely modern contamination, due to the degradation of ancient DNA. Poinar also suggests the consideration of the amplification strength in comparison to the size of the fragment. However, no difference in amplification strength was seen between the X and Y chromosomal bands, due to their very small 6bp difference in size.

Poinar also suggests the use of Quantitative Real Time PCR (qPCR) or competitive PCR assay in order to determine the copy number of amplifiable DNA in the sample. While this would have been preferred, the time constraints upon the project meant that this was not a possible option. The use of qPCR would have helped to assess the sensitivity of the neonatal PCR, and to identify whether degradation or inhibition was the cause of non-amplification in the results which showed strong primer dimer formation, yet no target amplicons.

Poinar also suggests the reproduction of the results, with the cloning and sequencing of a minimum of 10 clones in order to verify the validity of the amplicons. Reproduction of the results in this manner was not carried out due to time constraints. However, in further work, the cloning and sequencing of the amplified DNA would allow for the identification of errors in the sequence caused by DNA damage, and also identify any contaminant sequences and the ratio of endogenous ancient DNA sequences to contaminant modern sequences to determine the level of contamination in the samples.

In addition, Poinar suggests the reproduction of all of the work carried out, including cloning and sequencing, in an independent laboratory utilising different scientists. Due to time and financial constraints upon the project, this was not possible. This is suggested for any further work, to identify any contamination originating from the researcher. However, as noted by Deguilloux et al (2011), this would not identify any contamination originating from the archaeologists that had entered the samples during excavation or storage before the project began.

The assessment of biochemical preservation of the remains is also suggested, to corroborate evidence for the survival of ancient DNA. A detailed assessment of organic solids and composition of the remains has not been carried out, due to time constraints, but a visual assessment of the remains finds them in very good physical condition, with little surface erosion and a well preserved macrostructure, especially for neonatal remains. However, as discussed in Misner et al (2009), the physical degradation of the skeleton shows no correlation with the condition or survival of ancient DNA within the remains.

Finally, the suggestion is made to extract DNA from any associated animal remains that are in context with the human burials. Animal burials were associated with the remains excavated at the site, but were not accessible to the researcher for this project, as they are owned by a separate entity than the University. If these remains could be accessed, the recovery and amplification of DNA is suggested as further work.

Although the suggestions of Poinar (2003) have been followed wherever possible, it still remains that contamination with modern DNA gives a possible explanation as to why so few of the samples amplified to detectable levels. While the 10ng mass of DNA placed into the amplifications remained a constant, the actual copy number of amplifiable DNA in degraded aDNA samples will be much less than the copy number of amplifiable DNA in freshly extracted modern DNA. Therefore, contaminated samples would have a higher concentration of amplifiable DNA than uncontaminated samples and may therefore yield results where others fail.

Contamination would also explain why all three of the successful amplifications provided male genotypes. However, with such a small sample size it is very difficult to say that due to the successful amplification of three males from 63 unknown individuals, the samples must have been contaminated. By using binomial distribution, it can be calculated that the probability of there being at least 3 males in a sample of 63 individuals, assuming that there is no gender bias and therefore males and females appear at an approximate 50:50 ratio, is effectively $99.\overline{9}$. The probability of there being two males or less within the sample size of 63 is 1.569×10^{-50}%. Therefore, probability states that the amplification of three male genotypes from the neonatal remains cannot be statistically significant and should be considered coincidental. With a larger sample size of successful amplifications, it may become more apparent that contamination was a potential source for male genotypes.

To further assess whether contamination was the cause of these results, the presence of contamination must be assessed. Contamination with 106 and 112bp amplicons did occur in some of the results, such as those shown in Figure 26, and a further 3 amplifications shown in Appendix 9.4, as Figures 42, 43, and 44. Of the total 82 amplifications carried out (64 final results, in addition to the 18 results shown in Appendix 9.4, which were repeated to eliminate the contamination), 10.9% of samples (9 results) showed definite contamination with male genotype DNA, as a result of 4 contaminated negative controls. Those results

which indicated the presence of contamination, shown in Appendix 9.4, were then repeated in order to obtain genuine results for the affected neonatal remains. Of these repeated results, 1 gel showed contamination in the negative controls. This one contaminated gel suffered from PCR inhibition and as such contained no amplicons regardless of contamination. Therefore, the repetition of contaminated data has drastically reduced the presence of amplified contamination in the final results. Considering the observations of Deguilloux et al (2011) and Yang et al (2003), it is possible that there remains some very low-level contamination or "background DNA" present in the samples, but that this is not amplified to a detectable level with the lower 40-cycle PCR used in this experimentation.

A further band was also seen in Figures 23 and 31, with an approximate size of 75bp in length. As there is no standard allele that provides a 75bp band in human amelogenin, the specificity of the Identifiler Amelogenin primers was examined. Lazaruk et al (2001) and Wallin et al (1998) studied the amplicons produced from the use of the Identifiler kit on primates, including chimpanzee, gorilla, orang-utans and macaques and found that all primate DNA samples amplify, producing fragments exclusively within the 100-350bp region, which would rule out primate DNA producing the 75bp fragment.

The AmpFISTR Identifiler Direct PCR Amplification Kit user manual provided by Applied Biosystems (2012) also states that non-primates including chickens, cats, hamsters, rabbits, rats and mice do not yield any detectable products, and a microorganism mixture containing *C. albicans, E. faecalis, E. coli, F. nucleatum, L. casei, S. aureus, S. mitis, S. mutans, S. salivaris* and *S. viridians* also produced no detectable product. However, it was noted that horse, cow, dog and pig DNA produce a 104bp fragment that is near to the Amelogenin locus. Again, the lack of a 75bp fragment produced by these species further rules out potential non-human or bacterial contamination as the source for the 75bp fragment.

An alternative explanation would be anomalous band migration of the 106 and 112bp bands, caused by denatured DNA or incorrect electrophoresis conditions. However, if this were the case then it would be expected that the other bands shown on the gel would also undergo incorrect band migration, and as such would appear at unusual base pair lengths. The 75bp band appears in the positive control in Figure 31, alongside the 106 and 112bp bands that are located in the correct place, comparable to the DNA ladder. Therefore, it is unlikely that anomalous band migration is the cause of this band.

Therefore, it must be concluded that the band has been caused by non-specific binding on either human DNA, or the non-human DNA that provides banding such as those mentioned in Lazaruk et al (2001), Wallin et al (1998) or the Applied Biosystems (2012) user manual. This would explain the presence of the 75bp band alongside the 106 and 112bp banding seen in the positive control of Figure 31 and also provides an explanation as to why the positive control bands at 106 and 112bp are weaker than expected, due to competitive inhibition caused by the presence of the non-specific amplicon.

5.3.1. DNA Recovery & Age

During the experimentation, a hypothesis predicted a link between the age of the neonate at the time of death and the probability of amplification. This was based upon the previously made observation that while visual indication of weathering and DNA recovery rates are not correlated, generally, intact bones with a harder macroscopic structure and a better preserved microstructure provide typable DNA more regularly than soft or brittle bones with microstructural damage (Misner et al, 2009). The reason for this is that spongy bone is very porous, allowing access for chemical or biological entities which then cause DNA degradation. In comparison, the cortical bone provides a larger area of protected DNA due to its hard mineral structure. Misner et al therefore suggest the use of the petrous portion of the temporal bone, as used in this experimentation, as it is the hardest and densest bone in the body, claiming successful amplifications with a high number of individual remains, including infant remains.

As a newborn ages from the neonatal stage to early infancy, the bones grow and develop in size, producing more cortical bone and providing a harder and stronger skeleton. Therefore, the bones are less likely to become damaged after burial, or degrade as readily, and may preserve DNA better.

This would cause a correlation between the age of the neonate and the chance of DNA recovery and amplification and may provide an explanation for the successful amplification of the DNA of some neonates, but not all. The three neonates recovered showed potential evidence for the preservation of DNA in hard bone material. SK26846 and SK25544 had DNA extracted from the femur, a dense bone that is constructed of cortical bone all the way through to the medullary cavity in the diaphysis, only containing spongy trabecular bone in the metaphyses and epiphyses. SK25272 had DNA extracted from the left petrous portion of the temporal bone, described in Misner et al as the hardest and most dense bone in the human skeleton.

The age at death of the individuals that provided successful DNA amplification was also somewhat consistent with the hypothesis that older neonates may show better DNA survival rates. SK25272 has a predicted combined age of 38-40 prenatal weeks, while SK26846 has a predicted age of 40 prenatal weeks. SK25544 had an age calculated using incomplete remains and therefore only has a lower boundary of 26+ prenatal weeks and therefore cannot be used to test this hypothesis.

Again, due to the low number of samples that provided successful amplification, it cannot be determined whether this hypothesis has any statistical basis. It should be noted that in the successful amplifications that also allowed for a full combined age range to be determined, both were amongst the older neonatal remains. However, 32 of the 63 total individuals measured had a maximum predicted age of 40 prenatal weeks or more.

Therefore, if it were the case that their age provided greater protection against DNA degradation, it would be expected that more of these neonates would have provided successful amplification. A wider variation in ages and a much larger sample size would be required in order to determine the validity of this hypothesis.

6. Chapter Six: Conclusions

Inhibition in ancient DNA amplifications remains a considerable challenge. Amplicons around 100bp in size should theoretically amplify consistently due to their long-term survival in degraded DNA. In the present study, primer dimers acted as an internal standard to indicate the presence and extent of inhibition in the amplification. The lack of amplification of the 106 and 112bp amplicons from the neonatal remains is therefore due to inhibition. This inhibition is caused by humic acid present in the burial soil at the grave site, which has leached into the bone over time and caused the loss of amplicons of approximately 100bp in size (Opel et al, 2009).

The PowerClean Kit for Ancient DNA performed well in preliminary trials using 10ng of modern DNA. However, in the more challenging extractions of the neonatal remains, the success became intermittent. This may be due to the fact that the degradation of aDNA means that although 10ng of DNA was used in both the modern and ancient amplifications, the amplifiable concentration of DNA in the aDNA extractions is lower. Also, the addition of a solution of modern DNA to the aDNA extraction in the testing phase simultaneously increases the concentration of amplifiable DNA and dilutes the concentration of inhibitors in the sample, assuming that there were no inhibitors in the modern DNA extraction.

The initial Arnay-de-la-Rosa primers chosen for this investigation were used to substantial success in Arnay-de-la-Rosa's (2007) experimentation, achieving unambiguous sex identification in 75% of cases. However, in this experimentation the primers were completely unsuccessful; failing to amplify highly concentrated modern DNA consistently. A potential explanation for this lies in inhibition. In the present study, primer dimer formation was intermittent, indicating inhibition. However, the DNA being tested was modern DNA extracted via the Chelex method explained in Section 3.3 and should therefore not contain inhibitors. An alternative explanation lies in the concentration of DNA used in PCR. Arnay-de-la-Rosa report the DNA used in their PCR as a volume of non-specified concentration. Therefore, the mass of DNA in their PCR mixture may be substantially higher than in this experimentation, which would cause of a lack of PCR product, or may instead be much lower, causing the PCR in this experimentation to be overloaded.

The neonatal remains provided three positive results, all of which are male. Due to the low number of amplified samples, there is a possibility of contamination. Therefore, the results have been considered in a self-critical approach, as suggested by Gilbert et al (2005). This self-critical evaluation has been carried out using the authentication points proposed by Poinar (2003) and can be seen in Section 5.3. Combining the authentication techniques of Poinar with the suggestions of self-criticality by Gilbert et al (2005) and the problems highlighted with the techniques by Deguilloux et al (2011), the validity of the amplified DNA remains in question. Reasonable steps have been taken to reduce contamination at every opportunity and contamination in negative controls has remained at a low percentage in

neonatal results. Contaminated tests have been repeated in order to provide accurate results.

However, inhibition has proved the process of DNA extraction and amplification to be very problematic. It appears that the success of the amplification relies on the success of the PCR clean-up kit used. The wide variation in primer dimer formation is evidence of the intermittent success of the PowerClean kit and has lead to this very small sample size of positive results. This low sample size and the fact that all three obtained results provide a male genotype makes it very difficult to determine whether the source of the amplified DNA was in fact aDNA from the neonatal remains. Therefore, further work is suggested to introduce more rigorous inhibitor removal methods and create a larger sample size of neonatal DNA. This will allow for the assessment of the validity and relevance of the results of this investigation, alongside the surrounding literature.

The age determination of the neonatal remains was successful. 72% of the individuals have an age range including the 38 prenatal week age that indicates a full term child (Fehling et al, 1907). A further 8% indicated an age above 24 prenatal weeks, the age which defines a stillbirth in the Births and Registrations Act (1926). This suggests that the neonates at this site likely died during or shortly after the event of birth.

Physical degradation caused problems in the morphological assessment of age, highlighting the inherent problems with morphological assessments of neonatal remains. 55% of petrous portions showed damage that caused problems with age determination and 67% of the remains using post-cranial measurements had damage that prevented the calculation of a full combined age range. 16% of individuals had skeletal damage of such severity to prevent any accurate age calculation.

A correlation between DNA recovery probability and the age of the individual could not be assessed. Two of the three successful amplifications came from neonates 40 prenatal weeks or older, amongst the eldest of the individuals. The other neonate had damaged remains indicating a lower boundary age of 26+ prenatal weeks, with the potential to be an older individual. However, with such a small sample size and damaged skeletal material, it is impossible to provide rigorous statistical testing to assess this hypothesis.

7. **Chapter Seven: Further Work**

- Further work that needs to be undertaken is a study into the inhibitors present within the samples and the production and optimisation of a better technique of inhibitor removal. This would greatly improve the success rate of all amplifications and would allow for better reproducibility of the results. It is suggested that this study is carried out initially on medieval remains from a similar burial site with similar soil conditions, or from an adult skeleton from the same excavation as the neonates. While there would be variation in inhibitor content between medieval and the roman remains, there would be a greater mass of source material that is not as scientifically valuable as the neonatal remains. This preliminary study with adult remains would give valuable transferrable data in the method of inhibitor removal once the inhibitor content of the neonatal remains had been evaluated.

- In addition, the use of FTIR to analyse soil recovered from the burial site may indicate the presence of humic acid or other inhibitors in the soil. This would provide an explanation as to why the inhibitors are present within the remains. Modern DNA could then be tested with varying concentrations of the identified inhibitors in order to determine the level of inhibitors present within the skeletal samples.

- The use of qPCR would allow for the assessment of the limit of detection of the PCR and the sensitivity of the technique. This would provide valuable information as to the mass of DNA required for a successful PCR and also assess the percentage degradation to the ancient DNA in terms of actually amplifiable target DNA versus the mass of DNA in the PCR mixture. The use of qPCR will also help to determine whether inhibitors are present (Opel et al, 2009).

- The inclusion of additional primers to amplify an additional locus would allow for the identification of modern contamination if used alongside the cloning and sequencing technique. A larger fragment should be used up to 1000bp in size to assess the possibility of modern contamination, as fragments of this size are rarely amplified in ancient DNA (Poinar, 2003). With the addition of sequencing of the amplicons produced at this locus, the sequences could be compared to samples from the researcher for confirmation of contamination. The use of a locus that provides larger amplicons than 106 & 112bp would also allow for the assessment of whether or not the amplification strength is inversely proportional to the size of the amplicon, as suggested in Poinar.

- Reproduction of the results in a second laboratory, carried out by separate scientists. This would effectively eliminate the effect of contamination by the researcher as comparison of the results would show any variation in amplicon patterns. These results could then be repeated.

- DNA analysis of the animal remains which were excavated at the burial site could allow for more insight as to the extent of DNA degradation present in the samples and allow for assessment into the chance of genuine aDNA recovery from the neonatal skeletons.

- An assessment of biochemical preservation via the use of Scanning Electron Microscopy (SEM) in order to determine the level of damage to the microstructure of the bone. The use of SEM can help to provide information on the level of bacterial degradation of the organic collagen component of the bone and the loss of mineral hydroxyapatite due to the collagen loss (Jackes et al, 2001).

- A larger study sample is required to determine the possible correlation between chance of DNA recovery and the age of the individual at time of death. A sample with a wider variation of age ranges, from neonatal to adult, would also be required. Modern samples would allow for the rapid sampling of a wide variety of known ages, but would not show the high levels of DNA degradation that ancient remains do. Therefore, a large well documented sample such as the Spitalfields collection or a broad medieval collection is suggested.

- In combination, the suggestions above should improve the recovery rate of DNA from the neonatal remains. In doing this, a larger sample size of neonatal skeletons with known sex is generated. From this, the possibility of infanticide can be investigated. A statistically significant imbalance between male and female skeletons may indicate infanticide of female babies in a roman society which placed greater value upon a male heir.

- With a larger group of neonatal skeletons of known sex as a baseline, investigation into the morphological features of sex in juvenile and neonatal remains can be carried out. Currently, the morphological determination of sex in juvenile remains a problem in forensic anthropology due to the lack of sexual characteristics developed during puberty (Cardoso, 2008). However, some progress has been made using the teeth and craniofacial features of juvenile remains (Molleson et al, 1998, Gonzalez, 2012, and Viciano et al, 2011). These methods could be utilised on the neonatal remains in order to determine the extent of their reliability in differing populations and in very young individuals.

8. Chapter Eight: References

8.0. Books

Alberts, B., Johnson, A., Lewis, J., Raff, M., Roberts, K., and Walter, P., Molecular Biology of the Cell, 5th ed, Garland Science, 2007.

Bartlett, J.M.S, and Stirling, D., PCR Protocols (Methods in Molecular Biology), Volume 226, 2nd ed, Humana Press, 2003

Bloom, M. V., *Human DNA fingerprinting by polymerase chain reaction* in 'Tested Studies for laboratory teaching, Volume 15 (C. A. Goldman, ed.) Proceedings of the 15th Workshop/Conference of the Association for Biology Laboratory Education 1994

Brown, T.A., Gene Cloning & DNA Analysis: An Introduction, 6th ed., Wiley-Blackwell, 2010

Butler, J.M., Fundamentals of Forensic DNA Typing, Academic Press, 2009

Chhem, R.K., and Brothwell, D.R., Paleoradiology: Imaging Mummies and Fossils, Springer Science & Business Media, 2007.

Dorak, M.T., Real-time PCR, Garland Science, 2007

Fazekas, I.Gy, and Kósa, F., Forensic Fetal Osteology, Budapest: Akadémiai Kiadó, 1978

Fehling, H., Naegele, F.K., and Walcher, G., Lehrbuch der Geburtshilfe für Hebammen, Laupp, 1907.

Komar, D.A., and Buikstra, J.E., Forensic Anthropology: Contemporary theory and practice, Oxford University Press, 2008.

Maurer, J., PCR Methods in Food, Birkhauser, 2006.

Pinhasi, R., and Mays, S., Advances in Human Palaeopathology, Wiley-Blackwell, 2007.

Popping, B., Diaz-Amigo, C., and Hoenicke, K., Molecular Biological and Immunological Techniques and Applications for Food Chemists, John Wiley & Sons, 2010

Quigley, C., Skulls and Skeletons: Human Bone Collections and Accumulations, McFarland, 2001

Robertson, J.R., Ross, A.M., and Burgoyne, L., DNA In Forensic Science: Theory, Techniques and Applications, CRC Press, 2002.

Sapse, D., and Kobilinsky, L., Forensic Sience Advances and Their Application in the Judiciary System, CRC Press, 2011.

Schaefer, M., Black, S., and Scheuer, L., Juvenile Osteology: A Laboratory and Field Manual, Academic Press, 2009

Seeberg, E. And Kleppe, K, Chromosome Damage and Repair, Plenum Press, 1981.

Shapiro, R., *In* "Chromosome Damage and Repair" (Seeberg, E., and Kleppe, K., eds), Plenum Press, 1981

Sparks, D.L., Environmental Soil Chemistry, 2nd ed., Academic Press, 2003

Teschler-Nicola, M., and Prossinger, H., Sex determination using tooth dimensions. In: Alt, K.W., Rösing, F.W., Teschler-Nicola, M., editors. Dental Anthropology: Fundamentals, limits and prospects, New York: Springer-Verlag Wien, 1998.

Tropp, B.E., Molecular Biology: Genes to Proteins, 4th ed., Jones & Bartlett Publishers, 2012.

Turner, P., McLennan, A., Bates, A., and White, M., Molecular Biology, 3rd ed., Taylor and Francis Group, 2005.

Turnpenny, P.D., and Ellard, S., Emery's Elements of Medical Genetics, 14th ed., Elsevier Health Services, 2011.

Van Pelt-Verkuil, E., Van Belkum, A., and Hays, J.P., Principles and Techniques of PCR Amplification, Springer, 2008.

Walker, P., in Buikstra, J.E., and Ubelaker, D.H., Standards for Data Collection from Human Skeletal Remains: Proceedings of a Seminar at the Field Museum of Natural History (Arkansas Archeological Report Research Series), Arkansas Archaological Survey, 1994

White, T.D., and Folkens, P.A., The Human Bone Manual, Academic Press, 2005.

Wisshak, M., and Tapanila, L., Current Developments in Bioerosion, Springer Science & Business Media, 2008.

World Health Organisation, Air Quality Guidelines, 2nd ed., WHO Regional Office for Europe, 2000.

World Health Organisation, Carbon Tetrachloride: 208 (Environmental Health Criteria), World Health Organisation, 1999.

8.1. **Journal Articles**

Abyzov, S., Fukuchi, M., Imura, S., Kanda, H., Mitskevich, I., Naganuma, T., Poglazova, M., Savatyugin, L., and Ivanov, M., Biological investigations of the Antarctic ice sheet: review, problems and projects, *Polar Bioscience,* **17** (2004) 106-116

Adler, C.J., Haak, W., Donlon, D., Cooper, A., and The Genographic Consortium, Survival and recovery of DNA from ancient teeth and bones, *J. Archaeological Sci.* **38** (2011) 956-964

Alonso, A., Martín, P., Albarrán, C., García, P., García, O., Fernández de Simón, L., García-Hirschfeld, J., Sancho, M., Concepción de la Rúa, and Fernández-Piqueras, J., Real-time PCR designs to estimate nuclear and mitochondrial DNA copy number in forensic and ancient DNA studies, *Forensic Sci. Int.* **139** (2004) 141-149

Arnay-de-la-Rosa, M., González-Reimers, E., Fregel, R., Velasco-Vázquez, J., Delgado-Darias, T., González, A.M., and Larruga, J.M., Canary islands aborigin sex determination based on mandible parameters contrasted by amelogenin analysis, *J. Archaeological Sci.* **34** (2007) 1515-1522

Baker, L.E., McCormick, W.F., and Matteson, K.J., A silica-based mitochondrial DNA extraction method applied to forensic hair shafts and teeth, *J. Forensic Sci.* **46** (2001) 126-130

Bennett, C., and Kaestle, F.A., Investigation of Ancient DNA from Western Siberia and the Sargat Culture, *Human Biology*, **82** (2010) 143-156

Bergsjø, O., Denman, D.W. 3rd, Hoffman, H.J., Meirik, O., Duration of human singleton pregnancy. A population-based study, *Acta. Obstet. Gynecol. Scand.* **69** (1990) 197-207

Black, T.K., Sex dimorphism in the tooth-crown diameters of the deciduous teeth. *Am. J. Phys. Anthropol.* **48** (1978) 77-82

Bouwman, A.S., Chilvers, E.R., Brown, K.A., and Brown, T.A., Identification of the authentic ancient DNA sequence in a human bone contaminated with modern DNA, *Am. J. Phys. Anthropol.* **131**(2006) 428-431

Briggs, A.W., Stenzel, U., Johnson, P.L.F., Green, R.E., Kelso, J., Prüfer, K., Meyer, M., Krause, J., Ronan, M.T., Lachmann, M., and Pääbo, S., Patterns of damage in genomic DNA sequences from a Neandertal, *Proceedings of the National Academy of Sciences of the United States of America,* **104** (2007) 14616-14621

Campos, P.F., Craig, O.E., Turner-Walker, G., Peacock, E., Willerslev, E., and Gilbert, M.T.P., DNA in ancient bone – Where is it located and how should we extract it? *Annals of Anatomy* **194** (2012) 7-16

Cardoso, H.F.V., Sample-specific (universal) metric approaches for determining the sex of immature human skeletal remains using permanent tooth dimensions. *J. Archaeol. Sci.* **35** (2008) 158-168

Chilvers, E.R., Bouwman, A.S., Brown, K.A., Arnott, R.G., Prag, A.J.N.W., and Brown, T.A., Ancient DNA in human bones from Neolithic and Bronze Age sites in Greece and Crete, *J. Archaeological Sci.* **35** (2008) 2707-2714

Collins, P.J., Hennessy, L.K., Leibelt, C.S., Roby, R.K., Reeder, D.J., and Foxall, P.A., Developmental validation of a single-tube amplification of the 13 CODIS STR loci, D2S1338, D19S433, and amelogenin: the AmpFISTR Identifiler PCR Amplification kit, *J. Forensic Sci.* **49** (2004) 1265-1277

Daskalaki, E., Anderung, C., Humphrey, L., and Götherström, A., Further developments in molecular sex assignment: a blind test of 18th and 19th century human skeletons, *J. Archaological Sci.* **38** (2011) 1326-1330

Deguilloux, M., Ricaud, S., Leahy, R., and Pemonge, M., Analysis of ancient human DNA and primer contamination: One step backward one step forward, *Forensic. Sci. Int.* **210** (2011) 102-109

Dent, B.B., Forbes, S.L., and Stuart, B.H., Review of human decomposition processes in soil, *Environmental Geology,* **45** (2004) 576-585

Eckhart, L., Bach, J., Ban, J., and Tschachler, E., Melanin binds reversibly to thermostable DNA polymerase and inhibits its activity, *Biochem Biophys Res Commun*, **271** (2000) 726-730

Eckhart, L., Bach, J., Ban, J., and Tschachler, E., Melanin binds reversibly to thermostable DNA polymerase and inhibits its activity. *Biochem Biophys. Res. Commun.* **271** (2000) 726-730

Ehrlich, M., Norris, K.F., Wang, R.Y.-H., Kuo, K.C., and Gehrke, C.W., DNA Cytosine Methylation and Heat-Induced Deamination, *Bioscience Reports*, **6** (1986) 387- 393

Elsner, H.I., and Lindblad, E.B., Ultrasonic degradation of DNA, *DNA*, **8** (1989) 697-701

Fessler, D.M.T., Haley, K.J., and Lal., R.D., Sexual dimorphism in foot length proportionate to stature, *Annals of Human Biology*, **32** (2005) 44-59

Frutos, L.R., Metric determination of sex from the humerus in a Guatemalan forensic sample. *Forensic Sci. Int.* **147** (2005) 153-157

Garn, S.M., Lewis, A.B., and Bonné, B., Third molar formation and its development course. *Angle Orthodontist* **32** (1962) 271-279

Garn, S.M., Lewis, A.B., Kerewsky, R.S., Sex difference in tooth size. *J. Dent. Res.* **43** (1964) 306

Gates, K.S., An Overview of chemical processes that damage cellular DNA: Spontaneous Hydrolysis, Alkylation and Reactions with Radicals, *Chem. Res. Toxicol.* **22** (2009) 1747-1760

Gilbert, M.T.P., Bandelt, H-J., Hofreiter, M., and Barnes, I., Assessing ancient DNA studies, *TRENDS in Ecology and Evolution* **20** (2005) 541-544

Gilbert, M.T.P., Rudbeck, L., Willerslev, E., Hansen, A.J., Smith, C., Penkman, K.E.H., Prangenberg, K., Nielsen-Marsh, C.M., Jans, M.E., Arthur, P., Lynnerup, N., Turner-Walker, G., Biddle, M., Kjølbye-Biddle, B., and Collins, M.J., Biochemical and physical correlates of DNA contamination in archaeological human bones and teeth excavated at Matera, Italy, *J. Anthropological Sci.* **32** (2005) 785-793

Gonzalez, R.A., Determination of sex from juvenile crania by means of discriminant function analysis. *J. Forensic Sci.* **57** (2012) 24-34

Goray, M., Mitchell, J.R., and van Oorschot, R.A.H., Evaluation of multiple transfer of DNA using mock case scenarios, *Legal Medicine*, **14** (2012) 40-46

Gorham, E., The Development of Peat Land, *Quarterly Review of Biology* **32** (1957) 145-166

Graves, R.J., Coutts, C., and Green, T., Methylene chloride induced DNA damage: an interspecies comparison, *Carcinogenesis* **16** (1995) 1919-1926

Grokhovsky, S.L., Specificity of DNA Cleavage by Ultrasound, *Molecular Biology*, **40** (2006) 276-283

Gülekon, I.N., and Turgut, H.B., The external occipital protuberance: can it be used as a criterion in the determination of sex? *J. Forensic Sci. **48** (*2003) 513-516

Hecker, K.H., and Roux, K.H., High and Low Annealing Temperatures Increase Both Specificity and Yield in Touchdown and Stepdown PCR, *Biotechniques*, **20** (1996) 478-485

Hoff-Olsen, P., Mevåg, B., Staalstrøm, E., Hovde, B., Egeland, T., and Olaisen, B., Extraction of DNA from decomposed human tissue: An evaluation of five extraction methods for short tandem repeat typing, *Forensic Sci. Int.* **105** (1999) 171-183

Höss, M., and Pääbo, S., DNA extraction from PLeisocene bones by a silica-based purification method, *Nucleic Acids Res.* **21** (1993) 3913-3914

Iscan, M.Y., Loth, S.R., King, C.A., Shihai, D., and Yoshino, M., Sexual dimorphism in the humerus: a comparative analysis of Chinese, Japanese and Thais. *Forensic Sci. Int.* **98** (1998) 17-29

Jackes, M., Sherburne, R., Lubell, D., Barker, C., and Wayman, M., Destruction of microstructure in archaeological bone: a case study from Portugal, *International Journal of Osteoarchaeology,* **11** (2001) 415-432

Jans, M.M.E., Nielsen-Marsh, C.M., Smith, C.I., Collins, M.J., and Kars, H., Characterisation of microbial attack on archaeological bone, *Journal of Archaeological Science* **31** (2004) 87-95

Kashyap, V.K., Sahoo, S., Sitalaximi, T., and Trivedi, R., Deletions in the Y-derived amelogenin gene fragment in the Indian population, *BMC Med Genet.*, **7** (2006) 1471-2350

Kieler, H., Axelsson, O., Nilsson, S., and Waldenström, The length of human pregnancy as calculated by ultrasonographic measurement of the fetal biperietal diameter, *Ultrasound in Obstetrics & Gynecology,* **6** (1995), 353-357

Kieler, H., Axelsson, O., Nilsson, S., Waldenströ, U., The length of human pregnancy as calculated by ultrasonographic measurement of the fetal biparietal diameter, *Ultrasound in Obstetrics & Gynecology* **6** (1995) 353-357

Kinra, P., The use of mitochondrial DNA and short tandem repeat typing in the identification of air crash victims, *Ind. J. Aerospace Med.,* **50** (2006) 54-65

Krüttli, A., Bouwman, A., Akgül, G., Casa, P.D., Rühli, F., and Warinner, C., Ancient DNA Analysis Reveals High Frequency of European Lactase Persistence Allele (T-13910) in Medieval Central Europe, *PLOS ONE*, **9** (2014) e86251, viewed 20th August 2014 (http://www.plosone.org/article/fetchObject.action?uri=info%3Adoi%2F10.1371%2Fjournal.pone.0086251&representation=PDF)

Lazaruk, K., Wallin, J., Holt, C., Nguyen, T., and Walsh, PS., Sequence variation in humans and other primates at six short tandem repeat loci used in forensic identity testing, *Forensic Sci. Int.* **119** (2001) 1-10

Lindahl, T., and Nyberg, B., Rate of depurination of native deoxyribonucleic acid, *Biochemistry* **11** (1972) 3610-3618

Lindahl, T., Instability and decay of the primary structure of DNA, *Nature,* **362** (1993) 709-715

Liu, Y., Prasad, R., Beard, W.A., Kedar, P.S., Hou, E.W., Shock, D.D., and Wilson, S.H., Coordination of steps in single-nucleotide base excision repair mediated by apurinic/apyrimidinic endonuclease 1 and DNA polymerase β, *J. Biol. Chem.* **282** (2007) 13532-13541

Lovell, N.C., Test of Phenice's technique for determining sex from the os pubis. *Am. J. Phys. Anthropol.* **79** (1989) 117-120

Maca-Meyer, N., Cabrera, V.M., Arnay-de-la-Rosa, M., Flores, C., Fregel, R., González, A.M., and Larruga, J.M., Mitochondrial DNA diversity in 17th-18th Century remains from Tenerife (Canary Islands), *Am. J. Phys. Anthropol.* **127** (2005) 418-426

MacLaughlin, S.M., and Bruce, M.F., The accuracy of sex identification in European skeletal remains using the Phenice characters. *J. Forensic. Sci.***35** (1990) 1384-1392

Mall, G., Hubig, M., Buttner, A., Kuznik, J., Penning, R., and Grawn, M., Sex determination and estimation of stature from the long bones of the arm. *Forensic Sci. Int.* **117** (2003) 23-30

Malmström, H., Svensson, E.M., Gilbert, M.T., Willerslev, E., Götherström, A., and Holmlund, G., More on contamination: the use of asymmetric molecular behaviour to identify authentic ancient human DNA, *Mol. Biol. Evol.* **24** (2007) 998-1004

Manifold, B.M., Differential preservation of children's bones and teeth recovered from early medieval cemeteries: possible influences for the forensic recovery of non-adult skeletal remains, *Anthropological Review*, **76** (2013) 23-49

Manifold, B.M., Intrinsic and Extrinsic factors involved in the preservation of non-adult skeletal remains in archaeology and forensic science, *Bull. Int. Assoc. Paleodont.* **6** (2012) 51-69

Matheson, C.D., Gurney, C., Esau, N., and Lehto, R., Assessing PCR Inhibition from Humic Substances, *Open Enzyme Inhibition Journal* **3** (2010) 38-45

Miller, F. J., Rosenfeldt, F.L., Zhang, C., Linnane, A.W., and Nagley, P., Precise determination of mitochondrial DNA copy number in human skeletal and cardiac muscle by a PCR-based assay: lack of change with copy number with age, *Nucleic Acids Research,* **31** (2003) Pp. e61, viewed 17th August 2014, (http://nar.oxfordjournals.org/content/31/11/e61)

Misner, L.M., Halvorson, A.C., Dreier, J.L., Ubelaker, D.H., and Foran, D.R., The correlation between skeletal weathering and DNA quality and quantity, *J. Forensic Sci.,* **54** (2009) 822-828

Mitchell, D., Willerslev, E., and Hansen, A., Damage and Repair of Ancient DNA, *Mutation Research* **571** (2005) 265-276

Molak, M., and Ho, S.Y.W., Evaluating the Impact of Post-Mortem Damage in Ancient DNA: A Theoretical Approach, *Journal of Molecular Evolution*, **73** (2011) 244-255

Molleson, T., Cruse, K., and Mays, S., Some sexually dimorphic features of the human juvenile skull and their value in sex determination in immature skeletal remains, *J. Archaeological Sci.* **25** (1998) 719-728

Nakahori, Y., Takenaka, O., and Nakagome, Y., A human X-Y homologous region encodes "amelogenin", *Genomics*, **9** (1991) 264-269

Nicholson, R.A., Bone degradation, burial medium and species representation: debucking the myths, an experiment-based approach. *Journal of Archaeological Science,* **23** (1996) 513-533

Nudelman, F., Pieterse, K., George, A., Bomans, P.H.H., Friedrich, H., Brylka, L.J., Hilbers, P.A.J., de With, G., and Sommerdijk, N.A.J.M., The role of collagen in bone apatite formation in the presence of hydroxyapatite nucleation inhibitors, *Nature Materials,* **9** (2010) 1004-1009.

Okungbowa, F.I., Ghosh, A.K., Chowdhury, R., Choudhuri, P., Basu, A., and Pal, K., Mechanical lysis of *Candida* cells for crude protein and enzymatic activity estimation: Comparison of three methods, *World J. Med. Sci.* **2** (2007) 101-104

Okazaki, M., Yoshida, Y., Yamaguchi, S., Kaneno, M., and Elliot, J.C., Affinity binding phenomena of DNA onto apatite crystals, **22** (2001) 2459-2464

Opel, K.L., Chung, D., and McCord, B.R., A Study of PCR Inhibition Mechanisms using Real Time PCR, *J. Forensic Sci.* **55** (2009) 25-33

Pääbo, S., Ancient DNA: Extraction, characterization, molecular cloning, and enzymatic amplification, *Proc. Natl. Acad. Sci. USA* **86** (1989) 1939-1943

Phenice, T.W., A newly developed visual method of sexing the os pubis. *Am. J. Phys. Anthropol* **30** (1969) 297-301

Poinar, H.N, The top 10 list: criteria of authenticity for DNA from ancient and forensic samples, *International Congress Series* **1239** (2003) 575-579

Robe, P., Nalin, R., Capellano, C., Vogel, T.M., and Simonet, P., Extraction of DNA from soil, *European Journal of Soil Biology* **39** (2003) 183-190

Saiki, R.K., Gelfand, D.H., Stoffel, S., Scharf, S.J., Higuchi, R., Horn, G.T., Mullis, K.B., and Erlich, H.A., Primer-directed enzymatic amplification of DNA with a thermostable DNA polymerase, *Science*, **239** (1988) 487-491

Sampietro, M.L., Gilbert, M.T.P., Lao, O., Caramelli, D., Lari, M., Bertranpetit, J., and Lalueza-Fox, C., Tracking down human contamination in ancient human teeth, *Mol. Biol. Evol.* **23** (2006) 1801-1807

Schutkowski, H., Sex determination of infant and juvenile skeletons. I. Morphognostic features. *Am. J. Phys. Anthropol.* **90** (1993) 199-205

Sepp, R., Szabó, I., Uda, H., and Sakamoto, H., Rapid techniques for DNA extraction from routinely processed archival tissue for use in PCR, *J. Clin. Pathol.* **47** (1994) 318-323

Smith, C.I., Chamberlain, A.T., Riley, M.S., Cooper, A., Stringer, C.B., and Collins, M.J., Neanderthal DNA: not just old but old and cold? *Nature*. **10** (2001) 771-772

Smith, C.I., Chamberlain, A.T., Riley, M.S., Stringer, C., and Collins, M.J., The thermal history of human fossils and the likelihood of successful DNA amplification, *J. Hum. Evol.* **45** (2003) 203-217

Sullivan, K.M., Mannucci, A., Kimpton, C.P., and Gill, P., A rapid and quantitative DNA sex test: fluorescence-based PCR analysis of X-Y homologous gene amelogenin. *BioTechniques* **15** (1993) 636-638, 640-641

Sutherland, L.D., and Suchey, J.M., Use of the ventral arc in pubic sex determination, *J. Forensic. Sci* **36** (1991) 501-511

Sutovsky, P., Moreno, R.D., Ramalho-Santos, J., Dominko, T., Simerly., C and Schatten, G., Development: Ubiquitin tag for sperm mitochondria, *Nature*, **402** (1999) 371-372

Thangaraj, K., Reddy, A.G., and Singh, L., Is the amelogenin gene reliable for gender identification in forensic casework and prenatal diagnosis? *Int. J. Legal Med.* **116** (2002) 121-123

Thomas, C.E., and Aust, S.D., Free radicals and environmental toxins, *Ann. Emerg. Med.*, **15** (1986) 1075-83

Ubelaker, D.H., and Volk, C.G., A test of the Phenice method for the estimation of sex. *J. Forensic Sci.* **47** (2002) 19-24

Viciano, J., Alemán, I., D'Anastasio, R., Capasso, L., and Botella, M.C., Odontometric sex discrimination in the Herculaneum sample (79 AD, Naples, Italy) with application to juveniles, *Am. J. Phys. Anthropol.* **145** (2011) 97-106

Wallin, J.M, Buoncristiani, M.R., Lazaruk, K.D., Fildes, N., Holt, C.L., and Walsh, P.S., SWGDAM validation of the AmpFISTR blue PCR amplification kit for forensic casework analysis, *J. Forensic Sci.* **43** (1998) 854-870

Walrath, D.E., Turner, P., and Bruzek, J., Reliability test of the visual assessment of cranial traits for sex determination, *Am. J. Phys. Anthropol.* **125** (2004) 132-137

Walsh, P.S., Metzger, D.A., and Higuchi, R., Chelex 100 as a medium for simple extraction of DNA for PCR-based typing from forensic material, *BioTechniques*, **10** (1991) 506-513

Willerslev, E., and Cooper, A., Review Paper. Ancient DNA, *Proceedings of the Royal Society B,* **272** (2005) 3-16

Xie, C.Z., Li, C.X., Cui, Y.Q., Zhang, Q.C., Fu, Y.Q., Zhu, H., and Zhou, H., Evidence of ancient DNA reveals the first European lineage in Iron Age Central China, *Proceedings of the Royal Society B,* **274** (2007) 1597-1602

Yang, D.Y., Eng, B., and Saunders, S.R., Hypersensitive PCR, ancient human mtDNA, and contamination, *Human Biology*, **75** (2003) 355-364

Yankson, K.K., and Steck, T.R., Strategy for Extracting DNA from Clay Soil and Detecting a Specific Target Sequence via Selective Enrichment and Real-Time (Quantitative) PCR Amplification, *Applied and Environmental Microbiology*, **75** (2009) 6017-6021

Zoltewicz, J.A., Clark, D.F., Sharpless, T.W., and Grahe, G., Kinetics and mechanism of the acid-catalyzed hydrolysis of some purine nucleosides, *J. Am. Chem. Soc.,* **92** (1970) 1741-1750

8.2. **Other**

Applied Biosystems, AmpFlSTR SGM Plus PCR Amplification Kit User Guide, Life Technologies Corporation, 2012

BBC News, 2006, 'Crime-fighting successes of DNA', *BBC News*, 4th October, viewed 7th September 2014 (http://news.bbc.co.uk/1/hi/uk/5405470.stm)

Births and Deaths Registration Act 1926, Chapter 48, viewed 6th September 2014, (http://www.legislation.gov.uk/ukpga/Geo5/16-17/48/enacted)

Crown Prosecution Service, 2011, *B4. Adventitious (chance) DNA Matches*, Crown Prosecution Service, viewed 11 August 2014, (http://web.archive.org/20110610231004/www.cps.gov.uk/legal/s_to_u/scientific_evidence/adventitious_dna_matches/)

Geddes, L., 2012, 'How DNA contamination can affect court cases', *New Scientist*, 13th January, viewed 19th August 2014 (http://www.newscientist.com/article/mg21328475.000-how-dna-contamination-can-affect-court-cases.html#.U_N3TmOik7c)

Hogenboom, M., 2014, 'Kercher trial: How does DNA contamination occur?', *BBC News*, 30th January, viewed 19th August 2014 (http://www.bbc.co.uk/news/science-environment-24534110)

Marhsall, C., 2009, 'DNA pioneer's 'eureka' moment', *BBC News*, 9th September, viewed 11 August 2014, (http://news.bbc.co.uk/1/hi/programmes/newsnight/8245312.stm)

McGrath, M., 2013, 'World's oldest bog body hints at violent past', *BBC News,* 24th September, viewed 19th August 2014 (http://www.bbc.co.uk/news/science-environment-24053119)

MoBio Laboratories, PowerClean DNA Clean-Up Kit Instruction manual, MoBio Laboroatories, 2014

National Library of Medicine, 2011, *Medical Subject Headings: Amelogenin*, National Library of Medicine, National Institutes of Health, viewed 11 August 2014, (http://www.nlm.nih.gov/cgi/mesh/2011/MB_cgi?mode=&index=24032&view=expanded)

Promega, 2011, *Protocol and Applications Guide: Nucleic Acid Amplification*, Promega, viewed 11 August 2014, (http://www.promega.co.uk/~/media/files/resources/paguide/a4/chap1a4.pdf?la=en)

QIAGEN, 2002, *Genomic DNA Purification: Technical hints, applications and protocols*, QIAGEN, viewed 6th September 2014, (http://www.uniscience.com/pdf/Qiagen/Genomic%20DNA%20Purification.pdf)

Raff, J.A., 2008, 'An Ancient DNA Perspective on the Prehistory of the Lower Illinois Valley', Doctor of Philosophy thesis, Indiana University

World Health Organisation, *Dichloromethane in Drinking-water: Background document for development of WHO Guidelines for Drinking-water Quality.* World Health Organization, 2003. Viewed 17th August 2014, (http://www.who.int/water_sanitation_health/dwq/chemicals/dichloromethane.pdf)

9. Chapter Nine: Appendices

9.0. Thermal Age

Thermal age is described in Molak et al (2011), as a potential method to assess DNA preservation. Using temperatures that range from -30 to +30°C, an equation produced by Smith et al (2003) can be used to determine thermal age.

Equation 1:

$$t_{10°C} = t_c \left(\frac{k_T}{k_{10°C}} \right)$$

Where:

t is the age of the sample, either thermal age ($t_{10°C}$) or chronological age (t_c)

k is the rate of reaction, either at sample deposition temperature (*T*) or at 10°C

Rate of reaction is calculated using the Arrhenius equation, using values for pre-exponential constant and activation energy estimated by Lindahl and Nyberg (1972).

Equation 2:

$$k_r = Ae^{-E_a/RT}$$

Where:

A is the pre-exponential constant (A = 1.45 x 10^{11} s^{-1})

E_a is the activation energy (E_a = 127 kJ)

R is the gas constant (R = 8.314 J mol^{-1} K^{-1})

T is the temperature (K)

These two equations can be combined to give the following equation for calculating the thermal age of skeletal remains:

Equation 3:

$$t_{10°C} = t_c \cdot e^{-E_a\left(T^{-1}-\frac{1}{283.15}\right)R^{-1}}$$

9.1. **Arnay-de-la-Rosa Primers**

The primer sequences are as follows.

Amel-A Primer (Sullivan et al, 1993): CCCTGGGCTCTGTAAAGAATAGTG

Amel-C Primer (Meyer et al, 2005): AATRYGGACCACTTGAGAAAC

9.2. **Age Determination**

9.2.1. **Petrosa**

Maximum Length of the Pars Petrosa – Maximum anteroposterior distance across the bone. (Labelled as '4')

Maximum Width of the Pars Petrosa – Maximum distance at right angles to length across arcuate eminence. (Labelled as '5')

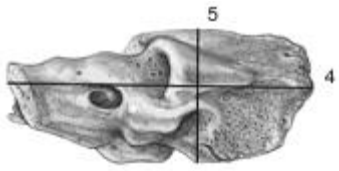

Fig 34: The pars petrosa, showing measurements of maximum length and width. Reproduced from Schaefer et al (2009).

9.2.2. **Tibia**

Maximum Length of the Tibia – The maximum distance from the most superior part of the proximal epiphysis to the most inferior part of the distal epiphysis. Due to the unfused epiphyses, the intercondylar eminence on the proximal epiphysis does not need to be discounted from the measurement.

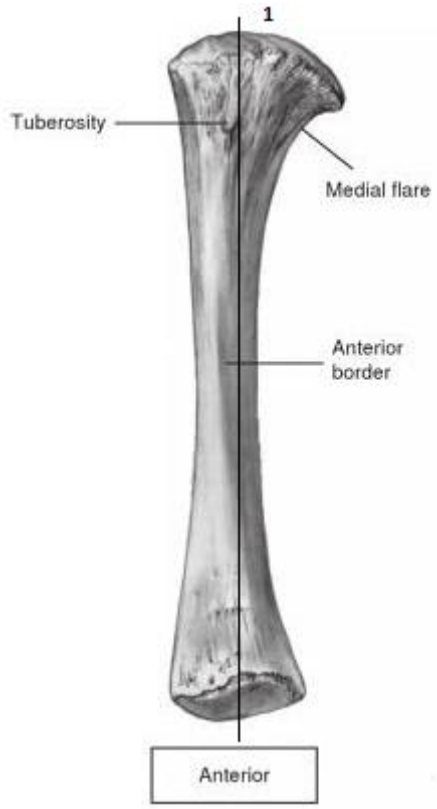

Fig 35: The anterior juvenile tibia. Maximum length measurement is shown labelled as '1'. Reproduced from Schaefer et al (2007).

9.2.3. **Sphenoid**

Body Length: Midline distance between the synchondrosis intrasphenoidalis and spheno-occipitalis. (Labelled as '1')

Body Width: Maximum transverse distance in the mid-hypophyseal fossa. (Labelled as '2')

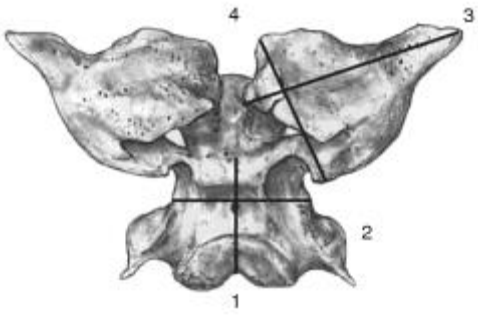

Fig 36: Intracranial view of the sphenoid showing measurements of the sphenoid body labelled as ‘1’ and ‘2’. Reproduced from Schaefer et al (2007).

9.2.4. **Femur**

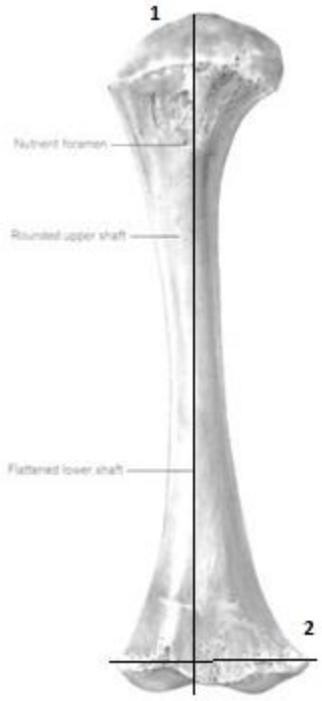

Fig 37: Anterior view of the perinatal femur, showing measurement of maximum length and distal width epiphysis as ‘1’ and ‘2’, respectively. Reproduced from Schaefer et al (2007).

Maximum Length: The maximum distance between the most superior point on the unfused proximal epiphysis and the most inferior part of the unfused distal epiphysis.

Distal width: The maximum distance between the most lateral point of the lateral condylar area and the most medial point of the medial condylar area.

9.2.5. **Humerus**

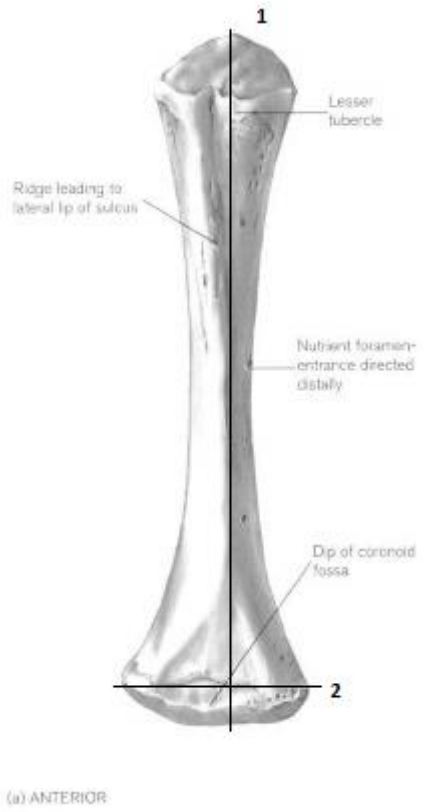

Fig 38: Anterior view of the perinatal humerus, showing measurements for maximum length (labelled '1') and distal width (labelled '2'). Reproduced from Schaefer et al (2007).

Maximum Length: The maximum distance between the most superior part of the unfused proximal epiphysis and the most inferior part of unfused distal epiphysis.

Distal Width: The maximum distance between the most lateral part of the lateral border of the unfused epiphysis and the most medial part of the medial border of the unfused epiphysis.

9.2.6. **Scapula**

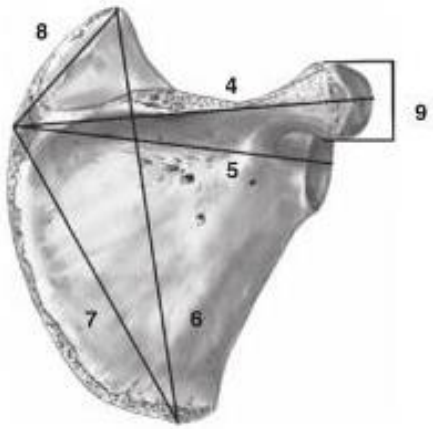

Fig 39: Posterior view of the perinatal scapula, showing the measurements for Scapula Width (labelled as '5') and Scapula Length (labelled as '6'). Reproduced from Schaefer et al (2007).

Scapula Width: Distance between the margin of the glenoid fossa and the medial end of the spine.

Scapula Length: Distance between the superior and inferior angles of the scapula.

9.2.7. **Ischium**

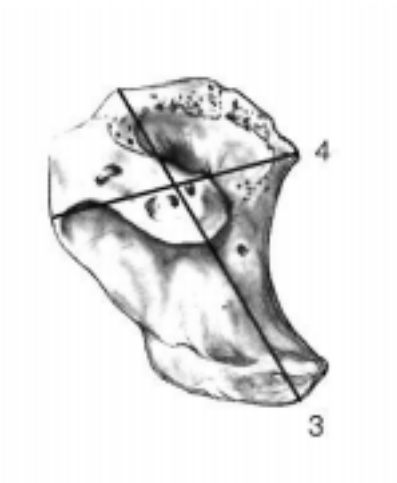

Fig 40: Lateral view of the perinatal ischium, showing the measurements for Maximum Ischium Length (labelled '3') and Maximum Ischium Width (labelled '4'). Reproduced from Schaefer et al (2007).

Maximum Ischium Length: Greatest distance between the convexity of the acetabular extremity and the tip of the ischial ramus.

Maximum Ischium Width: Greatest distance across the broad superior extremity.

9.3. **NEB Biolabs Low Molecular Weight Ladder**

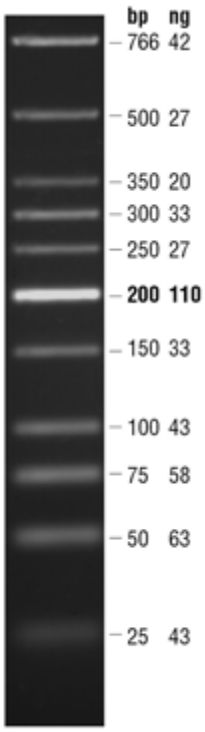

Fig 41: NEB Biolabs Low Molecular Weight Ladder fragment sizes. Ladder visualised with Ethidium Bromide staining on a 1.8% Agarose gel, with mass values for 0.5µg/lane. Reproduced from NEB Biolabs [https://www.neb.com/products/n3233-low-molecular-weight-dna-ladder]

9.4. **Contamination in Identifiler Results**

Three gels that were carried out during the testing of the neonatal remains with the Identifiler amelogenin primers, showed contaminated negative controls. The results, including the contamination, can be seen in the figures below.

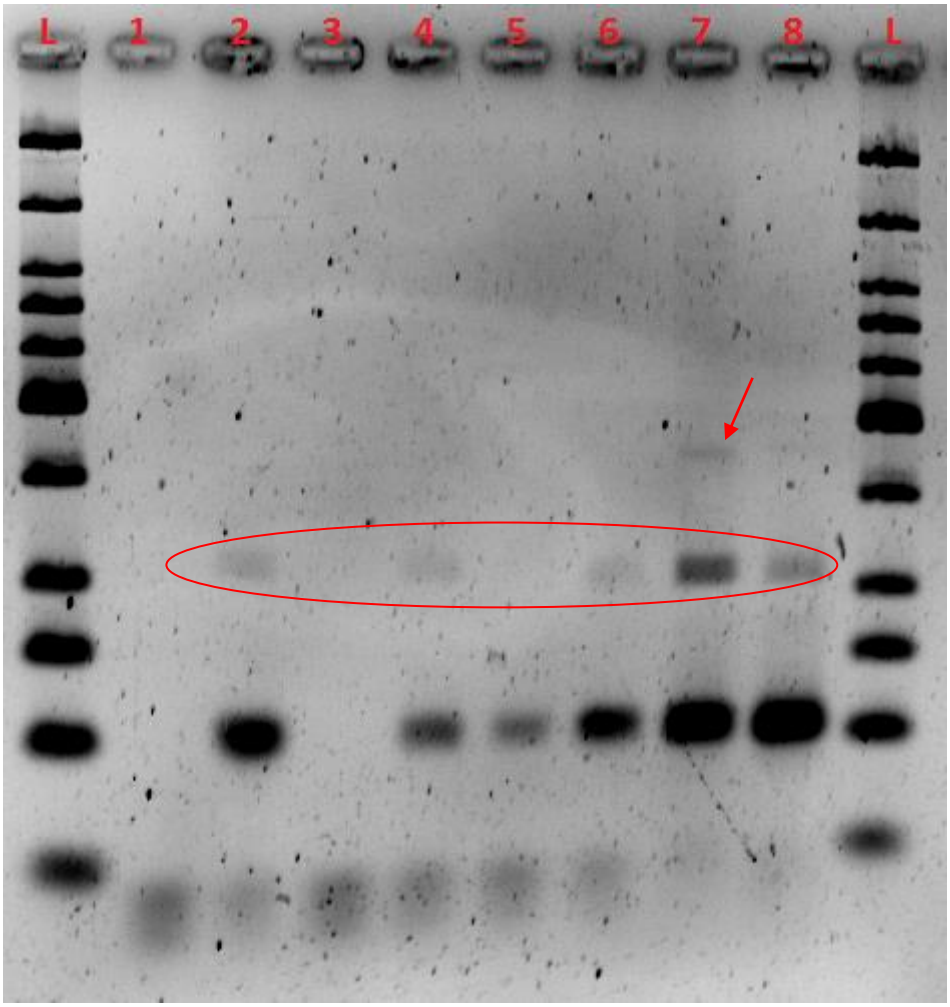

Gel Key: L – NEB Biolabs Low Molecular Weight Ladder, 1 – SK26320, 2 – SK27925, 3 – SK27447, 4 – SK27743, 5 – SK28224, 6 – SK26926, 7 – male positive control, 8 – blank, L – NEB Low Molecular Weight ladder.

Fig 42: Contaminated neonatal results 13-18. All tests carried out with 10ng of ancient DNA. Contamination can be seen in the negative control (blank) in lane 8. This contamination has also led to an XY genotype banding pattern in lanes 2, 4, and 6. Non-specific binding at approximately 175bp in length can be seen in Lane 7, the positive control.

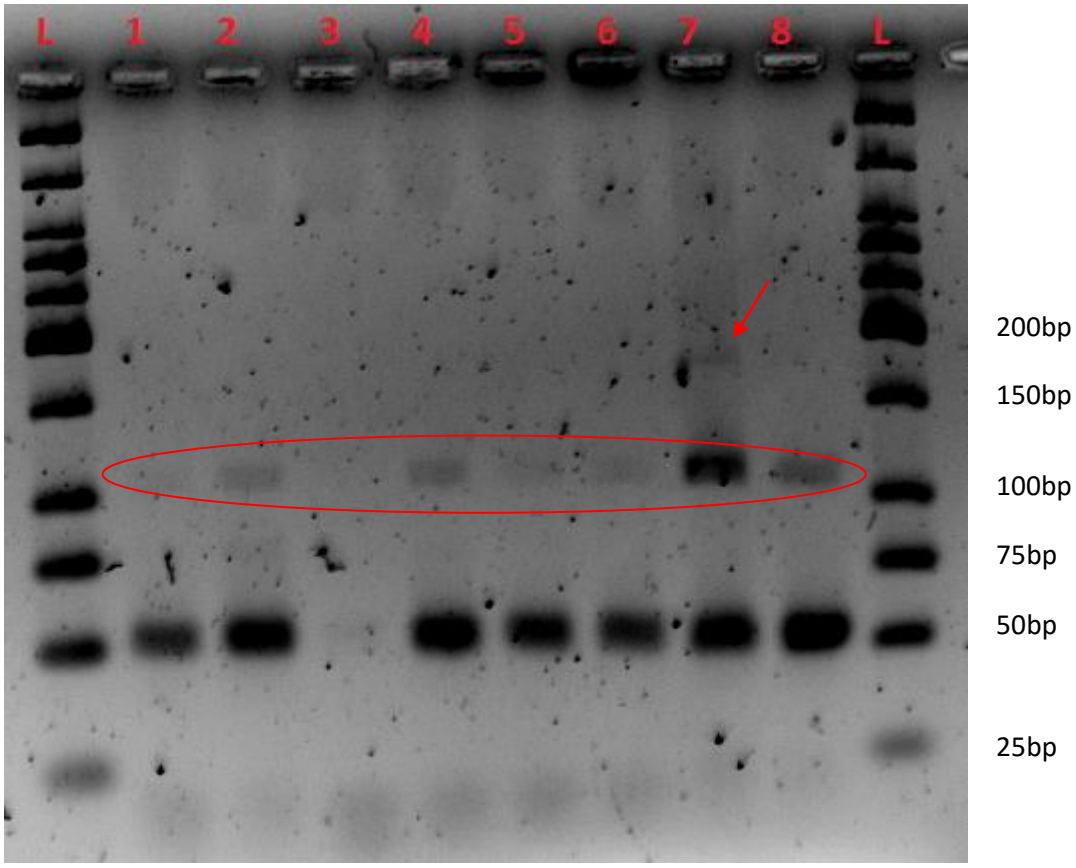

Gel Key: L – NEB Biolabs Low Molecular Weight Ladder, 1 – SK22684, 2 – SK25368, 3 – SK25167/25168, 4 – SK31225, 5 – SK25245/25244, 6 – SK27927, 7 – male positive control, 8 – blank, L – NEB Low Molecular Weight Ladder.

Fig 43: Contaminated neonatal results 19-24. All tests carried out with 10ng of Ancient DNA. Strong contaminant banding can be seen in the negative control in Lane 8. This contamination has also affected lanes 1, 2, 4, 5 and 6. Again, non-specific binding can be seen in the positive control (Lane 7) at approximately 175bp in length.

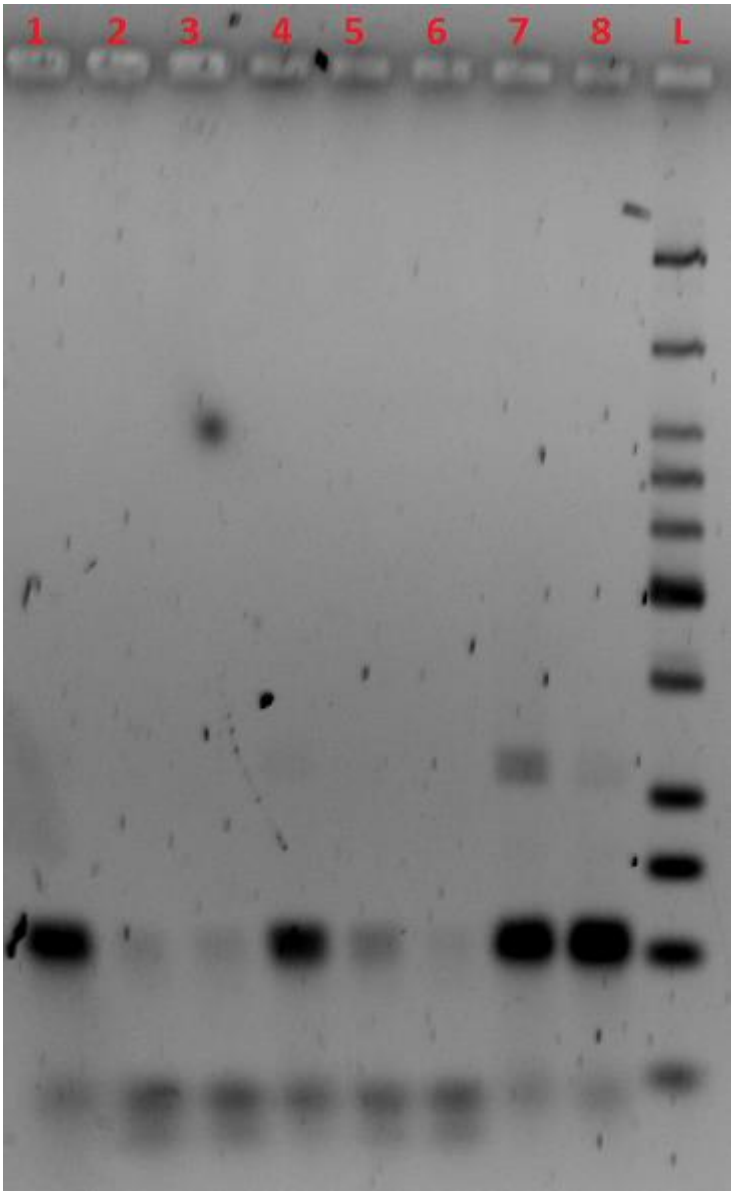

Gel Key: 1 – SK26851, 2 – SK27774, 3 – SK25209, 4 – SK33056, 5 – SK27392, 6 – SK26934, 7 – Male positive control, 8 – Blank, L – NEB Low Molecular Weight Ladder

Fig 44: Contaminated neonatal results 37-42. All testing carried out with 10ng of ancient DNA. Contamination can be seen in Lane 8, the positive control. Faint positive banding can be seen in lane 4, due to the contamination with modern DNA. Lanes 2, 3, 5 and 6 all show faint primer dimer formation due to PCR inhibition. Therefore, there may also be contamination in these lanes that simply has not amplified to a visible level.

These contaminated gels had entirely fresh extractions and amplifications carried out on the sample material, and the uncontaminated results that were gained from this repetition can be found in Section 4.4.